UNIVERSITY OF OKLAHOMA

GRADUATE COLLEGE

CHARACTERIZING THE BEHAVIOR OF CONCRETE CAST WITH TYPE K SHRINKAGE COMPENSATING CEMENT WHEN PLACED UNDER MECHANICAL RESTRAINT

A THESIS

SUBMITTED TO THE GRADUATE FACULTY

in partial fulfillment of the requirements for the

Degree of

MASTER OF SCIENCE

By

STEPHEN JOSIAH ROSWURM
Norman, Oklahoma
2018

CHARACTERIZING THE BEHAVIOR OF CONCRETE CAST WITH TYPE K SHRINKAGE COMPENSATING CEMENT WHEN PLACED UNDER MECHANICAL RESTRAINT

A THESIS APPROVED FOR THE
SCHOOL OF CIVIL ENGINEERING AND ENVIRONMENTAL SCIENCE

BY

_____
Dr. Chris Ramseyer

_____
Dr. Jeffery Volz

_____
Dr. Royce Floyd

This work is dedicated to my Lord Jesus Christ and the loving, beautiful, and amazing family that He gave me. I love you all so much!

Acknowledgments

I can hardly begin to express the depth of my gratitude to all those who have played such a crucial role in helping me to reach this point in my life and to accomplish the challenges that have been set before me. My thankfulness abounds because I know in my heart of hearts that I could never have fulfilled my hopes and dreams without the support of so many family, friends, coworkers, professors, and mentors.

First and foremost, I would like to thank my mentor, Dr. Chris Ramseyer, for his assistance throughout the completion of this research. He has been an invaluable resource and a great blessing throughout my college career. Dr. Ramseyer took a chance on hiring me when I was a sixteen year old kid who hadn't even started classes at OU yet, and stuck with me throughout the duration of both my undergraduate and graduate work. I never would have been able to navigate my way through the travails of this process without his help.

I want to also thank my incredible family for putting me in the best possible situation to succeed. Thanks first to my Mom and Dad who worked tirelessly to homeschool me, and ensure I had an excellent quality education. Thank you also for all the emotional, physical, and financial support throughout my time at OU. I could not have accomplished this without your spiritual guidance and loving support!

Thanks also go out to all my siblings. Katie, you mean the world to me, and I cannot express my gratitude for everything you've done for me while I have been so busy I'm not even seeing straight. You are the best sister I could ask for! Thank you to my oldest brother Sam, and his wife Kate. You two are such an inspiration to me, and

you have truly given me a vision for what God intended in a marriage. Thank you for always caring so deeply for all my ups and downs, and for all the fun times at the football games! Thank you to my next brother Jesse and his wife Amy, as well as my third oldest brother Seth, and his wife Brianna. You are a great encouragement to me. Jesse and Seth were such faithful stewards with what Dr. Ramseyer entrusted them that it greatly benefited me as I started down the same path that they did. Thanks additionally to Seth for recommending me to Dr. Ramseyer to first work at Fears Lab; I will remember the good times we had working there together for a long time.

Special thanks are also in order for my brother Jake. You mean so much more to me than I could possibly ever express to you. Throughout the last ten years of working and going to school with you, you have become the closest friend and confidant that I have ever known. I can say with confidence that I would not have been able to make it through all the hard times of my undergraduate degree and all the blood, sweat, and tears of graduate school without your cool, calm demeanor, steadying influence, and rock-solid faith and trust in the Lord. I love you, man, and nothing and no one can ever erase or replace the precious place you hold in my heart. We have truly been through the fire together and I love you so much!

I would also like to express my gratitude to my church family for their constant support and prayers. I know that you all were lifting me up before the Father, and I am forever thankful for all of you.

A single acknowledgment seems to pale in comparison to all that you mean to me, but I also want to specifically thank Ms. Trish Foor and Mr. Tracy Foor. Ms. Foor was a truly a life-changing influence for me, and completely changed the trajectory of

my life at such a critical time for me. It is not an understatement to say I would not be where I am today without your tender, loving care, which came at a time when I felt so ashamed and insecure that I hated to even speak. The Lord manifested His plan in my life through you, and I will be forever thankful for our friendship!

Finally, I want to express special thanks to all those in the CEES Department at OU that made my experience here successful and enjoyable. Thanks to my friends and coworkers from OU who assisted in various capacities on my research at Fears Lab, including Dakota Gennings, who worked tirelessly with Jake and I throughout our research. Others who were of great help include Dare Obasade, Connor Casey, Cameron Murray, Adam Aab, and Ousmane Ndure. Thanks also to Dr. Royce Floyd and Dr. Jeff Volz, whose research groups were often generous to share resources in the lab. Thank you to all the wonderful people from the CEES office who made my time here smooth, including Molly Smith, Susan Williams, and Audre Carter; for Susan and Audre, I hope you enjoy your retirement. Your hard work was such a blessing! Finally, I would like to thank Mike Schmitz, the shop supervisor at Fears Structural Engineering Laboratory. Mike, you have been an incredible influence on myself and hundreds of other students who have been the grateful beneficiaries of your vast knowledge, experience, and hard work. Thank you for your endless help, patience, and hard work and for helping me out when I was in a fix or stuck because of a dumb mistake that I made. I have learned so much from you, and I cannot thank you enough for the profound impact you had on this research and on my overall development as an engineer.

Special thanks also to the sponsors who made this research project possible. The primary sponsor for this project was the CTS Cement Manufacturing Corporation in Cypress, California. CTS provided all the Type K cement materials utilized in this project, as well as technical support. I would like to specifically thank Chris Davis of CTS for his direct role in obtaining some of this material. Additionally, thanks to the Dolese Brothers Company, which supplied all fine aggregate, coarse aggregate, and Portland cement used in this research.

Table of Contents

Chapter 1 – Introduction 1
1.1 Background 1
1.2 Objectives 3
1.3 Research Scope 4
Chapter 2 – Literature Review 6
2.1 Problem Statement 6
2.2 Practical Considerations 7
2.3 Advantages and Disadvantages of SCC 8
2.4 Case Study – Eskildsen et al. 9
2.5 Case Study – Rockford, IL Airport 11
2.6 Effects of Mechanical Restraint 18
Chapter 3 – Materials and Methods 43
3.1 Testing Overview 43
3.1.1 Compressive Specimens 43
3.1.2 ASTM C157, Unrestrained Expansion 43
3.1.3 ASTM C878, Restrained Expansion 45
3.1.4 Restrained and Unrestrained Expansion Cylinders 47
3.1.5 Restrained Columns 54
3.2 Raw Materials 63
3.3 Mix Designs 64
3.4 Casting Procedures 65
3.4.1 Batch Preparation 65
3.4.2 Mixing Procedure 66
3.4.3 Casting and Curing Procedure 67
Chapter 4 – Results 70
4.1 ASTM C157 Unrestrained Expansion 70
4.2 ASTM C878 Restrained Expansion 71
4.3 Unrestrained Expansion Cylinders 72
4.4 Restrained Expansion Cylinders 73
4.5 Restrained Column Expansion 74
4.5.1 15% Replacement - Cured with Cardboard Forms in Place 74
4.5.2 17% Replacement – Cured with Cardboard Forms in Place 77
4.5.3 15% Replacement - Cured with Sprinkler System 79

4.5.4 17% Replacement – Cured with Sprinkler System 81
4.5.5 19% Replacement – Cured with Sprinkler System 83
4.5.6 21% Replacement – Cured with Sprinkler System 85
4.6 Restrained Column Load Development 87
4.6.1 15% Replacement - Cured with Cardboard Forms in Place 87
4.6.2 17% Replacement - Cured with Cardboard Forms in Place 90
4.6.3 19% Replacement - Cured with Sprinkler System 92
4.6.4 21% Replacement - Cured with Sprinkler System 94
4.7 Compressive Cylinders 97
4.8 Fresh Properties 98
Chapter 5 – Discussion of Results 99
5.1 ASTM C157 Unrestrained Expansion 99
5.2 ASTM C878 Restrained Expansion 100
5.3 Unrestrained Expansion Cylinders 101
5.4 Restrained Expansion Cylinders 102
5.5 Comparing Unrestrained Cylinders to ASTM C157 Prisms 103
5.6 Comparing Restrained Cylinders to ASTM C878 Prisms 109
5.7 Comparing Expansion of Restrained Columns 113
5.7.1 Cured with Cardboard Forms in Place 113
5.7.2 Cured with Sprinkler System 116
5.8 Comparing Load Development of Restrained Columns 127
5.9 Analyzing Self-Induced Stress-Strain Behavior 134
5.9.1 15% and 17% Replacement 136
5.9.2 19% Replacement 136
5.9.3 21% Replacement 139
5.9.4 Overlaid Curves by Level of Restraint 142
5.9.5 Meaning of Stress-Strain Curves 145
5.10 Overall Shrinkage Compensation 146
5.11 Performance of VWSG 148
5.12 Comparisons with Previous Research 149
Chapter 6 – Summary 156
6.1 Conclusions 156
6.2 Recommendations for Future Work 158
6.2.1 Porosity Experiments 158

6.2.2 Restrained Column Protocol 159
6.2.3 Restrained Columns with Other Mix Designs 160
6.2.4 Restrained Columns with Chemical Prestress 161
References 163
Appendix A – Fresh Data and Mix Quantities 165
A.1 15% Replacement Mix 165
A.1.1 First Batch (Curing Alternative No. 1) 165
A.1.2 Second Batch (Curing Alternative No. 2) 166
A.2 17% Replacement Mix 167
A.2.1 First Batch (Curing Alternative No. 1) 167
A.2.2 Second Batch (Curing Alternative No. 2) 168
A.3 19% Replacement Mix 169
A.3.1 First Batch 169
A.3.2 Second Batch 170
A.4 21% Replacement Mix 171
A.4.1 First Batch 171
A.4.2 Second Batch 172
Appendix B – Strain Data for ASTM C878 and C157 Tests 173
Appendix C – 19% and 21% Restrained Columns (Invalidated Tests) 177
Appendix D – Long-Term Results 181

List of Tables

Table 1: Summary of Research Test Specimens 5
Table 2: Mixture Designs for Experimental Bridge Decks (Richardson et al., 2014) ... 23
Table 3: Raw Material for Research 64
Table 4: Mix Designs for Research 65
Table 5: Curing System Alternatives used for Restrained Columns 74
Table 6: Fresh Properties for Restrained Columns 98
Table 7: Comparison of SA/V Ratios for Length Change Specimens 108
Table 8: Comparison of Variation Between Column Expansion Curves 122
Table 9: Comparison of Variation Between Column Expansion Curves (Constant Restraint) 127
Table 10: Manually Measured Length Change Data (15% Komponent) 173
Table 11: Manually Measured Length Change Data (17% Komponent) 174
Table 12: Manually Measured Length Change Data (19% Komponent) 175
Table 13: Manually Measured Length Change Data (21% Komponent) 176

List of Figures

Figure 1: Airport Runway Slab with Steel Fiber Reinforcement at Greater Rockford Airport (Ramseyer, 2018) 13
Figure 2: Airport Runway Slabs at Greater Rockford Airport (Ramseyer, 2018) 14
Figure 3: Separation of Post-Tensioned Slab from Expansion Joint at Greater Rockford Airport (Ramseyer, 2018) 15
Figure 4: Transverse Crack Repair at Greater Rockford Airport (Chusid, 2006) 17
Figure 5: Vertical Slabs for Restrained Expansion (Russell, 1973) 19
Figure 6: Test Setup for Experimental Bridge Deck (Richardson et al., 2014) 22
Figure 7: Experimental Bridge Deck with Concrete (Richardson et al., 2014) 23
Figure 8: Locations of Strain Gages for Top Rebar (Richardson et al., 2014) 24
Figure 9: Locations of Strain Gages for Bottom Rebar (Richardson et al., 2014) 25
Figure 10: Strain Data for PCC Control Slab, Gages 1, 2, and 3 (Richardson et al., 2014) 26
Figure 11: Strain Data for Type K Slab, Gages 1 and 3 (Richardson et al., 2014) 27
Figure 12: Interaction of Mature Existing Slabs with Expansive Concrete (Seth Roswurm, 2013) 32
Figure 13: Comparison of Models for the Behavior of Expansive Concrete (Seth Roswurm, 2013) 33
Figure 14: Profile View of Test Frame (Seth Roswurm, 2013) 35
Figure 15: Profile View of Test Frame with Dimensions (Seth Roswurm, 2013) 36
Figure 16: Plan View of Test Frame Base Plate (Seth Roswurm, 2013) 37
Figure 17: Plan View of Test Frame Base Plate with Dimensions (Seth Roswurm, 2013) 37
Figure 18: Fully Assembled Test Frame with Concrete Column (Seth Roswurm, 2013) 39
Figure 19: 15% Komponent Column Expansion Results (Seth Roswurm, 2013) 40
Figure 20: ASTM C157 Unrestrained Prism 44
Figure 21: Dial Gage and Length Comparator for Unrestrained Prisms 44
Figure 22: ASTM C878 Restrained Prism 45
Figure 23: Dial Gage and Length Comparator for Restrained Prisms 46
Figure 24: Cross-Section of Geokon VWSG (Geokon, 2017) 47
Figure 25: 6"x 12" Cylinder Equipped with VWSG for Unrestrained Expansion 49
Figure 26: Top Down View of VWSG in 6”x12” Cylinder 50
Figure 27: 6"x 12" Cylinder for Restrained Expansion 51
Figure 28: Top Down View of Restrained Expansion Cylinder 52
Figure 29: 6"x 12" Cylinder for Restrained Expansion with Mold Removed 53
Figure 30: Curing Alternative 1, PVC Jackets with Cardboard Forms at Water Cure Stage (Seth Roswurm, 2013) 56
Figure 31: Plan View of Modified Test Frame Base Plate 57
Figure 32: Plan View of Modified Test Frame Base Plate with Dimensions 58
Figure 33: Curing Alternative 2, PVC Form with Hose Clamps at Form Stripping Stage 59
Figure 34: Restrained Columns Equipped with Sprinkler System for Wet Cure 60
Figure 35: Close-Up of Sprinkler System in Action 61
Figure 36: ASTM C157 Unrestrained Expansion Results 70

Figure 37: ASTM C878 Restrained Expansion Results 71
Figure 38: VWSG Unrestrained Expansion Cylinder Results 72
Figure 39: VWSG Restrained Expansion Cylinder Results 73
Figure 40: Restrained Column Expansion Results with Forms Left in Place (1/2" Restraint Rods, 15% Komponent) 75
Figure 41: Restrained Column Expansion Results with Forms Left in Place (5/8" Restraint Rods, 15% Komponent) 76
Figure 42: Restrained Column Expansion Results with Forms Left in Place (3/4" Restraint Rods, 15% Komponent) 76
Figure 43: Restrained Column Expansion Results with Forms Left in Place (1/2" Restraint Rods, 17% Komponent) 77
Figure 44: Restrained Column Expansion Results with Forms Left in Place (5/8" Restraint Rods, 17% Komponent) 78
Figure 45: Restrained Column Expansion Results with Forms Left in Place (3/4" Restraint Rods, 17% Komponent) 78
Figure 46: Restrained Column Expansion Results (1/2" Restraint Rods, 15% Komponent) 80
Figure 47: Restrained Column Expansion Results (5/8" Restraint Rods, 15% Komponent) 80
Figure 48: Restrained Column Expansion Results (3/4" Restraint Rods, 15% Komponent) 81
Figure 49: Restrained Column Expansion Results (1/2" Restraint Rods, 17% Komponent) 82
Figure 50: Restrained Column Expansion Results (5/8" Restraint Rods, 17% Komponent) 82
Figure 51: Restrained Column Expansion Results (3/4" Restraint Rods, 17% Komponent) 83
Figure 52: Restrained Column Expansion Results (1/2" Restraint Rods, 19% Komponent) 84
Figure 53: Restrained Column Expansion Results (5/8" Restraint Rods, 19% Komponent) 84
Figure 54: Restrained Column Expansion Results (3/4" Restraint Rods, 19% Komponent) 85
Figure 55: Restrained Column Expansion Results (1/2" Restraint Rods, 21% Komponent) 86
Figure 56: Restrained Column Expansion Results (5/8" Restraint Rods, 21% Komponent) 86
Figure 57: Restrained Column Expansion Results (3/4" Restraint Rods, 21% Komponent) 87
Figure 58: Restrained Column Load Development Results (1/2" Restraint Rods, 15% Komponent) 88
Figure 59: Restrained Column Load Development Results (5/8" Restraint Rods, 15% Komponent) 89
Figure 60: Restrained Column Load Development Results (3/4" Restraint Rods, 15% Komponent) 89
Figure 61: Restrained Column Load Development Results (1/2" Restraint Rods, 17%

Komponent) 90
Figure 62: Restrained Column Load Development Results (5/8" Restraint Rods, 17% Komponent) 91
Figure 63: Restrained Column Load Development Results (3/4" Restraint Rods, 17% Komponent) 91
Figure 64: Restrained Column Load Development Results (1/2" Restraint Rods, 19% Komponent) 93
Figure 65: Restrained Column Load Development Results (5/8" Restraint Rods, 19% Komponent) 93
Figure 66: Restrained Column Load Development Results (3/4" Restraint Rods, 19% Komponent) 94
Figure 67: Restrained Column Load Development Results (1/2" Restraint Rods, 21% Komponent) 95
Figure 68: Restrained Column Load Development Results (5/8" Restraint Rods, 21% Komponent) 95
Figure 69: Restrained Column Load Development Results (3/4" Restraint Rods, 21% Komponent) 96
Figure 70: Compressive Strength Results 97
Figure 71: ASTM C157 Unrestrained Expansion Results 99
Figure 72: ASTM C878 Restrained Expansion Results 100
Figure 73: VWSG Unrestrained Expansion Cylinder Results 101
Figure 74: Restrained Expansion Cylinder Results 102
Figure 75: Overlay of Unrestrained Expansion Cylinder with ASTM C157 (15% Komponent®) 103
Figure 76: Overlay of Unrestrained Expansion Cylinder with ASTM C157 (17% Komponent®) 104
Figure 77: Overlay of Unrestrained Expansion Cylinder with ASTM C157 (19% Komponent®) 105
Figure 78: Overlay of Unrestrained Expansion Cylinder with ASTM C157 (21% Komponent®) 106
Figure 79: Overlay of Restrained Expansion Cylinder with ASTM C878 (15% Komponent®) 109
Figure 80: Overlay of Restrained Expansion Cylinder with ASTM C878 (17% Komponent®) 110
Figure 81: Overlay of Restrained Expansion Cylinder with ASTM C878 (19% Komponent®) 111
Figure 82: Overlay of Restrained Expansion Cylinder with ASTM C878 (21% Komponent®) 112
Figure 83: Restrained Column Expansion Results with Forms Left in Place (All Restraint Rods, 15% Komponent) 114
Figure 84: Restrained Column Expansion Results with Forms Left in Place (All Restraint Rods, 17% Komponent) 114
Figure 85: Restrained Column Expansion Results with Sprinkler Curing (All Restraint Rods, 15% Komponent) 117
Figure 86: Restrained Column Expansion Results with Sprinkler Curing (All Restraint Rods, 17% Komponent) 118

Figure 87: Restrained Column Expansion Results with Sprinkler Curing (All Restraint Rods, 19% Komponent) 120
Figure 88: Restrained Column Expansion Results with Sprinkler Curing (All Restraint Rods, 21% Komponent) 121
Figure 89: Restrained Column Expansion Results with Sprinkler Curing (1/2" Restraint Rods, All Mix Designs) 123
Figure 90: Restrained Column Expansion Results with Sprinkler Curing (5/8" Restraint Rods, All Mix Designs) 125
Figure 91: Restrained Column Expansion Results with Sprinkler Curing (3/4" Restraint Rods, All Mix Designs) 126
Figure 92: Restrained Column Load Development Results (All Restraint Rods, 15% Komponent) 128
Figure 93: Restrained Column Load Development Results (All Restraint Rods, 17% Komponent) 129
Figure 94: Restrained Column Load Development Results (All Restraint Rods, 19% Komponent) 130
Figure 95: Restrained Column Load Development Results (All Restraint Rods, 21% Komponent) 131
Figure 96: Restrained Column Load Development Results (1/2" Restraint Rods, All Mix Designs) 132
Figure 97: Restrained Column Load Development Results (5/8" Restraint Rods, All Mix Designs) 133
Figure 98: Restrained Column Load Development Results (3/4" Restraint Rods, All Mix Designs) 134
Figure 99: Restrained Column Stress-Strain Curve (1/2" Restraint Rods, 19% Komponent) 137
Figure 100: Restrained Column Stress-Strain Curve (5/8" Restraint Rods, 19% Komponent) 137
Figure 101: Restrained Column Stress-Strain Curve (3/4" Restraint Rods, 19% Komponent) 138
Figure 102: Restrained Column Stress-Strain Curves (All Restraint Rods, 19% Komponent) 138
Figure 103: Restrained Column Stress-Strain Curve (1/2" Restraint Rods, 21% Komponent) 140
Figure 104: Restrained Column Stress-Strain Curve (5/8" Restraint Rods, 21% Komponent) 140
Figure 105: Restrained Column Stress-Strain Curve (3/4" Restraint Rods, 21% Komponent) 141
Figure 106: Restrained Column Stress-Strain Curves (All Restraint Rods, 21% Komponent) 141
Figure 107: Restrained Column Stress-Strain Curves (1/2" Restraint Rods, 19% and 21% Komponent) 143
Figure 108: Restrained Column Stress-Strain Curves (5/8" Restraint Rods, 19% and 21% Komponent) 143
Figure 109: Restrained Column Stress-Strain Curves (3/4" Restraint Rods, 19% and 21% Komponent) 144

Figure 110: 15% Komponent Column Expansion Results (Seth Roswurm, 2013) 150
Figure 111: Restrained Column Expansion Results with Sprinkler Curing (All Restraint Rods, 15% Komponent) 151
Figure 112: 15% Komponent Column Load Results (Seth Roswurm, 2013) 152
Figure 113: Restrained Column Load Development Results (All Restraint Rods, 19% Komponent) 153
Figure 114: 30% Komponent Stress-Strain Results (Seth Roswurm, 2013) 154
Figure 115: Restrained Column Stress-Strain Curves (All Restraint Rods, 21% Komponent) 155
Figure 116: Fresh Data and Mix Quantities for 15% Replacement, Mix #1 165
Figure 117: Fresh Data and Mix Quantities for 15% Replacement, Mix #2 166
Figure 118: Fresh Data and Mix Quantities for 17% Replacement, Mix #1 167
Figure 119: Fresh Data and Mix Quantities for 17% Replacement, Mix #2 168
Figure 120: Fresh Data and Mix Quantities for 19% Replacement, Mix #1 169
Figure 121: Fresh Data and Mix Quantities for 19% Replacement, Mix #2 170
Figure 122: Fresh Data and Mix Quantities for 21% Replacement, Mix #1 171
Figure 123: Fresh Data and Mix Quantities for 21% Replacement, Mix #2 172
Figure 124: Restrained Column Expansion Results (All Restraint Rods, 19% Komponent - First Trial) 178
Figure 125: Restrained Column Expansion Results (All Restraint Rods, 21% Komponent - First Trial) 179
Figure 126: Long-Term ASTM C157 Results 181
Figure 127: Long-Term ASTM C878 Results 182
Figure 128: Long-Term VWSG Unrestrained Cylinder Results 182
Figure 129: Long-Term VWSG Restrained Cylinder Results 183
Figure 130: Long-Term Results for 15% Restrained Column Expansion (Curing Alternative 1) 183
Figure 131: Long-Term Results for 17% Restrained Column Expansion (Curing Alternative 1) 184
Figure 132: Long-Term Results for 19% Restrained Column Expansion (Curing Alternative 1) 184
Figure 133: Long-Term Results for 21% Restrained Column Expansion (Curing Alternative 1) 185

Abstract

The purpose of this research was to determine whether shrinkage-compensating concrete (SCC) made with Type K cement is capable of offsetting the effects of early age drying shrinkage, specifically when the concrete is acted upon by a stiff external restraint. The effect of restraint on SCC is important because this effect resists the expansive behavior that provides shrinkage compensation. This research was intended to improve upon the 2013 work of Seth Roswurm. The test specimens used in this experiment very closely paralleled those used in Seth Roswurm's experiments; they consisted primarily of four sets of test specimens, each of which was cast with a unique mixture design. The test specimens included 4" diameter restrained columns, and each set consisted of three columns with varying degrees of stiffness in the restraint frame. The variation in stiffness was created by using a set of four steel restraint rods on each column, whose diameters were set at ½", ⅝", and ¾". The column specimens were instrumented using *Geokon*® vibrating wire strain gages (VWSG), which were embedded in the concrete, and load cells, which were affixed to the top of the columns using 2" steel reaction plates mounted to the restraint rods. The most significant result of this experiment was that the data showed that SCC can be effective even under stiff boundary conditions, meaning that SCC could be viable in applications for various structures such as pavements, bridge decks, pre-tensioned and post-tensioned beams, and even residential construction. Other results drawn from these experiments included data regarding what the optimal mix design is for full shrinkage-compensation, how the SCC should be cured in order to obtain satisfactory behavior, and what kind of stress-strain curves a self-expanding material will create.

Chapter 1 – Introduction

1.1 Background

The purpose of this research was to investigate the material behavior of shrinkage compensating concrete (SCC) made with Type K cement, particularly when placed under mechanical restraint. This mechanical restraint can come in many forms, but in the field, it is often due to the presence of reinforcing steel or adjacent slabs. The objective was to determine whether a concrete made with Type K cement can provide adequate shrinkage compensation when exposed to a stiff boundary condition.

The most common type of concrete used throughout the world today is made from Portland cement, and is typically referred to as Portland cement concrete (PCC). Although it can be an extremely robust product, PCC has certain deficiencies. One of the biggest issues with PCC is that, given enough time, it will nearly always develop cracks. These cracks allow water infiltration, and in cold climates, the resulting freeze-thaw cycle (coupled with the use of salt, sand, and other deicers) gradually degrades the concrete. At best, this results in unsightly aesthetic damage; at worst, the continued water infiltration begins to corrode the reinforcing steel and compromises the structure.

The mitigation of cracking in concrete is a difficult matter because it can arise from many different sources. First, whenever concrete is placed under load, if the cracking moment (Mcr) is exceeded, cracks will develop. Since concrete is relatively weak in tension, the cracking moment is usually lower than the moment demand placed on the structure, meaning that tension cracks often develop due to externally applied loads. One of the most common and serious forms of cracking, however, is due to restrained drying shrinkage. Other causes exist for the occurrence of shrinkage, but

drying shrinkage is the focus of this study because it is often the most significant. Restrained drying shrinkage occurs when a PCC element is cast, and the water in the fresh concrete begins to evaporate. The evaporation process causes a decrease in volume of the concrete, and since the concrete is not yet strong enough to resist the resulting tensile stresses, shrinkage cracks form. This is especially problematic when the concrete is at an early age, because it has not developed very much tensile strength. Although concrete is vulnerable at early age, drying shrinkage can continue past that period, and can cause shrinkage cracks as long as a year after casting.

The purpose of SCC is to use mineral admixtures or special cements that offset early age drying shrinkage, typically by increasing the early age volume of the concrete. The unavoidable drying shrinkage will still take place after curing (with the net change in length eventually returning to almost zero), but the shrinkage will be delayed enough that the concrete will have matured to the point that it can resist the tensile stress the shrinkage places on it. This research utilized Type K cement to create a shrinkage compensating concrete, with the objective of determining whether the concrete is capable of adequately offsetting shrinkage, even with a stiff boundary condition acting on it. These experiments were necessary because some researchers have proposed that a stiff boundary condition will make SCC ineffective. This suggestion is based on the fact that an infinitely stiff boundary condition will not allow any movement. This fact has been extended by some to conclude that since progressively stiffer restraint will reduce the expansion of SCC, these types of boundary conditions will prohibit effective shrinkage compensation.

This set of experiments utilized a group of mix designs with variable

percentages of Type K cement, subjected to different restraint systems of varying stiffness. The primary test specimens were a set of concrete columns, with a steel restraint system designed to mimic an in-situ slab-on-slab interaction. In addition to varying the stiffness of the restraint, the type of curing system was varied.

1.2 Objectives

The objectives that this series of tests are designed to accomplish are the following:

1.) Improve upon Ramseyer and Roswurm's 2013 research on Type K SCC.

2.) Determine if boundary conditions of varying stiffness will cause a significant difference in concrete expansion.

3.) Determine if a stiff boundary condition will materially hamper the ability of a Type K cement concrete to compensate for shrinkage.

4.) Determine if Type K shrinkage compensating concrete is capable of completely offsetting early age drying shrinkage.

The first step for these objectives is to characterize the length change of SCC in free expansion, using both manual measurements and strain gages. The second step is to characterize the length change of SCC in restrained expansion, using three different tests. One of those tests involves SCC column specimens, subjected to restraint systems of increasing stiffness. The third step is to characterize the load development of the SCC column specimens under consistent conditions. The final step is to study the self-induced stress-strain relationship created by the expansion of the concrete. In order for the results to be applicable in the real world, the following conditions must be in place. First, the boundary conditions that an actual SCC slab would be subjected

to in the field must be replicated. Second, the concrete must be cured in a manner that will achieve reasonable shrinkage compensation, yet still be practical in large scale construction work.

1.3 Research Scope

In order to fulfill the goals of characterizing the length change, load development, and stress-strain behavior of restrained SCC specimens, it was necessary to define the scope of the research and lay out exactly what kind of and how many tests would be performed. A brief treatment is given here concerning the scope of the experiments, and the purposes that they serve in accomplishing the research objectives.

The main goal of this research was to characterize the strain behavior of SCC, which requires taking measurements of length change (whether expansion or shrinkage) over an extended period of time. In this experiment, strain data was gathered in two different ways. First, to comply with ASTM standards, strain data was gathered by hand according to ASTM's C-157 and C-878, which employ a manual dial gage used to measure 3"x3"x10" prisms. The second means used to gather strain data were Geokon® vibrating wire strain gages (VWSG). These devices were embedded into larger scale test specimens, and allowed long term, continuous measurement of strain, whereas the ASTM tests yield only a few discrete data points. This means that the VWSG data produces smoother curves that are based on a larger number of measurements.

Another step in this research was to determine how much load would be developed when the expansive concrete was cast against a stiff restraint system. This was accomplished by casting specimens which were later attached to load cells that

continuously monitored load development for the duration of the experiments. This leads directly into the last step of the experiment, which was defining the self-induced stress-strain relationship for SCC. By simultaneously gathering length change data and load development data, it was possible to create plots of the stress-strain behavior of SCC. The final requirement for adequately defining the scope of this experiment was to determine the number of specimens that would be cast. A prerequisite to determining the number of specimens was to consider how many distinct mix designs would be tested. In this experiment, the expansive cement used was called Komponent©, which is a type K cement that is used to replace a portion of the Portland cement in the mix. The percentage of Portland cement replaced with Komponent© (or Type K cements in general) governs how much the concrete will expand, and therefore how much of the net shrinkage will be offset. For this research, it was chosen to perform a series of 4 batches, each with a slightly higher percentage of Komponent©. Within each batch, several different types of specimens were cast; Table 1 summarizes the purpose and quantity of test specimens that were cast in each batch.

Table 1: Summary of Research Test Specimens

Specimens	Quantity (per batch)	Purpose
4x8 Cylinders	15	Compressive Strength
6”x12” Cylinders	2	Small-Scale Restrained and Unrestrained Expansion
C-157 Prisms	3	ASTM Unrestrained Expansion
C-878 Prisms	3	ASTM Restrained Expansion
4x48 Columns	3	Full-Scale Restrained Expansion and Load

Chapter 2 – Literature Review

2.1 Problem Statement

One of the single most serious sources of bridge deck degradation is due to water infiltration, resulting in problems like freeze-thaw damage, rebar corrosion, and sulfate attack (Phillips et al., 1997). Furthermore, the most common means for water to infiltrate the bridge deck is due to deck cracking. Deck cracking can be due to many factors, but the restrained drying shrinkage of concrete is one of the primary causes of cracking in bridge decks (Phillips et al., 1997). SCC offsets drying shrinkage by forming ettringite, an expansive gel that induces a volume increase when hydrated. This early age volume increase offsets the eventual drying shrinkage and decreases (or perhaps eliminates) overall shrinkage. Therefore, using SCC could substantially reduce shrinkage cracking, therefore reducing water infiltration and increasing the serviceable lifespan of bridges (Phillips et al., 1997).

Bridge decks are not the only useful application for SCC. Reducing degradation due to shrinkage cracking using SCC has also been accomplished for airport runway pavements, slabs on grade, and elevated structural slabs in buildings. Furthermore, SCC has been successfully used in applications with all kinds of reinforcement, including ordinary rebar, steel fibers, and post-tensioning. Cases like these where SCC has been used show the potential for this product to have broad application in all kinds of construction projects.

2.2 Practical Considerations

There are several practical considerations for working with shrinkage compensating concretes that must be observed if they are to be successfully employed in the field. First of all, in order for shrinkage compensation to occur, the ettringite must be adequately hydrated. This requires at least seven days of the concrete being saturated or "water cured." This fact was shown in a parametric study which compared Type K cement mixes with ordinary Portland cement mixes, and cured the specimens under a number of different environmental conditions, such as hot, cold, dry, and wet (Pittman at al., 1999). The study concluded that while temperature had a slight effect on the expansion of the specimens, the presence of moisture during curing was critical; while wet-cured Type K mixes all demonstrated expansion, dry-cured Type K mixes actually did the opposite and shrunk (Pittman at al., 1999). Therefore, the 7 days of saturated curing is considered an absolute necessity for proper shrinkage compensation in all SCC mixes, and is standard practice when this material is used.

A second consideration is that concretes made with Type K cement require some special attention when being placed. The set-time is slightly shorter, and the rate of slump loss is slightly greater for mixes made with Type K cement compared to Portland cement. This means that concrete mixes that are designed to provide shrinkage compensation must be placed and finished more rapidly than conventional ones (Pittman et al., 1999). A third consideration is that shrinkage compensation does not mean that the concrete never shrinks. As soon as wet cure is terminated, and the ettringite hydration ceases, drying shrinkage starts to occur. The early expansion, however, induces compression stress in the concrete at an early age. Once the shrinkage

sets in, the concrete is mature enough to better resist the commensurate tensile stresses due to restrained drying shrinkage (Pittman et al., 1999).

2.3 Advantages and Disadvantages of SCC

There are many important concerns about the behavior of concrete that go beyond shrinkage and expansion. Some properties of interest are durability, abrasion resistance, flexural strength, and modulus of elasticity, to name a few. SCC actually performs as well as, if not better than, ordinary Portland cement concrete in all of these properties. In addition, SCC actually costs about the same as regular Portland cement concrete (Moffat, 2005).

However, there are some disadvantages to the use of SCC. SCC does require some special considerations in regard to placing and curing. Due to set-time concerns, the Ohio Turnpike Commission (OTC) recommends that SCC should not be poured if the ambient air temperature is greater than 80 degrees Fahrenheit (Phillips et al., 1997). The OTC also says that casting SCC at elevated temperatures can result in reduced strength and lower maximum expansion. Additionally, some researchers claim that SCC is more vulnerable to warping strains than Portland cement concrete, although this claim is not widely held (Moffat, 2005).

Another obstacle that historically stood between SCC and widespread use in industry is delayed ettringite formation (DEF). DEF is a premature deterioration of calcium sulfoaluminate (CSA) cements that occurs when ettringite formation is suppressed; DEF is also referred to as internal sulfate attack. It is important to note that SCC made with Type K cement is a CSA based material. When DEF occurs, the paste matrix de-bonds from the aggregate, severely damaging the concrete. Two of the

primary causes of DEF are low water-to-cement ratios which do not provide adequate water to hydrate the ettringite crystals and excessive heat during curing, which tends to dry out the concrete before all the ettringite has hydrated. If an expansive admixture is added to the SCC, the potential for DEF is removed; unfortunately, expansive admixtures are currently somewhat limited (Moffat, 2005). As long as best practices are observed when it comes to casting and placing the concrete, however, DEF is not usually problematic. These best practices include keeping the temperature of the mix down and always making sure that an adequate wet-cure condition is initiated after the concrete is placed. Since Type K cement is a CSA-based cement, one might suspect that it would be affected by delayed ettringite formation. This is, in fact, not the case. Because of the way Type K cement is manufactured, the material is over sulphonated, so that the production of ettringite goes to completion. Therefore, there is no risk of delayed ettringite formation for Type K SCC (Ramseyer, 2018).

2.4 Case Study – Eskildsen et al.

Case studies are especially helpful in determining how well SCC performs in real-life scenarios outside the laboratory. One such case study is presented by Eskildsen et al. (2009), and it discusses the use of SCC on a large scale construction project for the University of Alabama. The project in question involved constructing a very large (~345,000 ft^2) residence hall whose structural system was a post-tensioned concrete frame. Challenges for the project included an inflexible timeline, a relatively tight budget, and a poor subgrade due to years of dumping debris. The design of this structure required a large concrete slab, with dimensions of 325 x 270 ft. (87,750 ft^2). Ordinarily, a single plate of this size would have required pour strips to prevent the

accumulation of tensile stresses, which will lead to the development of cracks. The design team made the decision, however, that the number of pour strips required would be impractical, too slow to construct, and unnecessarily costly. Instead the decision was made to utilize SCC for the slab, so that the slab would expand, offsetting the normal shortening action of the post-tensioning process, and therefore eliminating the need for pour strips altogether. This shortening during post-tensioning is due to shrinkage, elastic shortening, creep shortening, and temperature change. The goal was to offset the effect all of these factors by using the shrinkage compensating concrete. The mix design employed was based on an expected expansion of between 0.05% and 0.07%, which was expected to fully compensate for all shortening effects (Eskildsen et al., 2009).

After placing the concrete, several methods were used to ensure that it would remain completely saturated for the first 7 days, which is crucial for SCC to reach its full expansion. First, a monomolecular film was applied to the slab while it was being finished, in an attempt to reduce evaporation. Second, the slabs were covered with burlap which was coated in polyethylene. Finally, soaker hoses were run continuously within the burlap (Eskildsen et al., 2009).

In order to quantify the performance of the SCC slab, it was instrumented with Vibrating Wire Strain Gages (VWSG). One frame line of the building along with two test slabs were instrumented, and three ASTM 878 expansion prisms were cast per 100 cubic yards of concrete placed. The performance of the SCC slab was excellent; the slab expanded for the first 7 days, then began shrinking after that time. Specifically, the ultimate shrinkage for the SCC (125 microstrain) was far less than that expected from ordinary concrete (350 microstrain). Therefore, the strain that the slab would have

experienced was reduced by more than 50% by using SCC, which is a far greater reduction than can be achieved using pour strips. Ultimately, the most convincing proof that Eskildsen presents for the success of the SCC slabs is that more 420,000 ft^2 of concrete that was cast remains crack free, the project was completed under budget (due to the cost savings of eliminating pour strips), and the project was completed more than a month ahead of schedule. Finally, Eskildsen concludes that from the results of the project, SCC is both a satisfactory and economical alternative to pour strips – in other words, the expansive properties of Type K materials can offset the effect of shrinkage of various kinds even under stiff restraint, in this case giving them significant value in large-scale construction (Eskildsen et al., 2009).

2.5 Case Study – Rockford, IL Airport

Another case study that concerns the successful application of Type K SCC is the 1993 expansion of the Greater Rockford, Illinois airport. This relatively small regional airport serves in a supplementary capacity to the Chicago O'Hare Airport, a little over 65 miles to its west (CMT, 1995) The Rockford airport was being limited by the fact that it only had one primary runway long enough for larger jet aircraft, making it an undesirable option for much air traffic. For this reason, it was determined that one of the secondary runways should be extended, in order to provide the extra capacity.

Expanding the capacity of the airport was not the only goal, however. The Federal Aviation Administration (the FAA) had long desired to implement innovative pavement technologies on a larger scale, which would allow the number of joints to be reduced in airport runways. This is because these joints, which are created in both the longitudinal and transverse directions in order to combat drying shrinkage and paving

limitations, are often the weak link that result in the degradation of airport runways. The joints are continually stressed by aircraft, snowplows, and other ground equipment, and they serve as location where the ends of the panels can warp. As the joints degrade, they crack and spall, and the loose debris which is created can cause foreign object damage (FOD) to jet aircraft. These facts led the FAA to consider Type K SCC as an option for runway pavements. By offsetting early age shrinkage strains, cracking issues can be avoided, thus either obviating these joints, or at the very least allowing them to be spaced further apart.

The Rockford project required the runway in question to be extended approximately one-half mile (CMT, 1993). It was determined that this length of runway would be comprised of three distinct segments. The first segment was constructed with conventional Portland cement concrete pavement and was 561’ long by 75’ wide. Additionally, this segment was 15” thick and had joints spaced every 20’ transversely and every 18’-9” longitudinally. The second segment was constructed out of Type K SCC with 85 lbs of steel fibers per cubic yard of concrete; this segment was 900’ long and the same width. The fiber reinforcement allowed the thickness to be reduced to only 10”, and it also was used to eliminate longitudinal joints, assuming that the expansion of the concrete coupled with the fibers would suffice to prevent cracking across the width of the slab. The transverse joints were placed at a variable spacing of 85’, 100’, 150’, or 200’. Figure 1 shows a photo of the steel fibers in the runway pavement.

Figure 1: Airport Runway Slab with Steel Fiber Reinforcement at Greater Rockford Airport (Ramseyer, 2018)

The purpose of the third segment was to totally eliminate joints throughout the entire run of pavement. This segment was 1200’ long and only 7” thick and was constructed with the same fiber-reinforced SCC concrete as the second panel, but it was post-tensioned in the longitudinal direction from both ends so that tensile stresses could be further reduced to the point that joints would be unnecessary. Post-tensioning was not performed in the transverse direction because the cost would have been high, and it was believed that the fiber-reinforced SCC would sufficiently offset the tensile strains developed over a shorter span. Figure 2 shows a photograph of the runway pavement at the Rockford Airport. In the right hand side of the photo are the conventional PCC slabs with joints in both directions, and in the left hand side of the photo is the post-tensioned SCC slab without joints.

Figure 2: Airport Runway Slabs at Greater Rockford Airport (Ramseyer, 2018)

Historically, post-tensioned concrete slabs have been limited to around 400’ in length mostly because beyond that length it becomes difficult to deal with shrinkage accumulation. But by using SCC, pavement can be laid down continuously for as long as the pavement is being water-cured (up to 7 days) because shrinkage will not occur during that time period. This allowed the third segment to be post-tensioned over a 1200’ span, which meant it could be cast without any joints. One downside to casting a single segment this long was that large stresses were developed due to thermal effects. It was intended to deal with this problem by placing expansion joints at either end of the span, which would allow the slab to expand and contract freely with temperature changes. Unfortunately, the expansion joint froze for an unknown reason, resulting in the end of the slab tearing away from the expansion joint, as shown in Figure 3. The

resulting gap has been sealed to prevent further damage to the joint interface.

Figure 3: Separation of Post-Tensioned Slab from Expansion Joint at Greater Rockford Airport (Ramseyer, 2018)

These segments of the runway were cast sequentially during the summer of 1993. The conventional PCC pavement with joints was cast on July 15 and 16, the fibrous SCC pavement was cast on July 21 and 29, and the post-tensioned fibrous SCC

pavement was cast on August 9 and 10. All the pavement that was cast was instrumented with strain gages and thermocouples, which are instruments that measure temperature, in order to characterize the stress, strain, and movement of the concrete. In addition, funding was obtained for the project, so that the behavior and performance of the pavement could be monitored over a prolonged time period (CMT, 1993).

The pavement monitoring was conducted by performing non-destructive tests, mapping any cracks discovered in the concrete, and taking measurements from the instruments every 3 months (Herrin and Naughton, 2003). One of the major points of interest in the monitoring program was tracking the behavior of a large crack that had developed in the post-tensioned pavement shortly after casting. When this segment was cast, rain forced the casting to be temporarily halted, and then resumed later, leaving a cold-joint in the pavement. This cold-joint, coupled with a 90 degree Fahrenheit temperature swing in the pavement overnight after casting, tore a large crack in the pavement, approximately 7/8” wide (Chusid, 2006). This crack occurred before the post-tensioning had been applied to the pavement. When the post-tensioning was applied the day after casting was complete (August 11/12), the crack began to close and was sealed with epoxy. Figure 4 presents a photograph of this crack being sealed.

Figure 4: Transverse Crack Repair at Greater Rockford Airport (Chusid, 2006)

Once the crack was sealed and the post-tensioning was applied, this crack did not re-open. Overall, the monitoring program showed that the use of the innovative Type K pavements performed excellently. Researchers performed a holistic performance review of these pavements at the Rockford Airport in 2003, 10 years after construction. One of the metrics used to describe the pavement performance was the Pavement Condition Index (PCI), which is a 0-100 scale that defines the level of "wear" a pavement has experienced, with 100 representing the best possible performance. The control panels, cast with conventional PCC and the normal jointing, were observed to have spalled along nearly all of the transverse joints and were rated "good" with a PCI value of 67 (Herrin and Naughton, 2003).

For the innovative Type K fibrous and prestressed pavements, the PCI surveys could not be conducted directly, because guidelines did not exist for pavements of this sort. An equivalent PCI value could still be determined, however. The non-prestressed pavement with steel fibers had experienced both longitudinal and transverse cracking,

but was rated as in “very good” condition with an equivalent PCI rating of 82. The post-tensioned Type K segment with steel fibers had performed the best; with the exception of the aforementioned crack which was closed when the 1200 foot slab was tensioned, there were very few transverse and longitudinal cracks, many of which were difficult to perceive. Based on a crack definition formulated for bridge decks by Darwin at the University of Kansas, these do not meet the criteria to even be considered as cracks (Ramseyer, 2017). This is because Darwin’s definition says that a crack must be visible to the naked eye when looking at the pavement from waist height. Also, the 5-year performance review determined that the large crack that opened when the 1200 foot slab was tensioned was not growing. Based on the very low level of distress on the pavement, it received a PCI score of better than 98 (Herrin and Naughton, 2003). This nearly perfect score indicates excellent behavior and shows that the materials and methods used in this project, including SCC concrete, fiber reinforcement, and post-tensioning, worked as planned and have great potential for many other applications, both individually and together. It is also worth noting that since the installation of the new runway slabs, Rockford has become a UPS shipping hub for the Chicago area. The UPS hangar is adjacent to the new taxiway, so it now receives significant nightly traffic with heavily loaded cargo planes (Ramseyer, 2017). Therefore, the fact that the pavement is in such good condition is even more promising.

2.6 Effects of Mechanical Restraint

In order to be a truly effective asset in the real-world, SCC must be able to reach its full expansion potential, even if a very stiff internal or external restraint exists. This can include reinforcing steel, adjacent structures, or even friction acting on a slab on

grade. The behavior of SCC under restraint has been debated, and it is the subject of ongoing research.

In 1973, Henry G. Russell, while working for PCA, investigated the use of several shrinkage compensating cements. He determined whether they could adequately reduce shrinkage, given certain restraint conditions, including both internal reinforcement and external boundary conditions. Russell was one of the first researchers to investigate the effects of various types of restraint on the mechanical behavior of shrinkage compensating cements. Russell cast 4'x2' concrete walls that were either unrestrained to replicate a simply supported slab or fully restrained to replicate a slab adjoining another structural member. His fully restrained specimens were placed in compression using hydraulic rams, which were used to readjust the walls to zero length change every day. Additionally, in his experiments, Russell used Whittemore strain gages to measure the length change of his specimens (Russell, 1973). Figure 5 presents a photo of the test setup for Russell's vertical slab specimens.

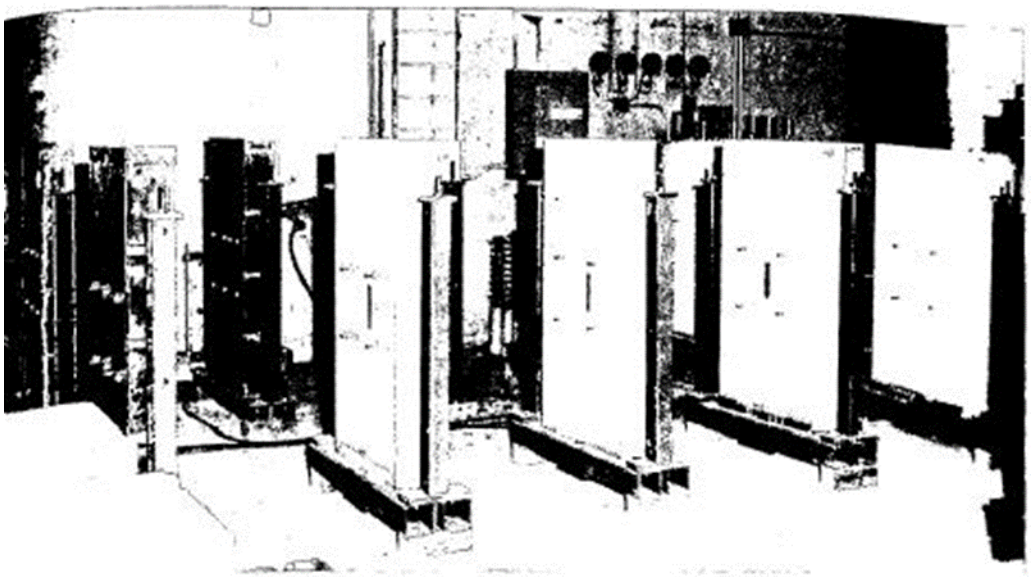

Figure 5: Vertical Slabs for Restrained Expansion (Russell, 1973)

In his study, Russell investigated three types of expansive cement; Type K, Type M, and Type S. Although all three are expansive cements that depend on ettringite formation, Type K is the only expansive cement used today. In addition to the large walls, Russell cast restrained and unrestrained prisms to measure expansive properties, and he cast cylinders to measure compressive strength. Russell concluded that there was virtually no difference in the expansive properties of the three different types of cement, and that the extent to which shrinkage could be compensated depended principally upon the degree of restraint, whether internal or external. He also concluded that full shrinkage compensation was only possible in very lightly reinforced slabs; therefore, a very stiff condition of restraint, Russell said, prevented the cement from fully compensating for shrinkage (Russell, 1973).

There have been other studies, however, whose conclusions stand in direct contrast to those of Russell. A study from 1973, performed by J.A. Hanson et al., discusses the usage of shrinkage compensating cements. In this study, the behavior of concrete specimens cast using ordinary Type I Portland cement was compared to that of specimens cast using Type M shrinkage compensating cement. It is important to note that although this research presents some insightful conclusions, it was performed using Type M cement; therefore, its behavior will not be identical to that of Type K, but it is analogous since both cements rely on ettringite for expansion. The testing program utilized both restrained and unrestrained specimens. The specimens were prisms, 6”x6”x30” and were cast vertically. For the restrained specimens, a hydraulic ram was used to apply an axial compressive force to the specimen, such that the net length change of the specimen would be zero. This replicated a fully restrained condition,

similar to the way Russell restrained his specimens. The unrestrained specimens included the same prisms without the restraint mechanism, as well as 6”x12” cylinders. Hanson arrived at several important conclusions. First, he determined that the use of shrinkage compensating cement offsets the effects of early-age shrinkage due to drying, even when a degree of restraint is provided that far exceeds what the specimen would face in the field. Second, he concluded that the reason shrinkage compensating cements are effective at reducing early-age drying shrinkage is because they delay the onset of the development of tensile stresses. Importantly, Hanson’s final conclusion was that using Type M shrinkage compensating concrete should provide structures that have fewer cracks (Hanson et al., 1973).

Between the fall of 2011 and the spring of 2013, Douglas Richardson et al. conducted an experiment which studied the effect of using Type K cement on bridge deck cracking. This study entailed the construction of a concrete slab which was analogous to a section of a typical Illinois Department of Transportation (IDOT) bridge deck. The slabs constructed were rectangular, measuring 10’ x 7’, with a thickness of 8”. The slab was supported using two W10x79 steel girders each 10’ long and spaced 5’ apart. These girders were connected to the slab using shear studs which ran along the length of the girders, 1’ apart from one another. Steel C-channels (10 x 15.3) were used around the perimeter of the slab which acted first as formwork for the slab and second to represent the mechanical restraint that adjacent slabs would provide in the real world (Richardson et al., 2014). The reinforcing steel within the slab was tied into these C-channels using epoxy. The test setup utilized in this experiment is shown in Figure 6.

Figure 6: Test Setup for Experimental Bridge Deck (Richardson et al., 2014)

As can be seen in Figure 6, the internal reinforcement of the bridge deck consisted of two layers of rebar. The top layer of rebar was placed 1” from the top of the deck, while the bottom layer of rebar was placed 2” from the bottom of the deck.

The testing program chosen by the researchers consisted of constructing two such bridge decks. The first bridge deck (the control) was cast with an ordinary IDOT Portland cement mixture, while the second was cast with a mixture containing Type K cement (at a replacement rate of approximately 16.5%). Each of the bridge decks were studied for 6 months. Table 2 displays the mixture designs for both the control and the experimental batches. The bridge deck is shown in Figure 7 following the addition of the concrete.

Table 2: Mixture Designs for Experimental Bridge Decks (Richardson et al., 2014)

	Control mix lbs./ft.^{3}	Type K mix lbs./ft.^{3}
Water	9.90	10.60
Cement (type I)	22.50	16.85
Cement (type K)	N/A	3.33
Fine aggregate	41.80	39.60
Coarse aggregate	67.60	67.80
w/c Ratio	0.44	0.52

Figure 7: Experimental Bridge Deck with Concrete (Richardson et al., 2014)

One important observation from Figure 7 is that there is apparently no provision for a wet cure of the bridge deck, which is critically important for SCC to be effective. Additionally, the authors make no mention of any kind of attempt to keep the surface of the slab saturated after casting. This fact proves important in considering and analyzing the results of this study.

After the test setup had been assembled, but before the concrete deck had been

cast, the reinforcing steel was instrumented with foil strain gages set as quarter bridges and thermocouples, which are devices used to measure temperature. The same pattern of instrumentation was used for both the control deck and the Type K deck. A total of twenty foil strain gages were placed throughout the deck, with more being placed on the upper rebar than on the lower rebar (since most relevant strains dominate in the upper region of the slab). These foil strain gages were placed in both the longitudinal and the transverse directions. Additionally, extra foil strain gages were also placed on both the top surface of the deck and on the steel girders supporting the deck. Figures 8 and 9 show the locations for the strain gages, on the top and bottom layers of reinforcement, respectively.

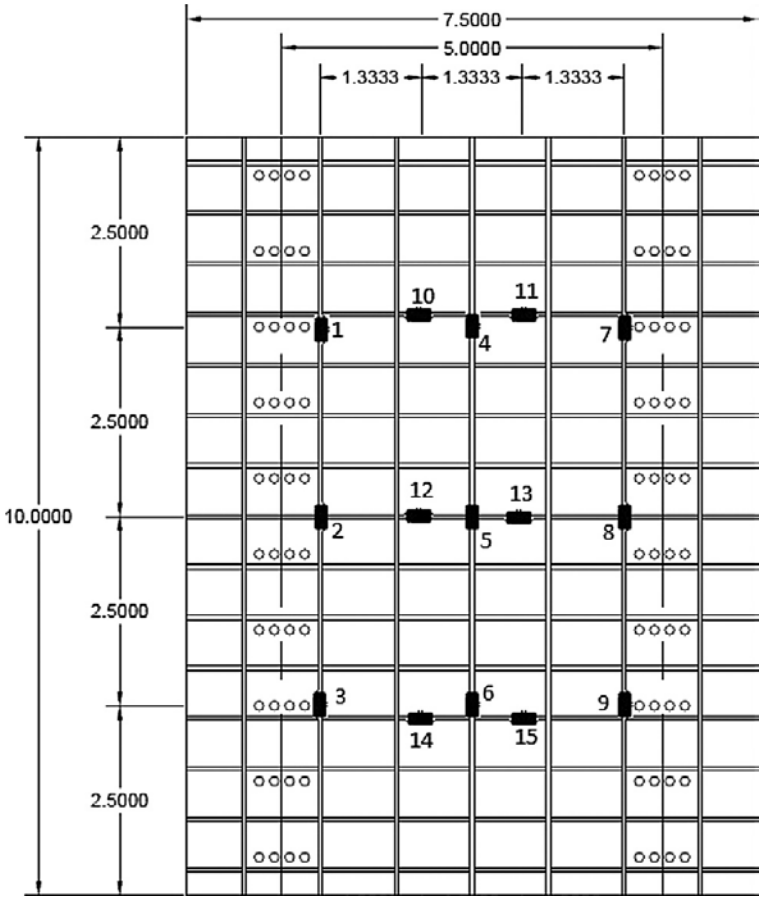

Figure 8: Locations of Strain Gages for Top Rebar (Richardson et al., 2014)

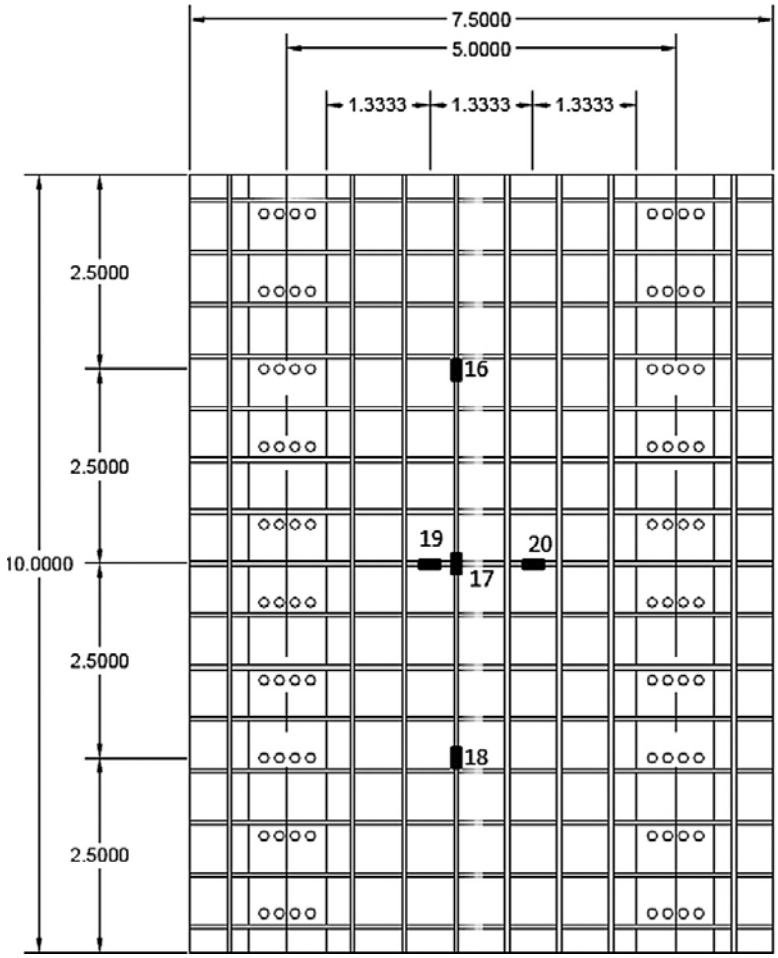

Figure 9: Locations of Strain Gages for Bottom Rebar (Richardson et al., 2014)

The only difference between the two slabs was their mix designs. Each one was instrumented the exact same way, and the slabs were even cast and monitored at the same time of year to account for temperature effects. It is worthwhile to note that the location of every strain gage in Figures 8 and 9 is also the location of a thermocouple. While standard ASTM tests like slump, air content, and compressive strength were also conducted, the most salient results come from the strain gage instrumentation of the slabs.

For the control slab (consisting of the ordinary Portland cement concrete) a zero point of 1 ½ hours after the completion of the pour was chosen as the zero point, and all strain values were normalized relative to this point. Unfortunately, quarter bridge strain gages do not compensate for temperature effects, and at 1.5 hours after casting, the heat of hydration would have elevated the temperature of the bridge panels. This means that the strain data presented in this work is likely incorrect. Virtually all of the strain gages throughout the slab displayed the same trend; a representative plot which shows this trend is presented in Figure 10.

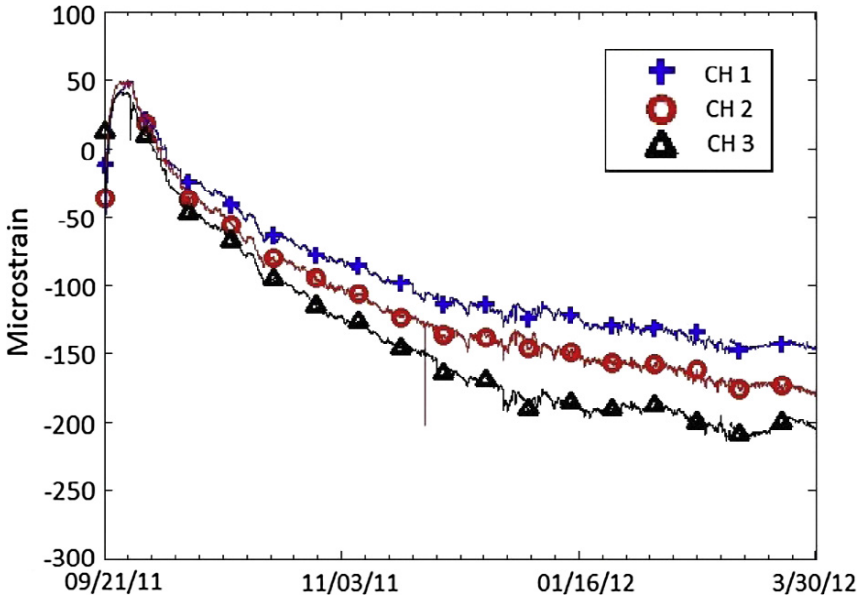

Figure 10: Strain Data for PCC Control Slab, Gages 1, 2, and 3 (Richardson et al., 2014)

In Figure 10, all positive strains denote tension, while negative strains denote compression (relative to the strain gage, not the concrete). Nearly all the strain gages throughout the slab behave like those in Figure 10; they initially spike upwards into tension at very early age due to expansion during the hydration of the cement, but then drying shrinkage quickly sets in and puts the gages in compression, resulting in negative

strains. For the top longitudinal rebar (those shown in Figure 6), the maximum expansion is around 50 microstrain, and gages 1 and 3 reach minimum strains of around -150 microstrain and -200 microstrain respectively.

For the slab cast with Type K shrinkage compensating cement, a zero point of 1 hour after the completion of the pour was chosen to normalize the data set. For both slabs this zero point was chosen arbitrarily to eliminate noise due to residual strains. Strikingly, all the plots of the strain data for the Type K slab show the exact same trend as those of the control slab. A plot that demonstrates the typical trend is shown in Figure 11.

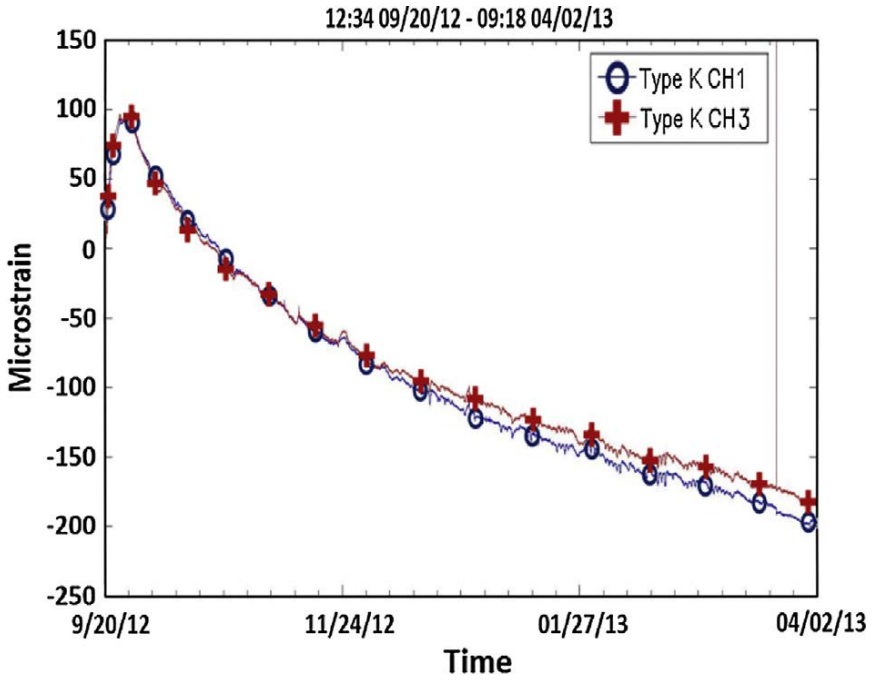

Figure 11: Strain Data for Type K Slab, Gages 1 and 3 (Richardson et al., 2014)

As Figure 11 shows, although the trend remains the same, the Type K deck experiences a higher initial expansion, which offsets some of the shrinkage, and therefore shifts the curve in the positive direction. Figures 10 and 11 show that for the

same gages (1 and 3), both in the same upper, longitudinal positions, the Type K slab expands around twice as much (100 microstrains compared to 50 microstrains for the control slab). Although this expansion dissipates rather quickly, the strain gages on the Type K slab remain 10-30 microstrain higher than their companions in the control slab by the end of the experiment. Additionally, it took a few weeks longer for the Type K slab to reach these strains than it did the control slab. Richardson concludes with the following points:

- The Type K cement caused an expansion in the experimental bridge deck 40-50 microstrains higher than that of the control deck. Although this effect has "worn off" by the end of the experiment (i.e. both bridge decks ultimately end up at the same degree of shrinkage), the Type K mix delays this shrinkage long enough for the concrete to reach mature strength.
- It took the Type K bridge deck 3 weeks longer to show signs of visible cracking, compared to the Portland cement bridge deck. Additionally, once these cracks were visible, they spread more slowly in the Type K deck.
- In order to link the results of the experimental analysis to a full scale bridge deck, further testing is required. The author hypothesizes that the difference in restraint between a real bridge deck and an experimental test setup could influence the degree of shrinkage compensation.

There were some issues with this research, however, that appear to have made the researchers fail to realize the full potential of Type K SCC. First, as to the issue of

the curing conditions of the slabs, it is absolutely imperative for SCC to be cured in saturated conditions for at least the first 7 days. The authors of the article do not explicitly mention whether or not this wet-cure was performed, and from visual evidence, it appears that it was not. In all likelihood, the slab was either not wet cured or it was not wet cured long enough because, as will be shown later, for a replacement percentage of more than 15%, the total expansion should be much higher than 100 microstrains. If the slabs were not wet cured, then this experiment demonstrates that the Type K cement can provide some degree of shrinkage compensation, even in adverse conditions when the product is not properly used.

Another concern with this work is the placement of the quarter bridge strain gages. In this experiment, the strain gages were applied directly to the reinforcing steel instead of being embedded in the plain concrete. This resulted in two problems. First, it caused the standard sign convention for tension and compression to be reversed, because expansion in the concrete (which causes compression in the concrete) causes tension in the reinforcing steel. More importantly, however, placing the strain gages on the reinforcing steel will result in flawed measurement of the strain in the concrete. Although the strains in the concrete and steel are theoretically the same according to strain compatibility, in reality, the strains will not be exactly the same unless the concrete is intimately bonded to the steel. By the time the concrete is mature that bond might be established, but during the early age of the test, when the concrete is still fresh, there will be no firm bond, the strains will be unequal, and therefore strain measurements gathered on the reinforcing bars will be fundamentally flawed. Another flaw that likely affected the strain measurements had to do with the foil strain gages that

were used. These types of measurement systems tend to have drift issues over long time periods, and they are usually applied in short-term experiments. The fact that they were used for several months likely resulted in the strain data being adversely affected.

Finally, the last issue with this research that will be discussed here pertains to temperature control. Any time that experimental research is being conducted on concrete of any kind, control of environmental factors is absolutely critical for the results to be accurate, consistent, and repeatable. The environmental factors that are typically the most important for concrete are temperature and humidity, and these conditions are usually controlled by casting the research specimens in some area that is insulated and air conditioned. In the experiment conducted by Richardson et al., however, the slabs were cast in an area which was neither temperature nor humidity controlled. This fact alone raises concern, but in addition, this experiment involved the comparison of the results from the Type K slab to the Portland cement slab. Since these slabs were not cast at the same time, they were exposed to different environmental conditions, affecting both the level of moisture and the temperature gradients throughout the slabs. This means that that important variables which affect shrinkage and expansion in concrete were not accounted for, potentially skewing the comparisons of the two slabs in the experiment.

In 2013, Dr. Chris Ramseyer and Seth Roswurm performed a set of experiments that were also concerned with studying the behavior of SCC under various forms of mechanical restraint. This was primarily because the ACI guide on shrinkage compensation, ACI 223, suggested in Chapter 5 that, if surrounded on all sides by a stiff boundary condition such as mature slabs or existing structure, SCC would be unable to

fully compensate for shrinkage (ACI 223). This hypothesis provided the impetus for the development of Seth Roswurm's testing program, which set out to show that stiff restraint will not materially hamper shrinkage compensation when using Type K cement (Seth Roswurm, 2013).

In order to dispute the assertion that a mature concrete slab would cause shrinkage compensation to be diminished, one of the major focuses of Seth Roswurm's research was to develop a testing apparatus which would reasonably simulate a slab-on-slab interaction. The prevalence of the idea that the usefulness of SCC would be diminished by a stiff boundary condition was due in large part to the work of Russell in 1973. A real-life example of what this kind of slab-on-slab interaction would look like is shown in Figure 12.

Figure 12: Interaction of Mature Existing Slabs with Expansive Concrete (Seth Roswurm, 2013)

For several reasons, casting a full-scale slab of this sort would be difficult. The primary challenge would be that the mature slabs would have to be cast far ahead of the time that the expansive slab were cast. This would require a significant investment of time, as well as considerable cost to cast multiple full-scale slabs. Therefore, instead of attempting to cast many large slabs, Seth Roswurm designed a testing apparatus which would mimic this restrained condition in a much more controlled fashion. When reduced to two-dimensional behavior, the expansion of the slab results in the concrete being placed in axial compression due to the opposing reactions of the mature concrete

slabs. This effect is therefore analogous to a concrete column being acted upon by restraints above and below it, as shown in Figure 13.

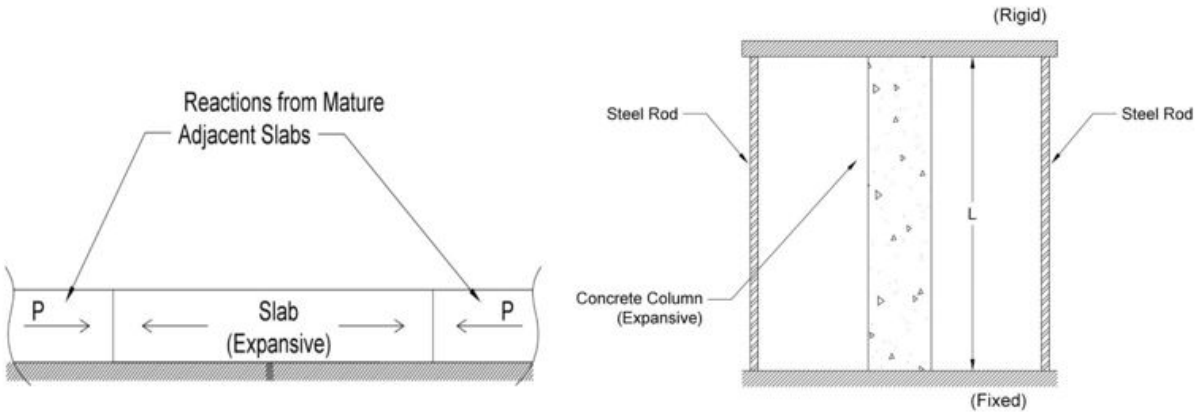

Figure 13: Comparison of Models for the Behavior of Expansive Concrete (Seth Roswurm, 2013)

The primary reason for using the simplified column model shown on the right side in Figure 13 is that the key variables in this experiment, the positive strain due to the expansive behavior of the concrete and the negative strain due to the axial compression on the concrete, need to be isolated. The following equation was derived by Seth Roswurm in his thesis research:

$$\varepsilon_{net} = \varepsilon_P - \varepsilon_C - \varepsilon_e - \varepsilon_{sh}$$ (Equation 1: Seth Roswurm, 2013)

where,

ε_p = potential chemical expansive strain

ε_C = creep strain

ε_e = elastic compressive strain

ε_{sh} = drying shrinkage strain

In this scenario, strain due to creep is ignored for several reasons. First, the duration of these tests is generally fairly short. Second, the force being exerted on the concrete is only caused by the expansion of the concrete itself. Hence, when the concrete ceases expanding and resumes drying shrinkage, the reaction force quickly dies off, and the possibility of creep is diminished. Third, although young concrete is more susceptible to creep, any effect of creep would be consistent across each set of specimens and would not affect the comparison of the trends significantly. In addition to the creep term being very small or entirely eliminated, the drying shrinkage term is zero as long as the expansion phase is still underway, and the concrete is being wet cured. Therefore, this experimental setup effectively isolates the relationship between the concrete's expansion and the boundary condition's restraint, until such a time as the drying shrinkage commences. Figures 14-17 show the apparatus that was designed to accomplish this purpose.

Seth Roswurm developed an analogy whereby the stiffness of a mature concrete slab that restrains an expansive concrete element can be reasonably simulated using a steel test frame as shown in Figures 14-17, equipped with four ⅝" diameter steel rods to restrain the expansive concrete column. In order to study the sensitivity of the shrinkage compensation to the degree of external restraint, he also fabricated test frames with less restraint (four ½" rods) and more restraint (four ¾" rods). Each mix design utilized was subjected to all three restraint conditions, and the effect on the concrete expansion was observed (Seth Roswurm, 2013).

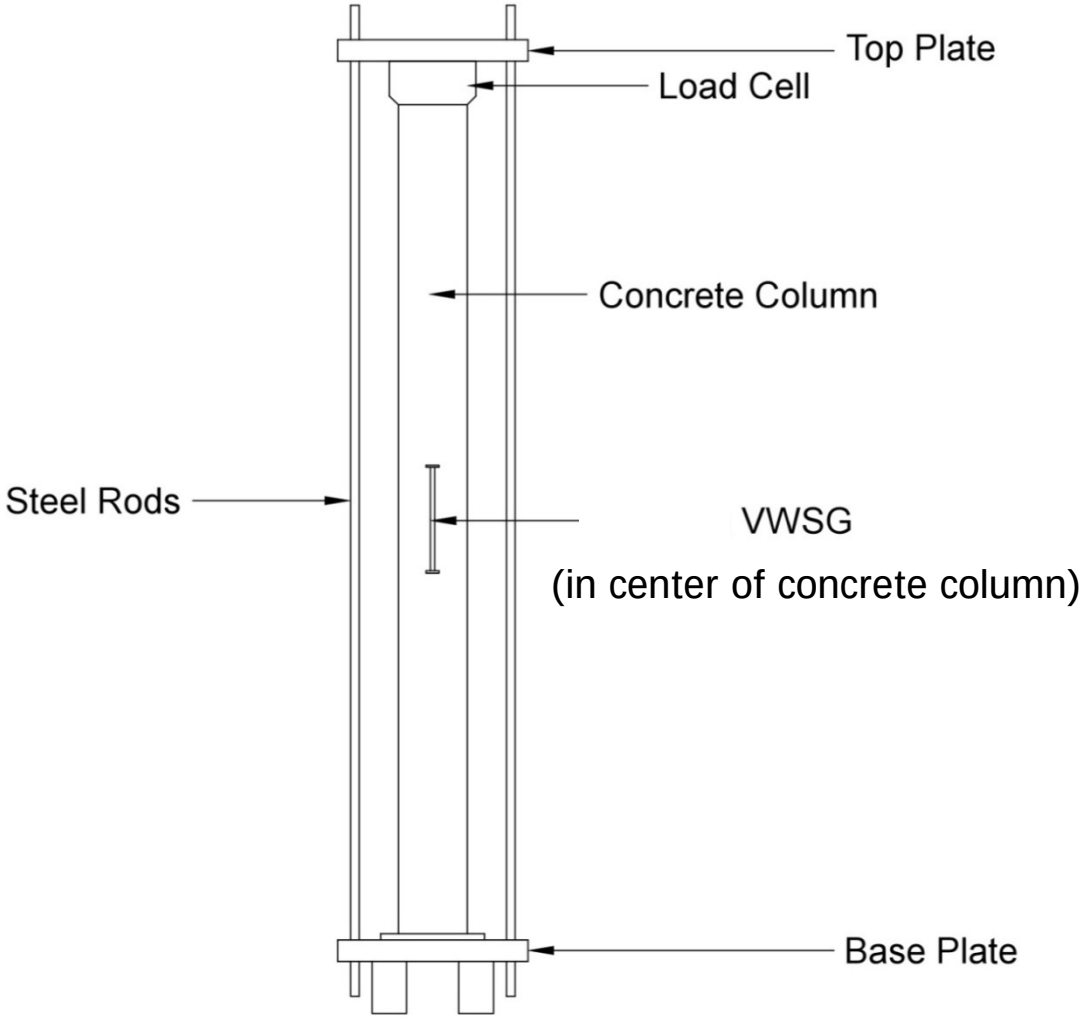

Figure 14: Profile View of Test Frame (Seth Roswurm, 2013)

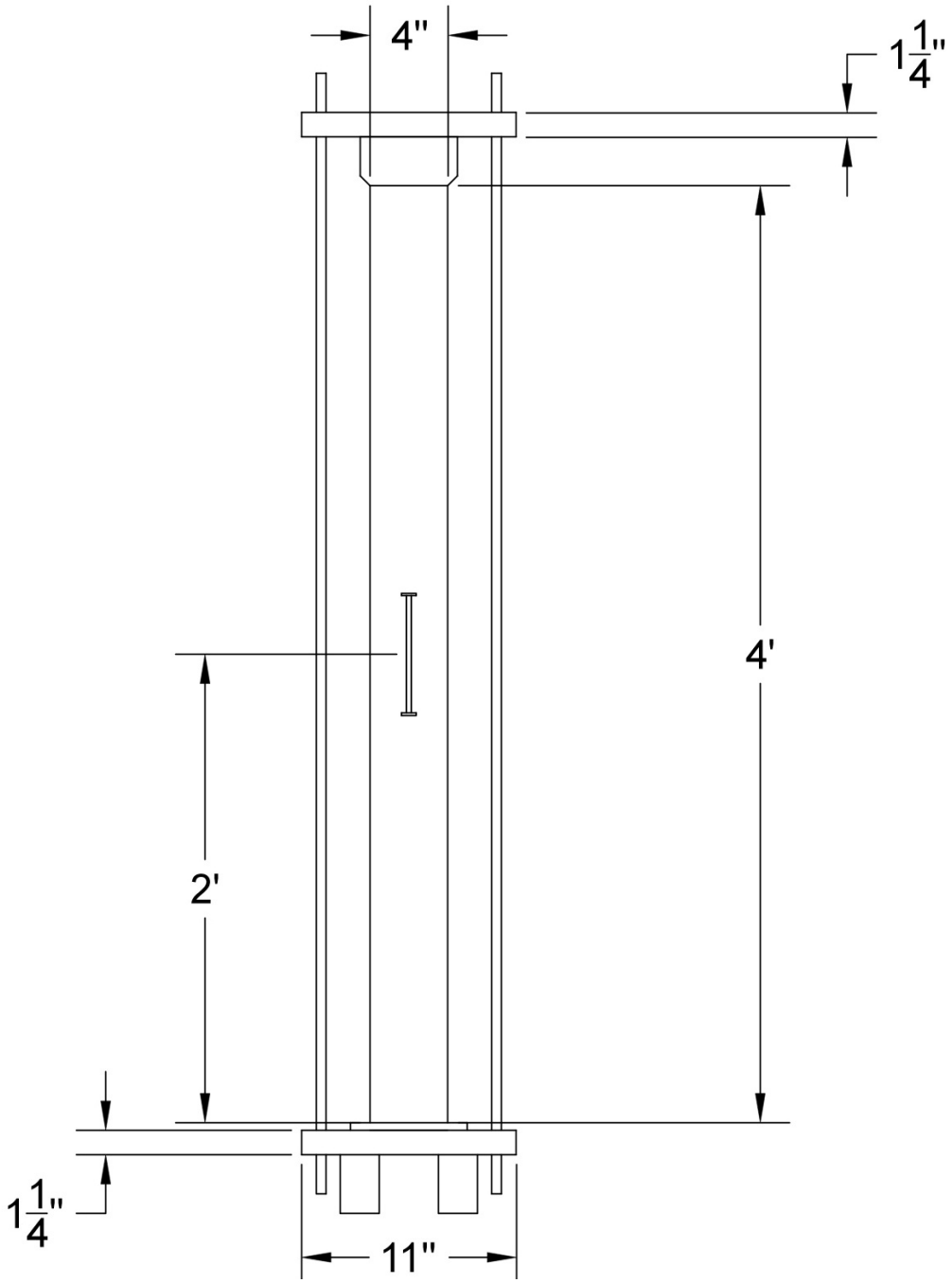

Figure 15: Profile View of Test Frame with Dimensions (Seth Roswurm, 2013)

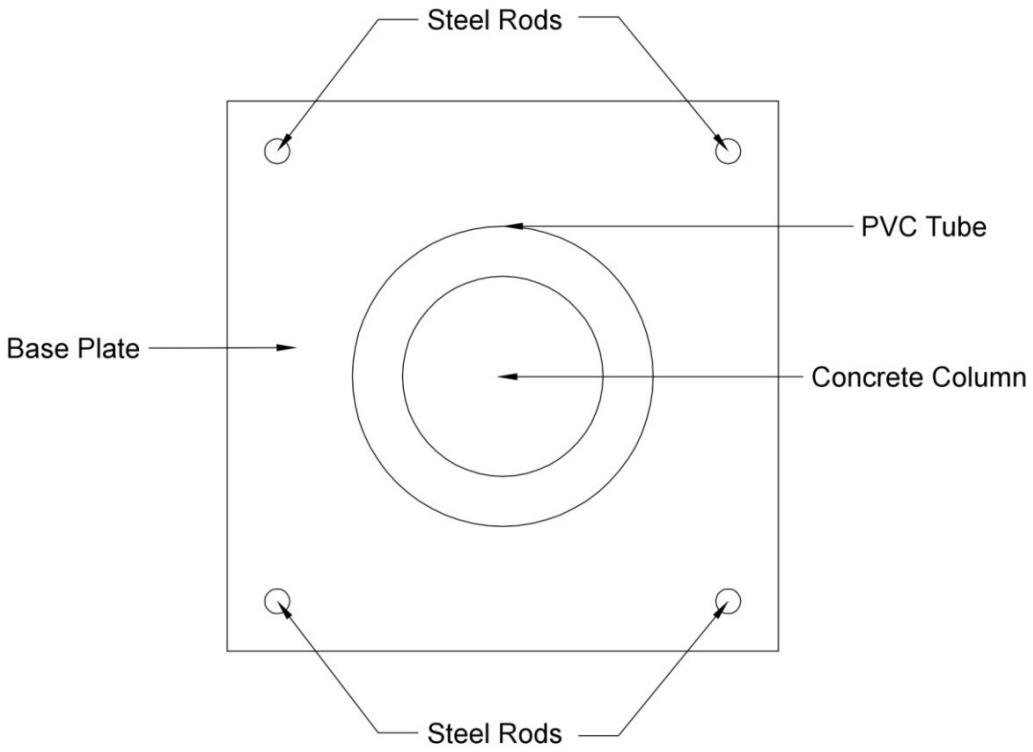

Figure 16: Plan View of Test Frame Base Plate (Seth Roswurm, 2013)

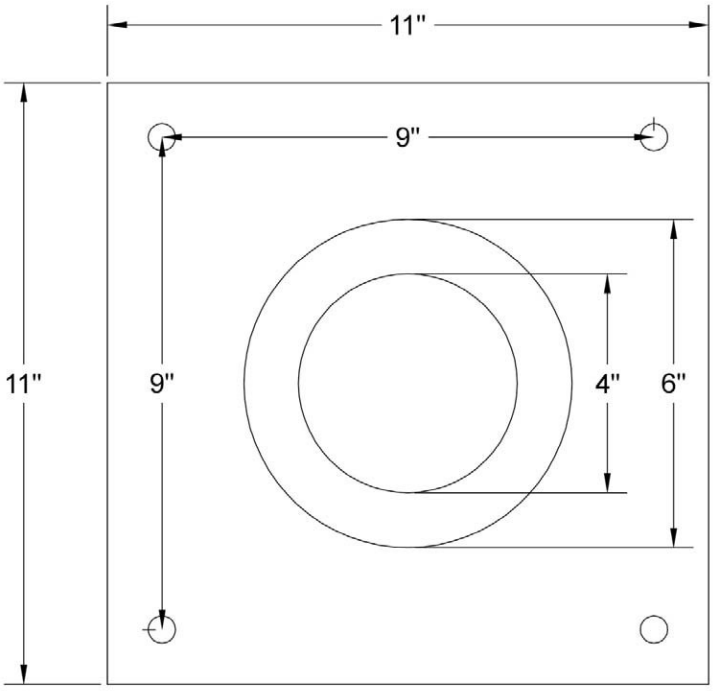

Figure 17: Plan View of Test Frame Base Plate with Dimensions (Seth Roswurm, 2013)

A photograph of the fully assembled test frame that Seth Roswurm used in his experiments is shown in Figure 18. The column specimens were cast with a Type K shrinkage compensating cement, using Komponent®. This additive was combined with the Portland cement in order to create an ASTM approved Type K shrinkage compensating cement. The concrete was cast into 4” diameter cardboard forms which were surrounded by a 6” PVC jacket. The columns were cured by flooding the jacket, which held the water against the column. These forms had to be removed by cutting the PVC and stripping away the cardboard. Some of the remnants of the cardboard can be seen on the column in Figure 18.

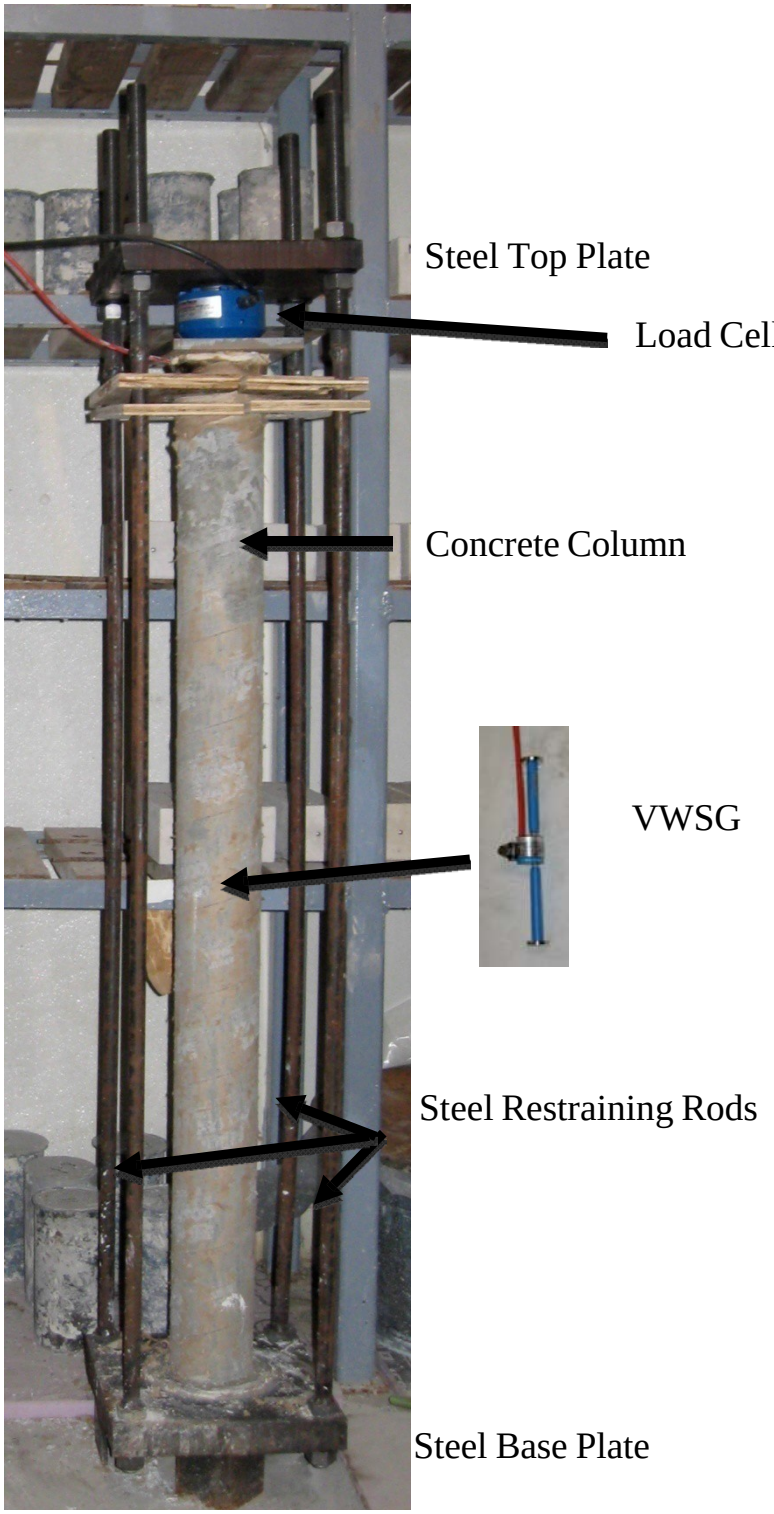

Figure 18: Fully Assembled Test Frame with Concrete Column (Seth Roswurm, 2013)

In this experiment, there were four sets of columns cast, each with increasing percentages of Komponent®. These batches used 15%, 17%, 19%, and 30% Komponent® replacement. Figure 19 shows the results obtained from the set of frames that contained the batch with 15% Komponent®.

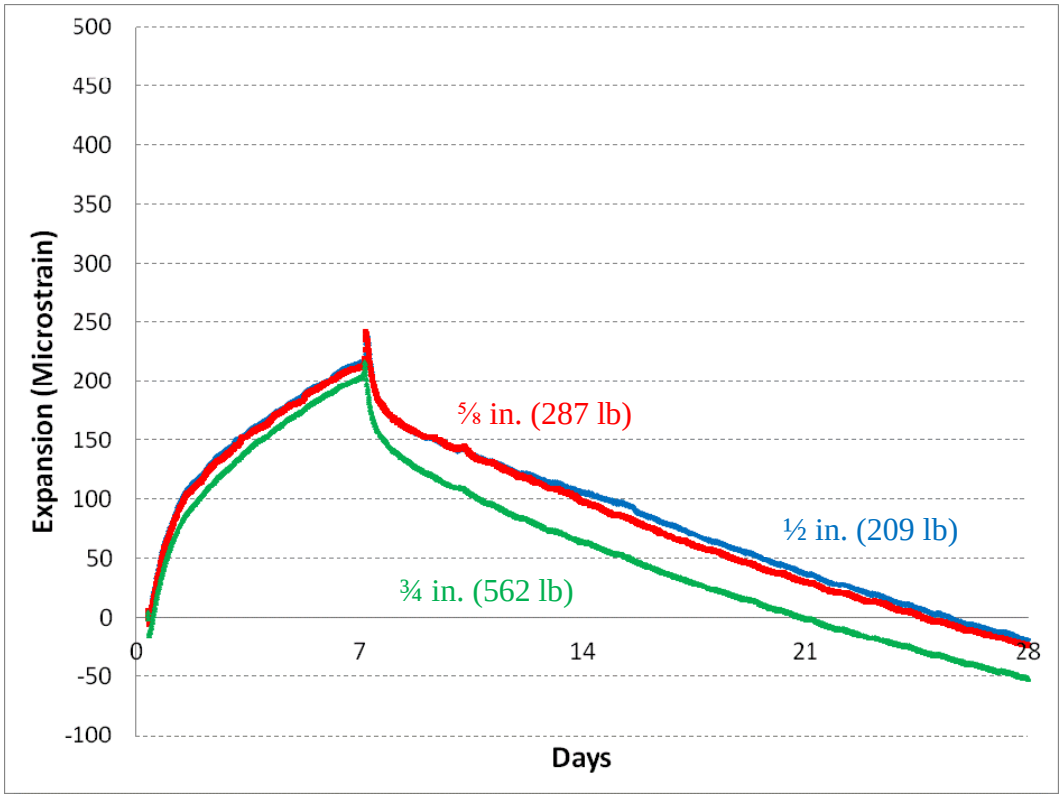

Figure 19: 15% Komponent Column Expansion Results (Seth Roswurm, 2013)

It should be noted that in Figure 19, the ½" and ⅝" curves are very close to each other, while the ¾" curve is significantly different. This may have to do with the significantly higher pre-compression load, or it may be due to more aggressive shrinkage caused by the stiffer restraint. There are several important conclusions that can be drawn from the results of the tests performed in this experiment. The first of these was the fact that increasing the percentage of Komponent® resulted in a corresponding increase in the expansion of the concrete, given the same level of

restraint. The second major conclusion is that for the same percentage of Komponent®, a higher level of external restraint generally resulted in a reduced degree of expansion; this trend is apparent in Figure 19. The column with the ¾" diameter rods (the stiffest external restraint) exhibits the least expansion, and it proceeds into the shrinkage phase more rapidly. The columns restrained with the ⅝" rods and the columns restrained with the ½" rods exhibit progressively higher expansions (though the difference between the two is miniscule) and they do not fall off as rapidly when shrinkage starts at 7 days (Seth Roswurm, 2013).

Another interesting behavior noted by Seth Roswurm in this research was the relatively slight impact that large changes in external restraint stiffness had on column expansion. Seth Roswurm points out in this work that the change in stiffness between the ⅝" restraint and the ½" restraint is 36%, and the change between ⅝" restraint and ¾" restraint is 44%. Yet it is apparent from Figure 15 that the gap between the curves is not necessarily strongly correlated to these differences in restraint, which may indicate that the relationship between expansion and restraint stiffness is not linear for this material. Based upon this observation, Seth Roswurm concluded that since large increases in external restraint stiffness have relatively little impact on shrinkage compensation, that the presence of stiff, mature concrete slabs will have little impact on the ability of a Type K SCC to offset shrinkage.

Although this work presented some very insightful conclusions, there were multiple issues that were brought up as recommendations for future work, in order to improve the quality of the data. First, the expected trends for the column expansion were skewed on several of the batches. It was proposed that one reason for this was that

the pre-compression loads (those loads induced on the column during installation of the top plate and load cell) were not carefully controlled, resulting in some columns receiving hundreds of pounds of load at time zero in the test. It was hypothesized that this influenced long-term expansion for the specimens.

The other primary recommendation for improvement had to do with the curing system. Since Type K SCC must be wet cured for the first 7 days after casting, the original test setup for this experiment utilized a 4” cardboard tube to cast the concrete column into, and a larger 6” PVC jacket placed concentrically around the cardboard tube. The PVC formed a reservoir which was filled with water to keep the column wet for 7 days. After the 7 day period ended, however, in order to achieve a dry condition, the PVC jackets had to be cut away, and the cardboard form, which had bonded intimately with the concrete column, had to be manually stripped away, bit by bit. This activity jostled the columns and caused temperature variations which created noise in the data, especially for the load development and the stress-strain curves. It was recommended that alternate methods be examined for the curing system, in order to improve the resolution of the data from the columns. Due to the issues which were encountered during the course of those 2013 experiments, it was intended for this work to improve upon the previous results for the restrained columns by decreasing or eliminating pre-compression loads, reducing physical trauma to the specimens, and adjusting the curing protocol.

Chapter 3 – Materials and Methods

3.1 Testing Overview

This testing program was designed to build upon that of Seth Roswurm's work in 2013, with several important improvements. The main changes that were implemented in this regard had to do with the 4" diameter restrained column specimens, which are the primary focus of this research. Other than the column specimens, there were many other specimens that were investigated in this research, including compressive cylinders, length change prisms, and length change cylinders.

3.1.1 Compressive Specimens

For this research, 4"x8" cylinders were cast for every mix in order to characterize the compressive strength of the concrete, in general accordance with ASTM C39. At least 15 specimens were cast for each mix so that cylinders could be tested at ages of 24 hours, 7 days, 14 days, and 28 days; each test consisted of the average strength of three cylinders. These cylinders were tested using the Forney compression testing apparatus at Fears Structural Engineering Laboratory.

3.1.2 ASTM C157, Unrestrained Expansion

Prisms were cast according to ASTM C157 for each mix design in order to measure the degree of expansion of the concrete with no external restraint. These prisms are 3"x3" square and have a single stainless-steel stud embedded in either end, so that the specimen can be read using a length comparator for the purpose of measuring its length change. The nominal length of the C157 prisms in this experiment was 11.25". Figure 20 shows a specimen of this type; note the end of the specimens where the stud can be seen in detail. Figure 21 shows the dial gage and comparator used to measure the

length change for all unrestrained prisms.

Figure 20: ASTM C157 Unrestrained Prism

Figure 21: Dial Gage and Length Comparator for Unrestrained Prisms

3.1.3 ASTM C878, Restrained Expansion

Prisms were cast according to ASTM C878 for each mix design in order to measure the degree of expansion of the concrete under a restrained condition. These prisms were 3”x3”x10”, but have a threaded rod embedded inside that is connected to steel restraint plates at either end. A stainless-steel acorn nut serves as the receptacle for the length comparator. Figure 22 shows a C878 prism, and Figure 23 shows the dial gage and comparator used to measure the length change for all restrained prisms. The primary difference between this dial gage and the one used for the C157 specimens is that this one has a wider receptacle to accept the acorn nut.

Figure 22: ASTM C878 Restrained Prism

Figure 23: Dial Gage and Length Comparator for Restrained Prisms

Both the restrained and the unrestrained prisms were tested according to the same schedule. For the first 7 days, while the specimens were cured in a water bath, the specimens were measured once a day. For the next 7 days, once the specimens were removed from the water bath, the specimens were still measured once a day. After that, readings were also taken at 21 days and 28 days.

The measurement procedures were the same for both the C157 and C878 specimens. The calibration rod was removed from the length comparator and was replaced by the specimen in its upright orientation. The top of the specimen was marked so that the same end pointed up on every reading. The specimen's length was read by choosing the value from the dial gage which was farthest counter-clockwise from the previous reading, while gently rotating the specimen in the length comparator.

3.1.4 Restrained and Unrestrained Expansion Cylinders

In addition to the C878 and C157 prisms, modified 6”x12” cylinders were utilized along with Geokon® vibrating wire strain gages (VWSG) to measure the expansion and shrinkage of the concrete. The VWSG’s used in this research are specifically designed for embedment in concrete, and the configuration of one of these instruments is shown in Figure 24.

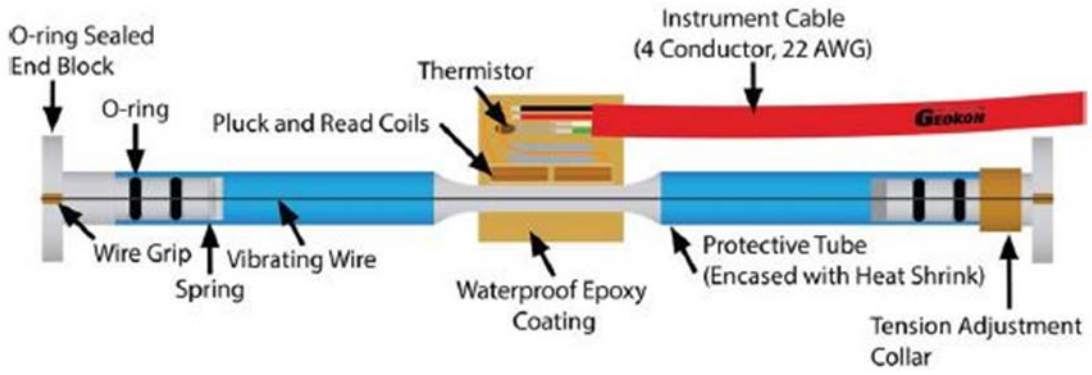

Figure 24: Cross-Section of Geokon VWSG (Geokon, 2017)

When placed into the desired orientation prior to casting, these instruments are then cast in place when the concrete is poured. The vibrating wire is plucked at specified intervals, and the frequency of the resulting motion is converted into a strain measurement. There are many advantages of using VWSG to measure length change compared to manual ASTM specimens. Primarily, the ASTM hand specimens are limited by the fact that they must be measured manually, which can only occur at certain discrete intervals (it is infeasible to read them more often than once a day). The VWSG, however, can take continuous strain measurements, as often as every 5 minutes, which greatly increases the clarity of the data and eliminates the need for constant handling of the specimens. An additional advantage of using the VWSG compared to

the ASTM hand specimens is that the VWSG eliminate the inherent user bias associated with the ASTM tests. This is due to the fact that performing the ASTM tests requires handling both the specimens and the dial gage, which can result in both physical and thermal disturbance. Also, the process of determining the length change by reading the dial gage carries an inherent user bias, meaning the same operator should perform all the readings. Even with one user, however, great care must be taken in order to avoid erroneous readings or disturbance of the sensitive length comparator. The VWSG, however, collect data constantly, without human intervention or handling, and without bias when taking measurements. Additionally, VWSG can measure strain with an accuracy of 1 microstrain, while the ASTM C-157 and C-878 tests have an accuracy of only 10 microstrain.

Due to these advantages, a test has been developed in previous research (Seth Roswurm, 2013) that is analogous to the ASTM restrained and unrestrained expansion tests that uses a VWSG to measure the strain over time. This test utilizes a standard 6”x12” cylinder mold with minor modifications to allow a VWSG to be suspended in the concrete. Similar to the ASTM tests, the unrestrained cylinder consists of plain concrete with the ends free of any constraints. An unrestrained 6”x12” with a VWSG installed is shown in Figure 25. At the stage of assembly shown in Figure 25, the cable ties holding the VWSG have not been tightened yet.

Figure 25: 6"x 12" Cylinder Equipped with VWSG for Unrestrained Expansion

This configuration is achieved by drilling holes in the cylinder which are diametrically opposed to one another and running cable ties through the holes from opposing sides. The VWSG is then run longitudinally through the four cable ties, which are then tightened down so as to hold the VWSG firmly in place in the center of the cylinder. The result is a VWSG centered in the cylinder with 3” of cover in all directions, including top, bottom, and radially. Figure 26 shows a top down view of the inside of the cylinder, where the VWSG runs through the cable ties.

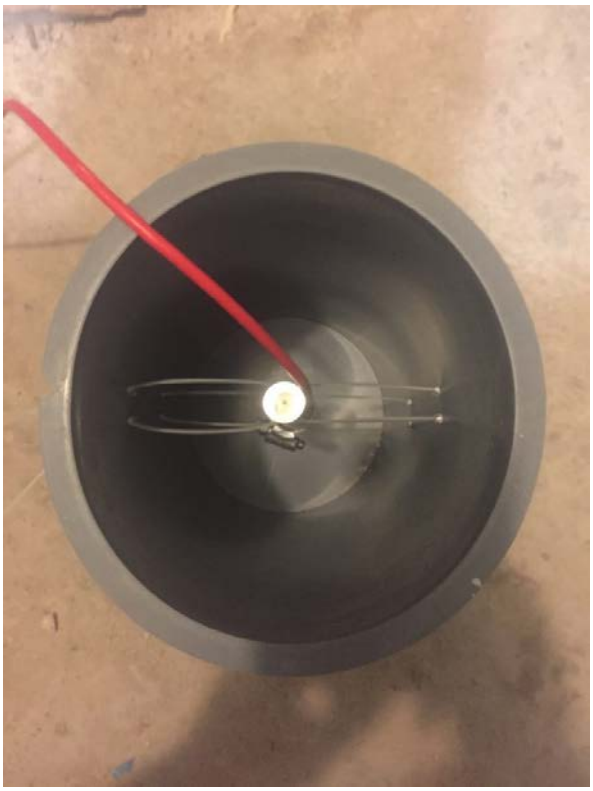

Figure 26: Top Down View of VWSG in 6”x12” Cylinder

Once the cable ties are tightened, as they are shown in Figure 26, the concrete is cast around the VWSG, and after the form is removed at an age of 24 hours, the cylinder is in a completely unrestrained condition, similar to an ASTM C157 prism.

The VWSG specimens for restrained expansion are created in a similar manner, with a few important modifications. In order to create a restrained condition, a threaded rod is run through the center of the specimen and is fastened to steel plates at either end (just like the ASTM C878 prisms), and the VWSG is still fastened in place with cable ties, in this case directly alongside the threaded rod. Figures 27 and 28 show what this configuration looks like.

Figure 27: 6"x 12" Cylinder for Restrained Expansion

In order to provide the necessary restraint, the bottom of the plastic cylinder mold is removed, and is replaced with a 6”x6” steel plate. The plate at the bottom of the form is fastened in place with duct tape which only serves to seal the bottom until the concrete sets. The plates at both the top and bottom of the form have holes drilled in them so that the rod can pass through. The rod is then held in place with nuts which are tightened until snug-tight. Since the intent of this test is to replicate the ASTM C878 test, the diameter of the threaded rod was chosen by matching the reinforcement ratio of a C878 prism. This diameter was determined to be most nearly 5/16” coarse-threaded rod. Figure 28 shows a top down view of the inside of a restrained cylinder assembly (VWSG is not pictured).

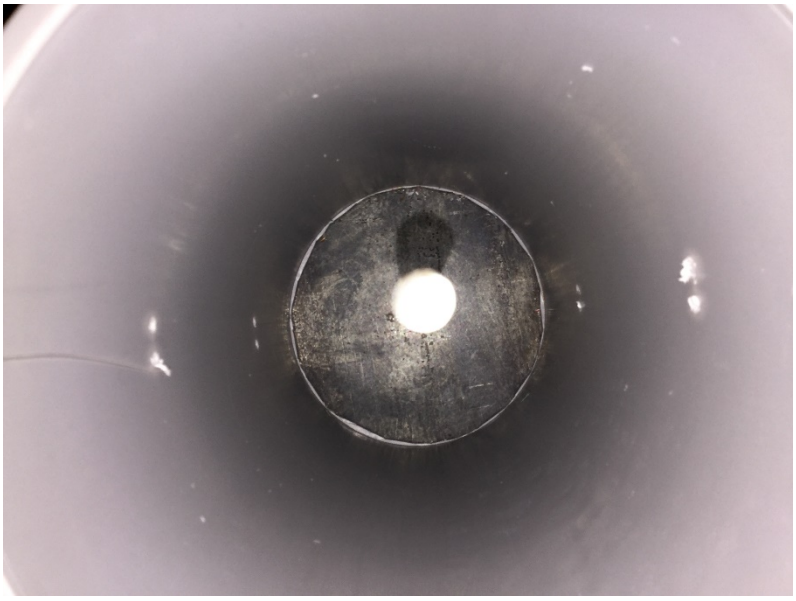

Figure 28: Top Down View of Restrained Expansion Cylinder

In Figure 28, the VWSG runs vertically alongside the threaded steel rod. Just like the unrestrained expansion cylinders, the plastic molds are removed from these specimens at an age of 24 hours, without disturbing the end plates. After cutting the duct tape at the base and stripping away the plastic, all that remains is the concrete cylinder with the VWSG and threaded rod embedded, and the steel restraint plates above and below, as seen in Figure 29.

Figure 29: 6"x 12" Cylinder for Restrained Expansion with Mold Removed

It is important to note that these unrestrained and restrained expansion cylinders were subjected to the same curing process as the other ASTM hand specimens and restrained columns. After they were cast, these cylinders were placed into 5-gallon buckets of water as soon as initial set was reached (typically this was around 6-8 hours after batching). As mentioned previously, the forms were stripped the next day, and the cylinders remained in wet cure for the first 7 days after casting, just like the other specimens. After 7 days, the cylinders were removed from the water and were set aside in the environmental chamber where they dried, and they remained at 73.4 degrees Fahrenheit and 50% relative humidity for the duration of the experiment (see Section 3.4 for more information on the casting and curing procedures). The variation in temperature in the environmental chamber was typically less than 2 degrees Fahrenheit.

3.1.5 Restrained Columns

The primary test specimens in this research were 4” diameter, 48” long restrained columns. Figures 10-13 present schematics that show the specifications for how these columns were assembled. Shrinkage-compensating concrete (SCC) must be wet-cured for the first 7 days after casting to hydrate and expand properly. For the small-scale test specimens, this was easily done by simply submerging them in a tub or bucket large enough to cover them in water. For the restrained columns, however, establishing a streamlined curing system was difficult because of their size and their vertical orientation.

Seth Roswurm’s research (2013) utilized restrained columns with 4” inside diameter cardboard tubes, which were used as the formwork for these specimens. These cardboard tubes were placed inside larger 6” PVC tubes which were sealed to the base of the frame and acted as jackets. The space between the cardboard and PVC tubes was then filled with water, which was contained by the PVC but soaked through the cardboard and hydrated the concrete (see Figures 12 and 13). The primary problem with this curing system, however, was the fact that the concrete intimately bonded to the cardboard form. But removing the cardboard proved to be extremely difficult because of how tightly the concrete and cardboard had bonded. This meant that the cardboard had to be stripped away bit by bit using hand tools; this process resulted in the columns being disturbed both physically and thermally, and the jostling of the specimens created noise in the data (especially for the load data, since it is measured on a very fine time increment).

Two alternatives were developed for improving the curing system for the restrained columns in this experiment. The first alternative was to modify the existing curing system. The cardboard forms and PVC jackets were used, but a ball valve was installed at the bottom of the PVC jackets, so that at the end of the first 7 days the valve could simply be opened, and the water would drain away. The cardboard forms would be left in place, removing the risk of damaging the columns or the data by removing them, and the columns would be left to dry gradually with the surface protected from direct evaporation. This alternative was used for the first two sets of restrained columns; for reasons that will be discussed later, this system was determined to be problematic, and was replaced in favor of the second alternative. Figure 30 presents a photograph showing the general layout of the first curing alternative, from Seth Roswurm's 2013 research; the only components of the system not visible in Figure 30 are the valves which were added at the base of the columns.

Figure 30: Curing Alternative 1, PVC Jackets with Cardboard Forms at Water Cure Stage (Seth Roswurm, 2013)

The second alternative for the curing system involved totally dispensing with the cardboard forms and PVC reservoir. The 6” diameter PVC jackets were removed, and the 4” inside diameter cardboard forms were replaced with 4” inside diameter PVC forms, which were split into halves down their longitudinal axis. The two halves were then placed in the restraint frame and were reassembled by using 6 stainless steel hose-clamps along the length of the PVC form. This meant that the forms were reusable and, as long as a form release agent of some kind was used, the PVC formwork could be easily removed after loosening the hose-clamps without disturbing the columns. In this alternative, the forms could not be removed until initial set was reached, at which time wet curing was initiated by turning on a series of micro-sprinklers that continuously

sprayed water on the surface of the restrained columns. Schematics showing the plan view of this configuration are shown in Figures 31 and 32.

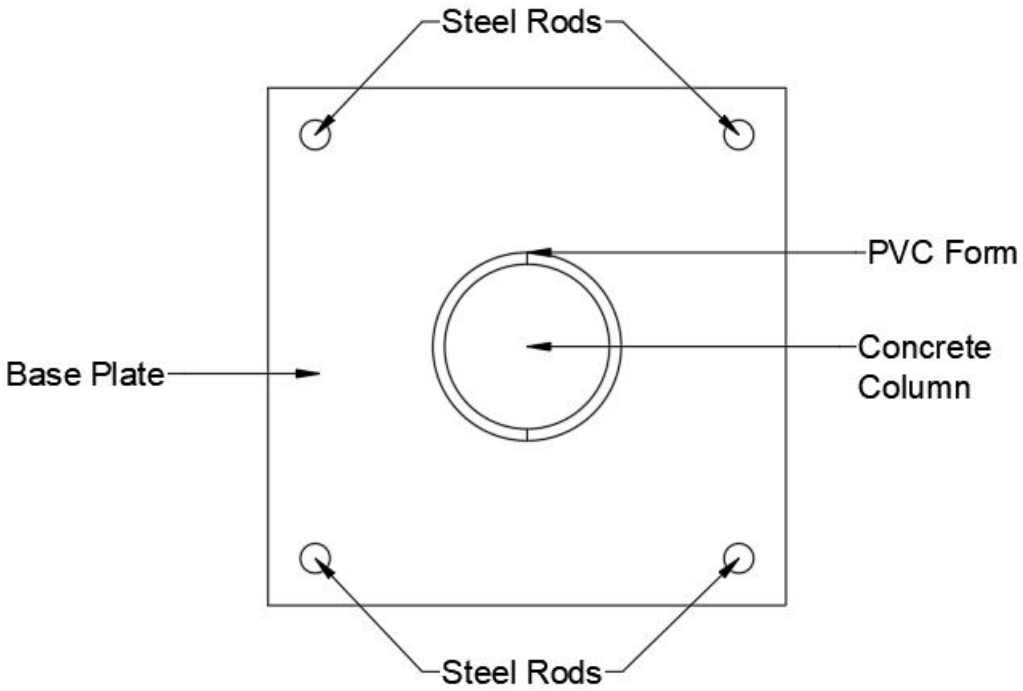

Figure 31: Plan View of Modified Test Frame Base Plate

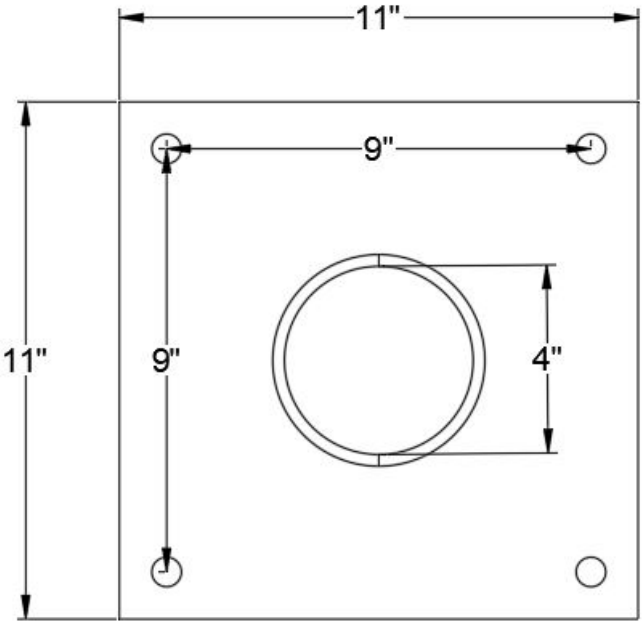

Figure 32: Plan View of Modified Test Frame Base Plate with Dimensions

For reference, Figure 33 shows a photograph of these forms in action. The two columns on the left have already had their PVC forms removed, while the column on the right still has its forms in place. To achieve the unmolded condition, the hose clamps need only to be loosened and removed, and the two halves of the PVC forms can be pulled gently away.

Figure 33: Curing Alternative 2, PVC Form with Hose Clamps at Form Stripping Stage

In Figure 33, thin plywood plates can be seen near the top of each column. The purpose of these plates is twofold. First, they hold the steel restraint rods square to one another. Since the restraint rods are more than 4’ long and are welded only at the base, the plywood plates prevent them from racking. The plywood top plate also serves to stabilize the columns. During early age, prior to installing the load cell at 6-8 hours, the columns are vulnerable to lateral movement. The plywood top plates serve to help minimize any such movements.

After initial set was reached, and the forms could be removed, a sprinkler system consisting of ¼” diameter plastic hose attached to 5-7 gallon per hour (gph) fogger/mister attachments was strung from column to column, with a minimum of 3 fogger/misters on each column. This configuration resulted in the columns, now totally

free of obstructions, being continuously drenched throughout the 7 day wet cure period. Plastic sheets were arranged around the test frames during the wet cure period to prevent direct overspray from the misters touching other specimens. Figure 34 shows how the sprinkler system was arranged to wet cure the restrained columns, and Figure 35 shows a close-up of the misters in action.

Figure 34: Restrained Columns Equipped with Sprinkler System for Wet Cure

Figure 35: Close-Up of Sprinkler System in Action

The primary disadvantage of this alternative was that the water being continuously sprayed in the environmental chamber caused the relative humidity to spike to 70-80% for the wet cure period, every time a set of columns was cast. This had the tendency to skew the shrinkage or expansion of other specimens in the chamber that were intended to be curing at 50% relative humidity. Another drawback was that if the spigot supplying water to the sprinkler system was turned off and not reactivated soon enough, the columns would dry out prematurely, which would adversely impact the results. After deliberation, however, this alternative was used for all the restrained columns after the first set because it caused no jostling or disturbance to the columns, and it provided much smoother and more reasonable data.

The testing heads, which are shown at the tops of the columns in Figure 34, consist of a 2” thick steel plate affixed to the load cell, which together weigh upwards of 50 lbs. When the nuts are tightened to bring the load cell into contact with the top of the column, which is covered in a gypsum cement leveling compound, a substantial amount of additional force can unintentionally be induced on the column. This occurred in Seth Roswurm’s research. Between the weight of the testing head and the compressive force from tightening the nuts to bring the load cell into contact with the top of the column, the resulting pre-compression loads ranged from around 200 lbs up to over 560 lbs. Seth Roswurm concluded that these pre-compression loads were adversely affecting the results of the experiments.

As a result, it was desirable to reduce or even eliminate these high pre-compression loads. This was achieved by carefully monitoring the load cell read-out while the test head was being installed. First, the data acquisition system was turned on and the adviser’s laptop was configured so that the load on the load cells could be monitored real-time. Next, the leveling compound was placed on the top of the first column, and then the test head was lowered carefully down the restraint rods until it was very nearly touching the top of the capping compound. See Figures 34 and 35; there are nuts above and below the restraint plate, and the nuts below the plate were set just above the top of the column. Finally, the nuts above the plate were tightened one at a time, and the nuts below the plate were raised or lowered until the load cell was firmly in contact with the column top.

The entire time that the adviser was engaged in the process of adjusting the test head into place, the author was monitoring the load cell read-out on the adviser’s laptop.

Every time the reading was updated (every 1 second or 10 seconds, depending on the sampling rate), the author called out the current load. In this manner, the adviser could tighten the nuts from above to achieve contact, but if a compressive load registered on the load cell, the nuts below the plate could be raised, in order to bring the load read-out back net zero. In this way, the nuts above and below the plate were adjusted one at a time, until the load cell was in intimate contact with the column leveling compound, and the compressive load on the column was very nearly zero (typically within a few lbs.). In this manner, any pre-compression loads were reduced by two orders of magnitude, when compared to Seth Roswurm's work. It was also noted that if the curing water misters were turned on before the leveling compound was completely hardened, some of the initial expansion was absorbed by deformation of the soft leveling compound.

3.2 Raw Materials

The raw materials used for the concrete in this experiment were identical to those used in ordinary concrete, with the only exception being the addition of a controlled amount of Komponent ®, the Type K cementitious material chosen to create the desired expansive behavior. Table 3 summarizes the nature of the raw materials used in this research, as well as the suppliers.

Table 3: Raw Material for Research

Material	Specifications	Supplier
Fine Aggregate	Dover sand meeting ASTM C33	Dolese Bros. Co, Norman OK
Coarse Aggregate	Number 67 crushed rock (limestone)	Dolese Bros. Co, Norman OK
Portland Cement	Type I/II Portland cement	Dolese Bros. Co, Norman OK
Type K Cement	Komponent®; shrinkage compensating additive	CTS Cement Corp, Cypress CA
Water	Ordinary tap water	City of Norman municipal water, Norman OK

3.3 Mix Designs

A total of four unique mix designs were utilized in this research; the only property that was varied for each mix was what percentage of Portland cement was replaced with Type K material (often referred to as percent replacement). The point of varying the percent replacement is to correspondingly manipulate the degree of expansion that the concrete exhibits. Every mix design used a 0.5 W/C ratio, and a total of 580 lbs of cementitious material per cubic yard of concrete. The four mix designs used Komponent at percent replacements of 15%, 17%, 19%, and 21%. A replacement percentage of 15% was chosen as the baseline mix design because it is typically considered the minimum when this material is used in industry. The mix design for each batch is summarized in Table 4; Note that all material quantities are shown in lbs/yd^3.

Table 4: Mix Designs for Research

Material	15% (lbs./yd^3)	17% (lbs./yd^3)	19% (lbs./yd^3)	21% (lbs./yd^3)
Portland Cement	493	481	470	458
Komponent	87	99	110	122
Total Cementitious Material	580	580	580	580
Coarse Aggregate	1772.6	1772.6	1772.6	1772.6
Fine Aggregate	1349.2	1348.2	1347.4	1346.4
Water	290	290	290	290
W/C Ratio	0.5	0.5	0.5	0.5

It is important to note that since the W/C ratio was held constant and the total cementitious material was held constant, Table 4 shows that the water in each batch was constant at 290 lbs/yd^3. This figure does not, however, represent the actual weight of water added to each batch, because the amount of mix water was adjusted for each batch based upon the measured moisture content of the aggregates.

3.4 Casting Procedures

The mixing, casting, and testing of all specimens studied in this research was performed at the University of Oklahoma Fears Structural Engineering Laboratory. The process for batch preparation and mixing was standardized in accordance with the appropriate ASTM standards and Dr. Ramseyer's standard operating procedures.

3.4.1 Batch Preparation

Anytime that a batch was to be conducted, the raw materials, including rock, sand, and cement, were removed from outside storage approximately 24 hours before the expected time of the batch. The rock and sand were stored in bins exposed to outdoor conditions, and they were therefore prone to variation in moisture content. When the rock and sand were gathered, representative samples were taken from the

gathered aggregate, and these samples were subjected to an oven-drying test during the 24 hours before the batch, so that the moisture content could be estimated. This process followed ASTM C566, the standard test method for determining aggregate moisture content. The moisture content of the aggregate was then used to adjust the batch quantities for the water to be added to the mix.

At the same time that the samples were taken for moisture content, the rock and sand to be used in the batch was separated into individual 5-gallon plastic buckets which were sealed with lids to avoid loss of moisture. Any cement that would be required was also placed into buckets and sealed. The required mix water was never measured out until immediately before the batch, so that leakage, evaporation, or spillage would not skew the W/C ratio.

3.4.2 Mixing Procedure

All concrete mixing occurred in the same portable concrete mixer at Fears Lab, outdoor, but underneath a protective awning. All concrete mixing was performed in general accordance with ASTM C192, the standard practice for producing concrete test specimens. The aggregate was placed in the drum first, alternating between adding equal buckets of coarse and fine aggregate, until all the aggregate was in the drum. The aggregate was then mixed thoroughly, and a small portion of the mix water was added. Once the aggregate was well blended, the cement was placed in the drum, alternating between Portland cement and Komponent® to make sure the cement was well-distributed throughout the mix. Finally, the remainder of the mix water was placed in the drum. According to ASTM C192, the mixing then proceeded for 3 minutes, the drum was stopped for the concrete to rest for 3 minutes, and then mixing was continued

for another 2 minutes (this process is referred to as a 3-3-2 mixing pattern). At this point, the mixing was complete, and the concrete was placed into wheelbarrows so that it could be distributed for casting the various specimens.

3.4.3 Casting and Curing Procedure

Once the concrete mixing was complete and had been divided up, so casting could begin, a complete battery of fresh testing was conducted. These fresh tests included measurement of slump, unit weight, entrapped air, and internal concrete temperature. The slump tests were conducted in accordance with ASTM C143, the unit weight tests were conducted in accordance with ASTM C138, and the entrained air was measured according to ASTM C231. The concrete temperature was measured using an ordinary probe thermometer which was inserted after the mixing was complete. In addition to fresh testing, outdoor environmental data (ambient temperature and relative humidity) were gathered for the exact date and time of the batch. This data was retrieved online from the National Weather Service local forecast office in Norman, OK. All fresh data and environmental data for each batch can be found in Appendix A.

At the same time that fresh testing was being conducted, the crew was also engaged in casting the research specimens. As shown previously in Table 1, these specimens included 4”x8” compressive cylinders, 6”x12” cylinders for both restrained and unrestrained expansion, ASTM C878 and C157 prisms for both restrained and unrestrained expansion, and 4”x48” columns for the primary restrained expansion specimens. Both the 4”x8” cylinders and the 6”x12” cylinders were cast following ASTM C192 for proper guidelines on tamping or vibration for consolidation, and the prisms were cast following the ASTM inherent to each of their names. Due to the length

and slenderness of the 4”x48” columns, internal vibration was the only feasible way to consolidate the concrete.

Every precaution possible was taken to ensure that the specimens were cast in a manner that would allow them to experience as little thermal variation or desiccation as possible at early age. The most vital specimens, the 4”x48” columns, were cast in the environmental chamber (the same location where all specimens were ultimately placed to cure). This was for two reasons; first, it was desired that, due to their criticality, the columns would be at a controlled temperature and humidity from time zero, and second, because the column frames and data acquisition equipment were located in the environmental chamber and were not portable. Therefore, since the 6”x12” cylinders also were connected to the data acquisition system, they were also cast in the environmental chamber. Because of limited space in this area, the remainder of the specimens, including the 4”x8” compressive cylinders and the ASTM prisms, had to be cast outside under to covered awning area. This posed no issues for the compressive cylinders, since any effect on strength due to early age exposure was not a concern for this experiment. On the other hand, great care was taken with the C-157 and C-878 prism specimens. These were cast as quickly as was practical, were then sealed with plastic wrap to avoid loss of moisture, and they were moved into the environmental chamber as soon as possible. The maximum time that any specimens had to wait outside before being moved into the chamber was approximately 30 minutes.

The environmental chamber at Fears Lab was the storage location for all specimens used in this research, from the day of casting, up through the time at which the specimen was terminated and discarded. This chamber is an insulated, air-

conditioned, and humidity-controlled room which meets ASTM standards for curing, by maintaining the temperature at 73.4 degrees Fahrenheit, within approximately 1 degree, which meets ASTM C192, which allows up to a 3.5 degree variation. The chamber is also equipped with a dehumidifier that maintains the relative humidity at approximately 50% under normal circumstances.

Chapter 4 – Results

4.1 ASTM C157 Unrestrained Expansion

Figure 36 shows an overlay of the ASTM C157 unrestrained expansion data, gathered for all four mix designs. The curves are color-coded according to the percentage replacement of Komponent® for that batch; the red curve corresponds to the 21% replacement, the purple curve corresponds to the 19% replacement, the green curve corresponds to the 17% replacement, and the blue curve corresponds to the 15% replacement. The initial reading was taken when each specimen was de-molded at an age of 6-8 hours. The variability in the time of the first reading was only due to space conflicts in the environmental chamber, because this was the same time that the columns were being capped.

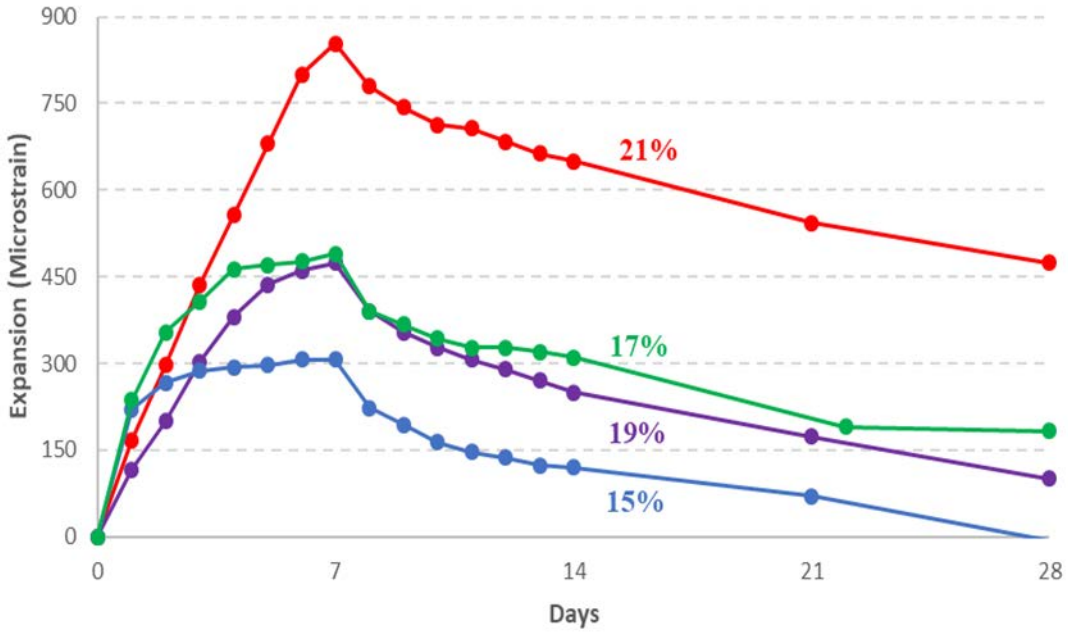

Figure 36: ASTM C157 Unrestrained Expansion Results

4.2 ASTM C878 Restrained Expansion

Figure 37 shows an overlay of the ASTM C878 restrained expansion data, gathered for all four mix designs. The color-coding scheme for these curves is the same as for Figure 36. These specimens were each initially read at an age of 6-8 hours, when they were de-molded.

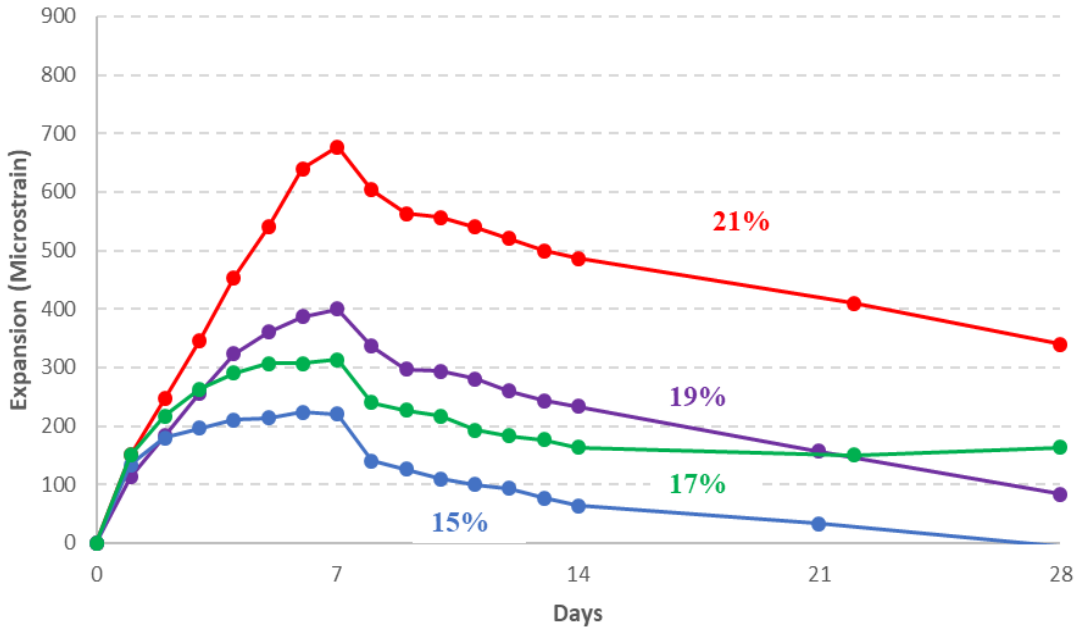

Figure 37: ASTM C878 Restrained Expansion Results

4.3 Unrestrained Expansion Cylinders

This section presents the data gathered by the VWSG's for the unrestrained expansion cylinders, for all 4 mix designs. The color-coding scheme for these curves is the same as for the previous figures. The curves shown are comprised entirely of continuous data points, except for those regions where the curve is thinner. In these locations, missing data (which occurs occasionally due to the memory on the data logger filling up or the battery running down) has been connected using straight lines. The strain readings for all 6"x12" cylinders were zeroed to the set-time of the concrete, which was approximately 6 hours after casting. Figure 38 presents the VWSG expansion data for the unrestrained cylinders, overlaid for all four mix designs.

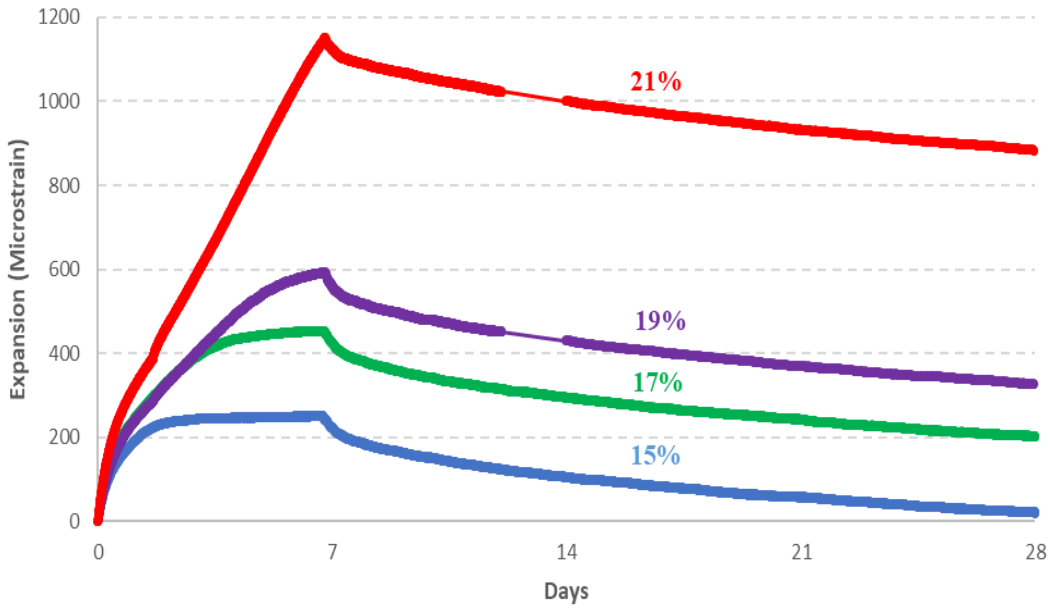

Figure 38: VWSG Unrestrained Expansion Cylinder Results

4.4 Restrained Expansion Cylinders

This section presents the data gathered by the VWSG's for the restrained expansion cylinders, for all 4 mix designs. The color-coding scheme for these curves is the same as for the previous figures. The curves shown are comprised entirely of continuous data points, except for those regions connected with straight line representing gaps in the data. The strain readings for all 6"x12" cylinders were zeroed to the set-time of the concrete, which was approximately 6 hours after casting. Figure 39 presents the VWSG expansion data for the restrained cylinders, overlaid for all four mix designs.

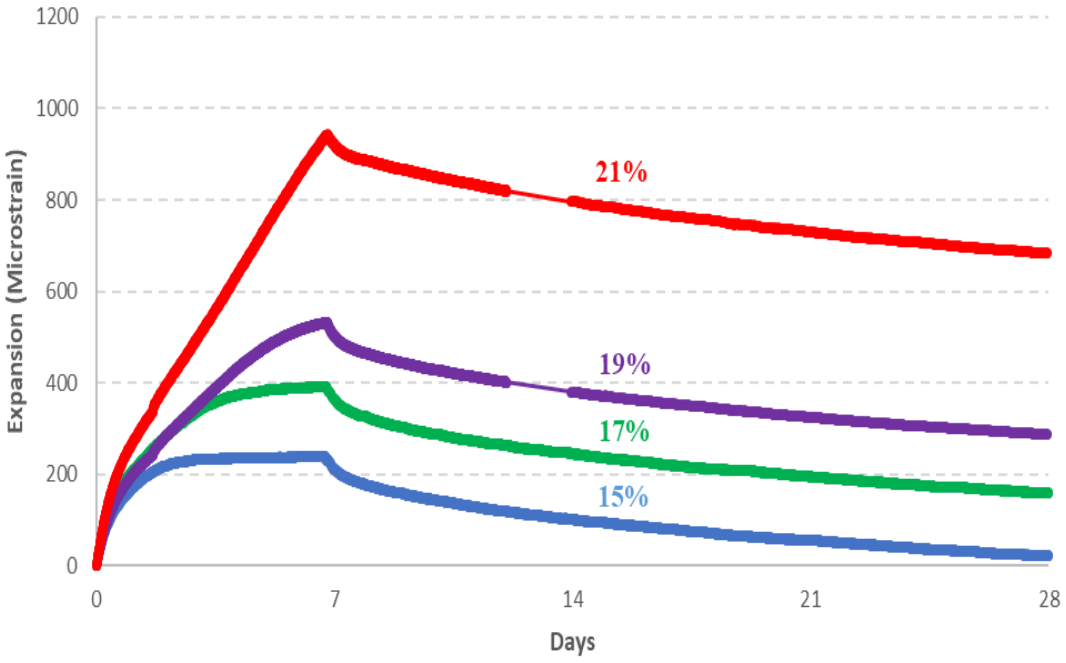

Figure 39: VWSG Restrained Expansion Cylinder Results

4.5 Restrained Column Expansion

This section presents the results gathered from the restrained column specimens. As previously mentioned, there were two different alternatives employed for wet-curing the columns, which are shown in Table 5. An x indicates that the curing alternative was used for a given mix, while hyphen indicates that the curing alternative was not used for that mix.

Table 5: Curing System Alternatives used for Restrained Columns

Curing System	Mix Designs			
	15% Replacement	17% Replacement	19% Replacement	21% Replacement
Alternative 1	X	X	-	-
Alternative 2	X	X	X	X

Alternative 1 involved leaving the cardboard forms in place and draining the water from the PVC jacket using a valve. Alternative 2 used removable PVC forms so that the columns could be sprayed with a micro-sprinkler system. The results from the first alternative will be presented first. The first curing alternative was determined to be unacceptable for this research, and it was discarded after preliminary batches with 15% and 17% Komponent® replacement. The second curing alternative (micro-sprinkler system) was used for all subsequent work.

4.5.1 15% Replacement - Cured with Cardboard Forms in Place

This section presents the results for the restrained columns, using the first curing alternative that was investigated. For a given percentage replacement, blue curves represent the columns under the lowest degree of restraint (1/2” rods), green curves represent the columns under the theoretical midpoint of restraint (5/8” rods), and red curves represent the columns under the highest degree of restraint (3/4” rods). These

curves are made up solely of data points collected from the VWSG's embedded in the columns, with the exception of areas where a straight line connects data points due to a gap in the data, as previously described. The strain values for these restrained columns were zeroed to the set-time of the concrete, at approximately 6 hours after casting. This also corresponded to the time that the load cells were installed, and the PVC jackets were filled with water. Figures 40-42 present the restrained column expansion data for the 15% mix for curing alternative 1.

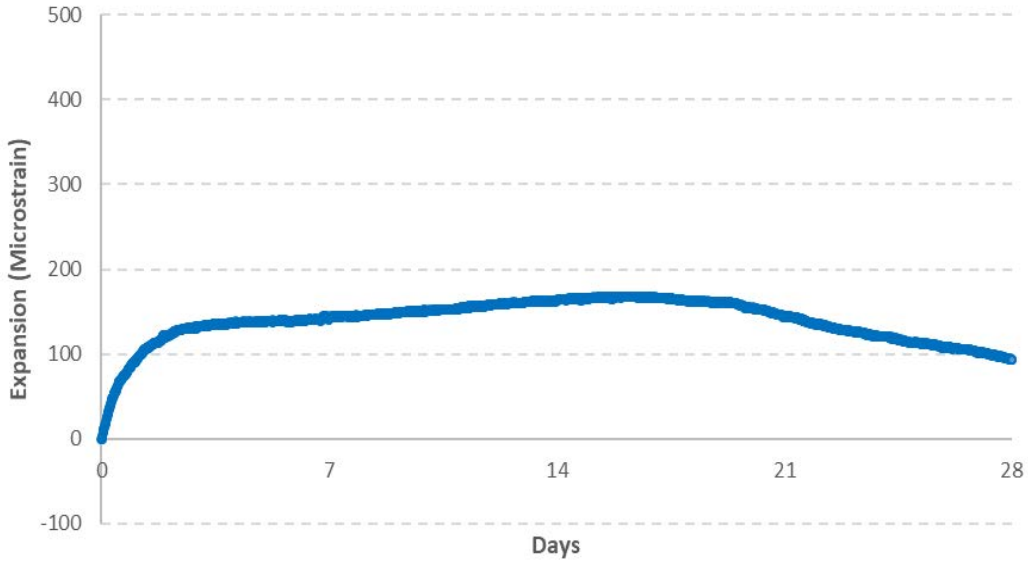

Figure 40: Restrained Column Expansion Results with Forms Left in Place (1/2" Restraint Rods, 15% Komponent)

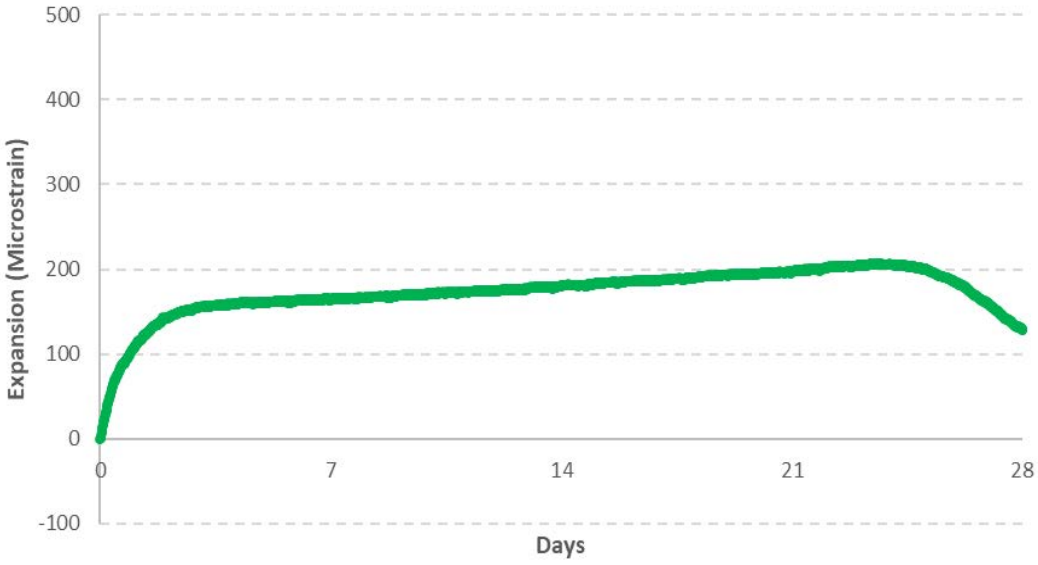

Figure 41: Restrained Column Expansion Results with Forms Left in Place (5/8" Restraint Rods, 15% Komponent)

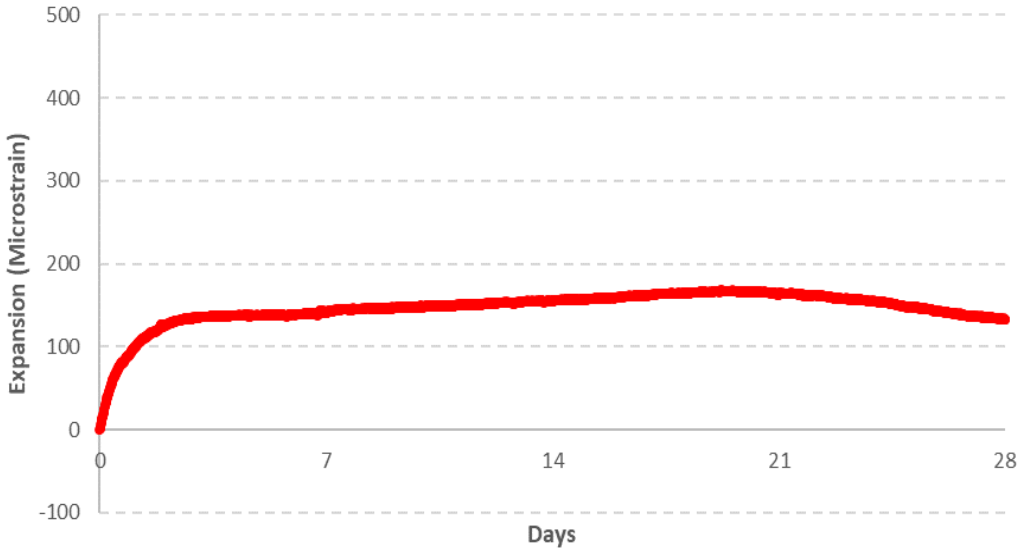

Figure 42: Restrained Column Expansion Results with Forms Left in Place (3/4" Restraint Rods, 15% Komponent)

4.5.2 17% Replacement – Cured with Cardboard Forms in Place

This section presents the VWSG data for the 17% Komponent® restrained columns cast with the first curing system. The color coding system is the same as what has been previously established. The strain values for these restrained columns were zeroed to the set-time of the concrete, at approximately 6 hours after casting. This also corresponded to the time that the load cells were installed, and the PVC jackets were filled with water. Figures 43-45 present the restrained column expansion data for the 17% mix for curing alternative 1.

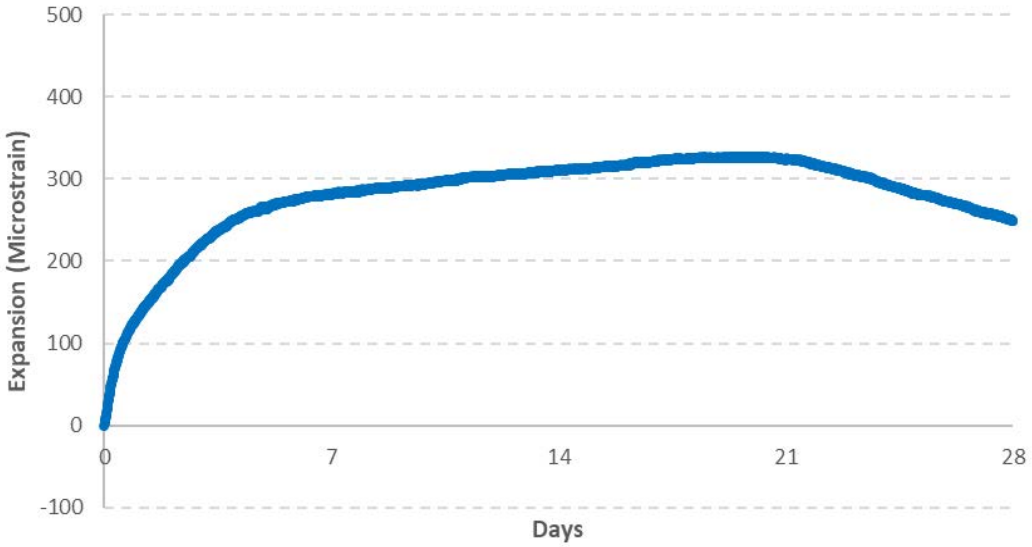

Figure 43: Restrained Column Expansion Results with Forms Left in Place (1/2" Restraint Rods, 17% Komponent)

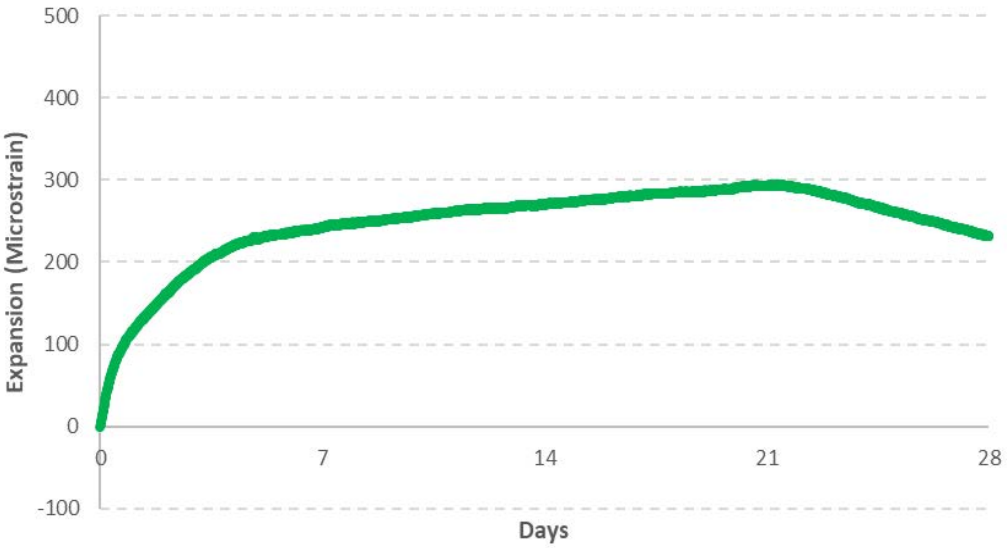

Figure 44: Restrained Column Expansion Results with Forms Left in Place (5/8" Restraint Rods, 17% Komponent)

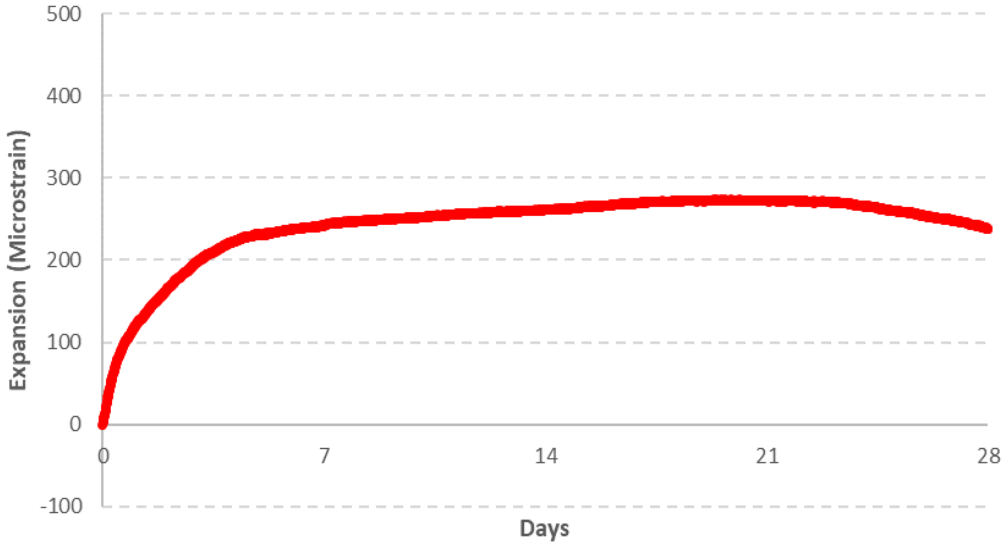

Figure 45: Restrained Column Expansion Results with Forms Left in Place (3/4" Restraint Rods, 17% Komponent)

The strain data produced from the restrained columns cast with curing alternative 1, which produced the curves in Figures 40-45, was influenced by unintended restraint from the presence of the cardboard forms. For this reason, curing alternative 1 was discontinued.

4.5.3 15% Replacement - Cured with Sprinkler System

This section presents the results for the restrained columns, using the second curing alternative that was investigated (removable PVC forms, allowing the concrete to be soaked with misters). This method proved superior to the first option, so it was used for the restrained columns for all 4 mix designs. For a given percentage replacement, blue curves represent the columns under the lowest degree of restraint (1/2” rods), green curves represent the columns under the theoretical midpoint of restraint (5/8” rods), and red curves represent the columns under the highest degree of restraint (3/4” rods). In addition, each curve has a label indicating its level of restraint. These curves are made up solely of data points collected from the VWSG’s embedded in the columns, with the exception of areas where a straight line connects data points due to a gap in the data, as previously described. Even where it appears that the data ends and a straight line continues on, that data has not been extrapolated; it picks back up again off the frame of the plot. Longer term data is supplied in Appendix D. The strain values for these restrained columns were zeroed to the set-time of the concrete, at approximately 6 hours after casting. This also corresponded to the time that the load cells were installed, and the micro-sprinklers were turned on shortly thereafter. Figures 46-48 present the restrained column expansion data for the 15% mix for curing alternative 2.

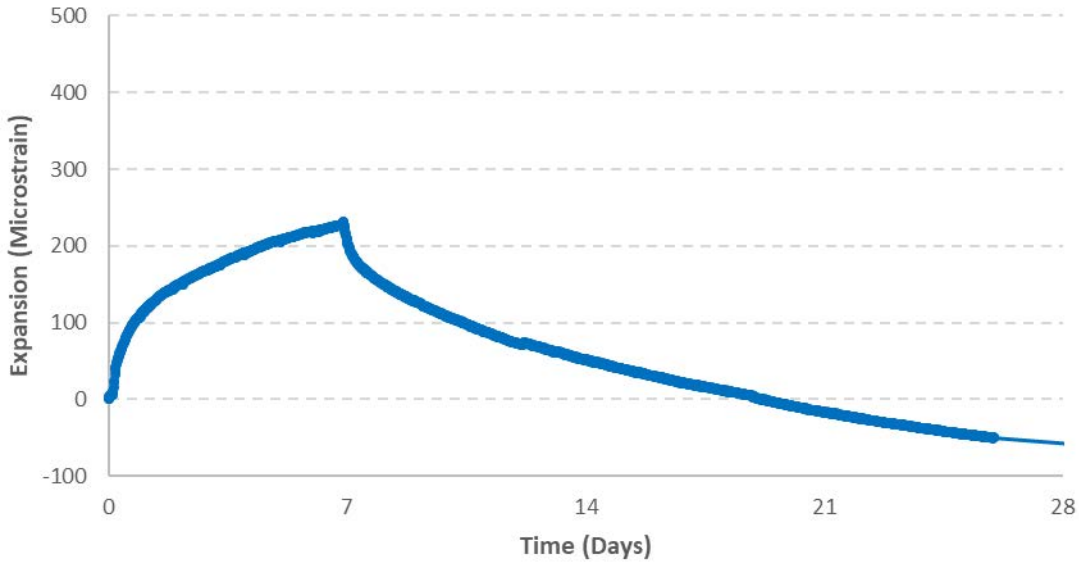

Figure 46: Restrained Column Expansion Results (1/2" Restraint Rods, 15% Komponent)

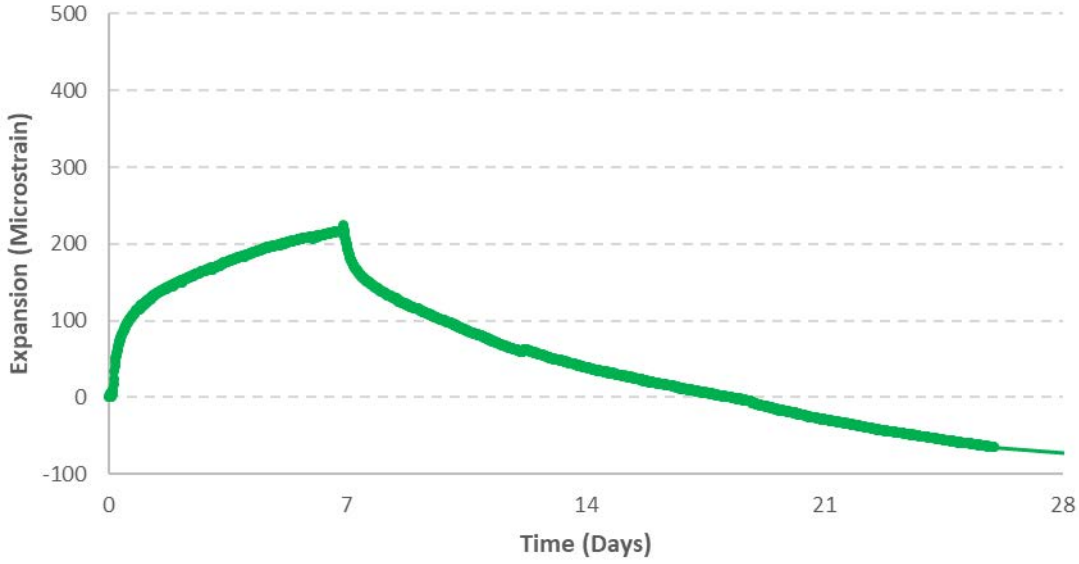

Figure 47: Restrained Column Expansion Results (5/8" Restraint Rods, 15% Komponent)

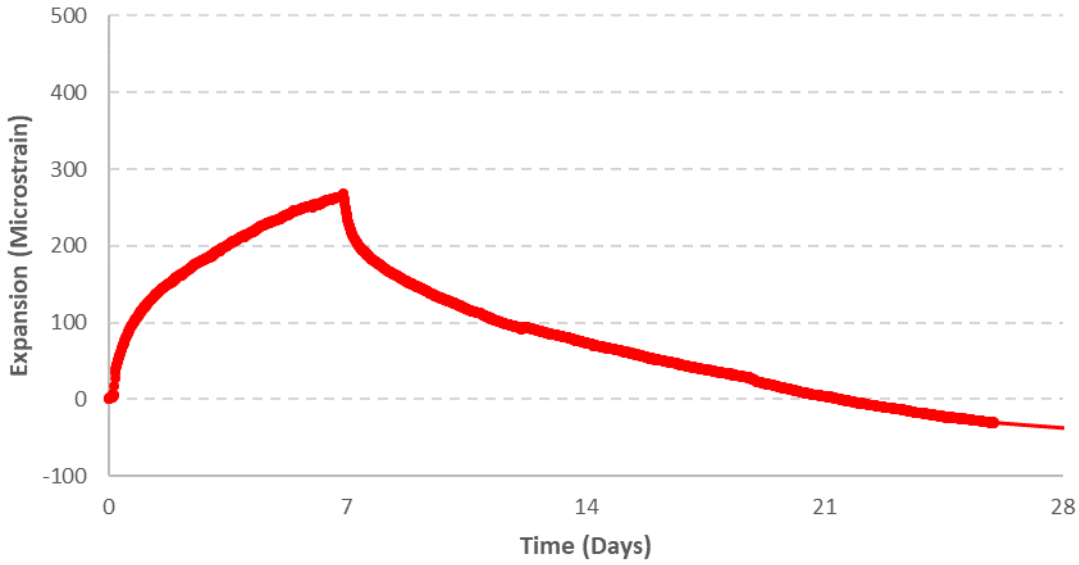

Figure 48: Restrained Column Expansion Results (3/4" Restraint Rods, 15% Komponent)

4.5.4 17% Replacement – Cured with Sprinkler System

This section presents the results for the restrained columns, using the second curing alternative, with 17% Komponent®. The color coding system is the same as for the previous section. The straight line represents a gap in the VWSG data, which recommences outside the frame of these plots. The strain values for these restrained columns were zeroed to the set-time of the concrete, at approximately 6 hours after casting. This also corresponded to the time that the load cells were installed, and the micro-sprinklers were turned on shortly thereafter. Figures 49-51 present the restrained column expansion data for the 17% mix for curing alternative 2.

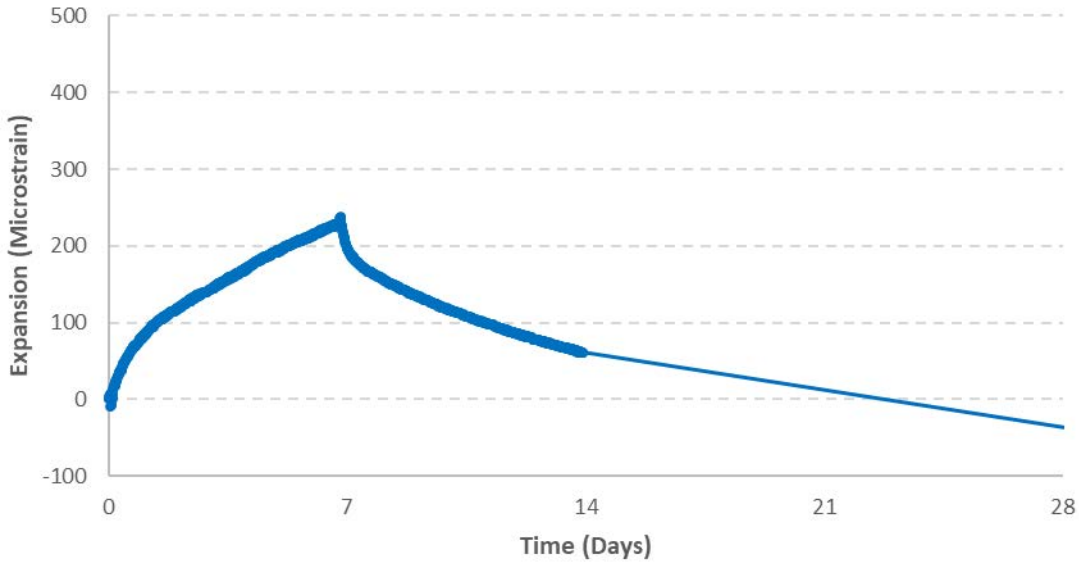

Figure 49: Restrained Column Expansion Results (1/2" Restraint Rods, 17% Komponent)

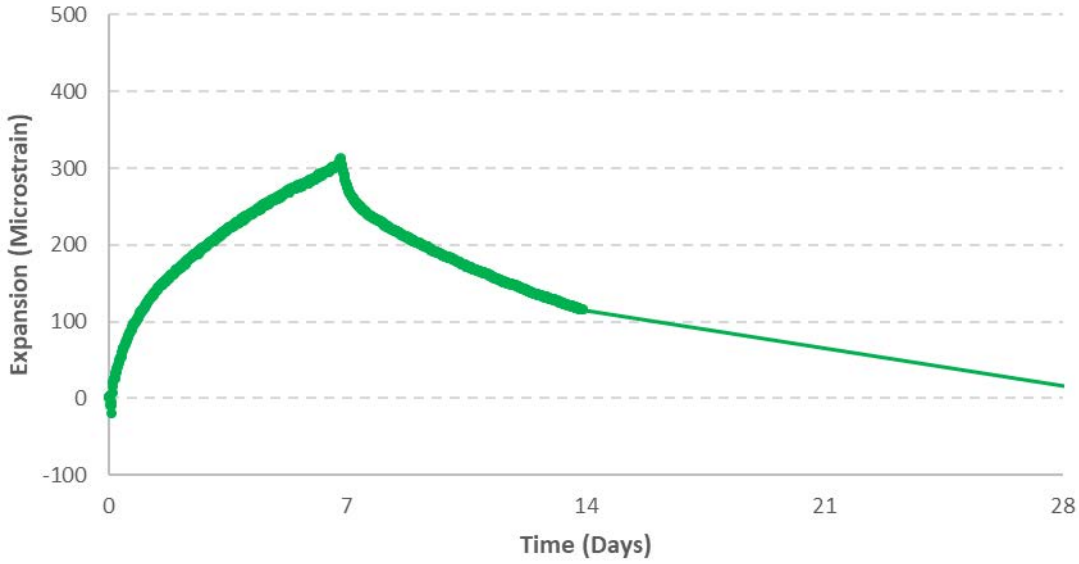

Figure 50: Restrained Column Expansion Results (5/8" Restraint Rods, 17% Komponent)

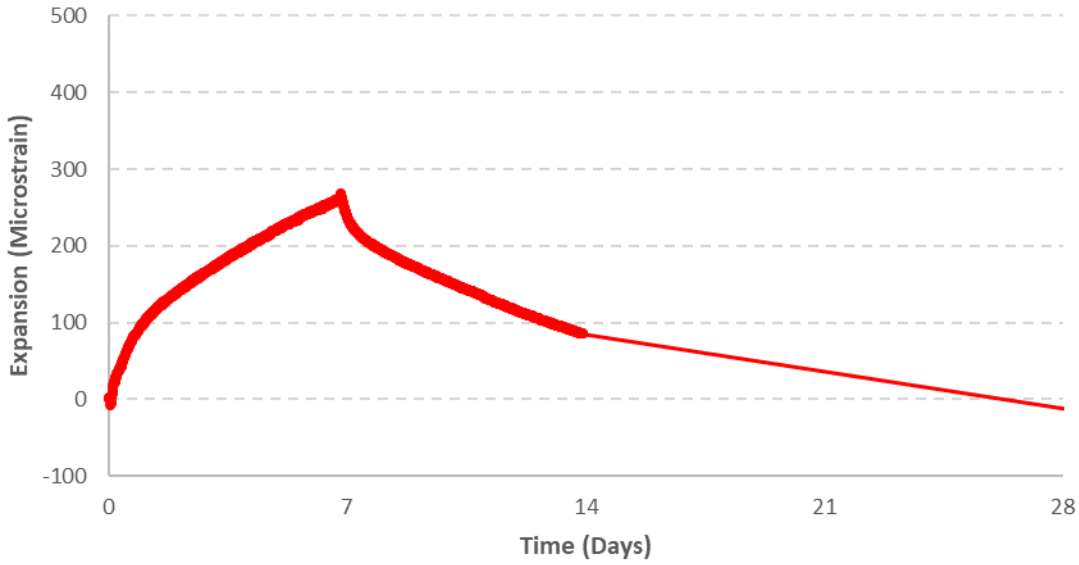

Figure 51: Restrained Column Expansion Results (3/4" Restraint Rods, 17% Komponent)

4.5.5 19% Replacement – Cured with Sprinkler System

This section presents the results for the restrained columns, using the second curing alternative, with 19% Komponent®. The color coding system is the same as for the previous section. The strain values for these restrained columns were zeroed to the set-time of the concrete, at approximately 6 hours after casting. This also corresponded to the time that the load cells were installed, and the micro-sprinklers were turned on shortly thereafter.

This data is actually a re-batch of the original mix, because the original restrained column test for the 19% and 21% batch was skewed due to an unexpected termination of the spigot which was running the sprinkler system. This required a re-batch late in the fall 2018 semester which was not originally scheduled; that is the data shown in the subsequent plots. The data from the original batch can be found in Appendix C. Figures 52-54 present the restrained column expansion data for the 19%

mix for curing alternative 2.

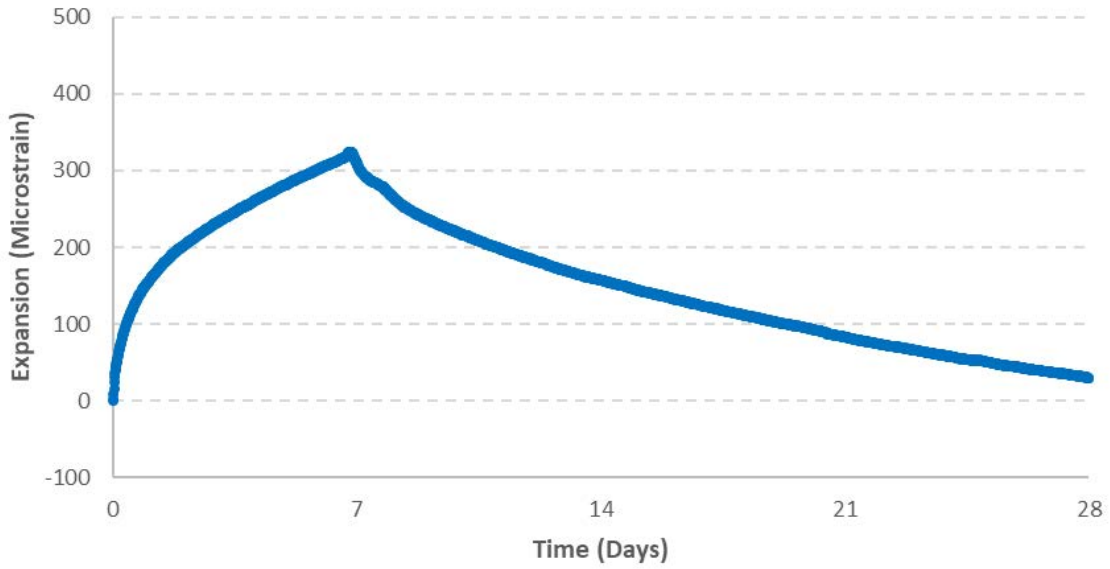

Figure 52: Restrained Column Expansion Results (1/2" Restraint Rods, 19% Komponent)

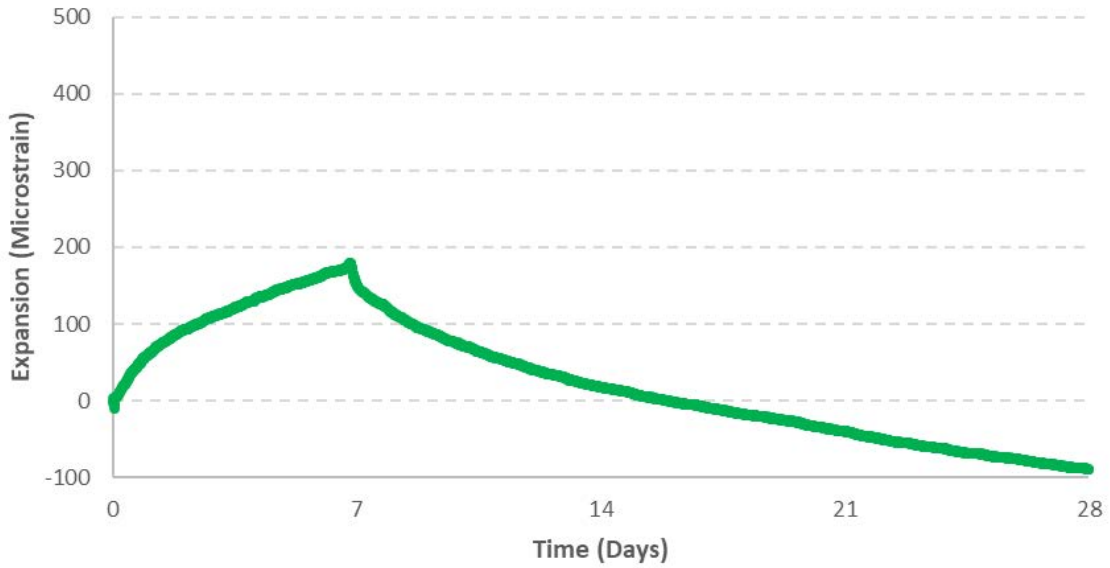

Figure 53: Restrained Column Expansion Results (5/8" Restraint Rods, 19% Komponent)

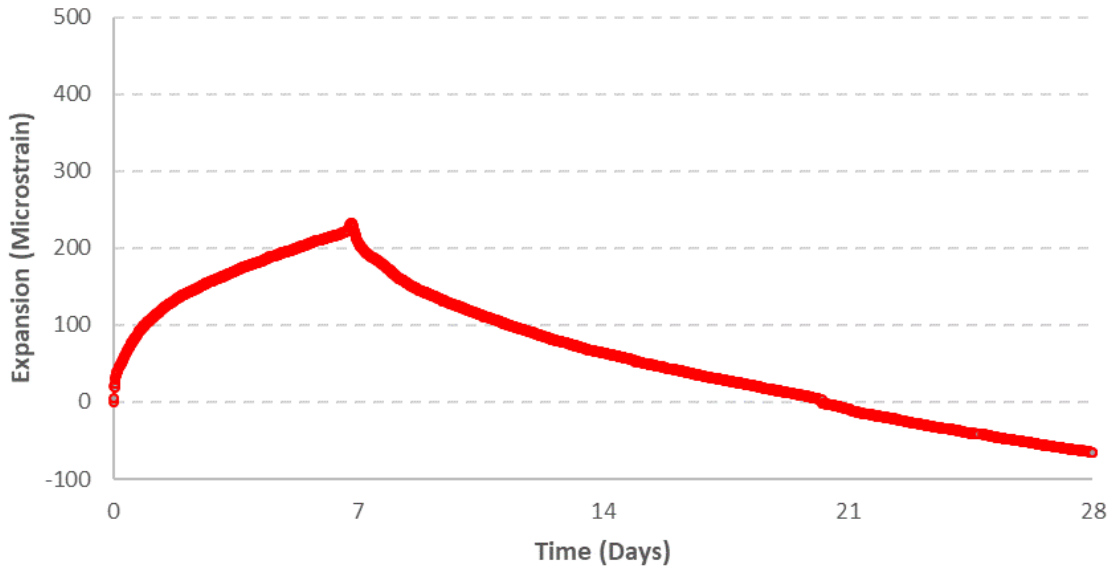

Figure 54: Restrained Column Expansion Results (3/4" Restraint Rods, 19% Komponent)

4.5.6 21% Replacement – Cured with Sprinkler System

This section presents the results for the restrained columns, using the second curing alternative, with 21% Komponent®. The color coding system is the same as for the previous section. The strain values for these restrained columns were zeroed to the set-time of the concrete, at approximately 6 hours after casting. This also corresponded to the time that the load cells were installed, and the micro-sprinklers were turned on shortly thereafter. The data shown in the subsequent plots is from the re-batch that occurred after the original 21% batch that was disrupted. Figures 55-57 present the restrained column expansion data for the 21% mix for curing alternative 2.

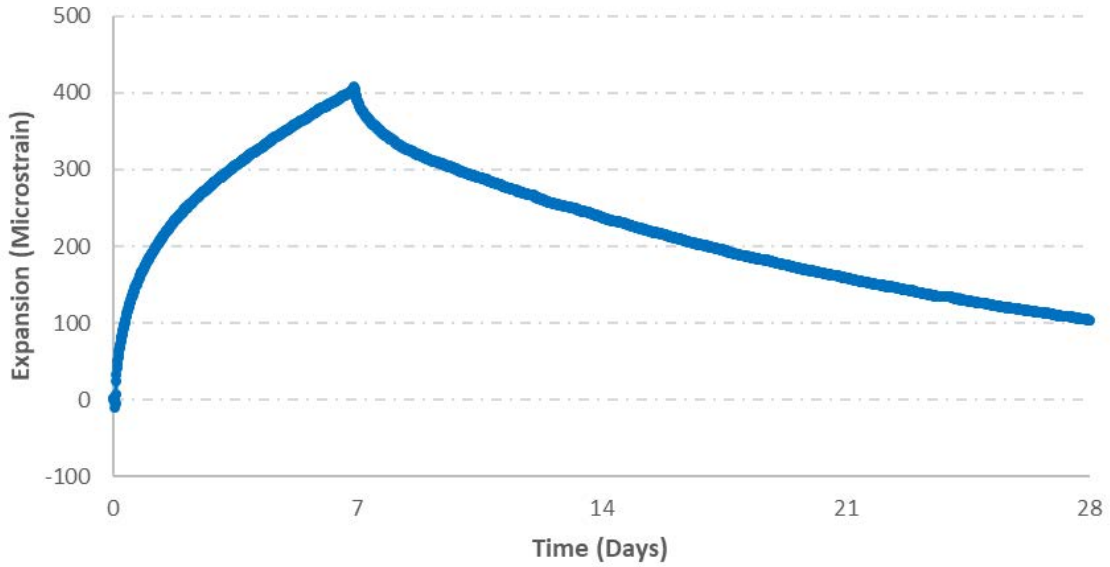

Figure 55: Restrained Column Expansion Results (1/2" Restraint Rods, 21% Komponent)

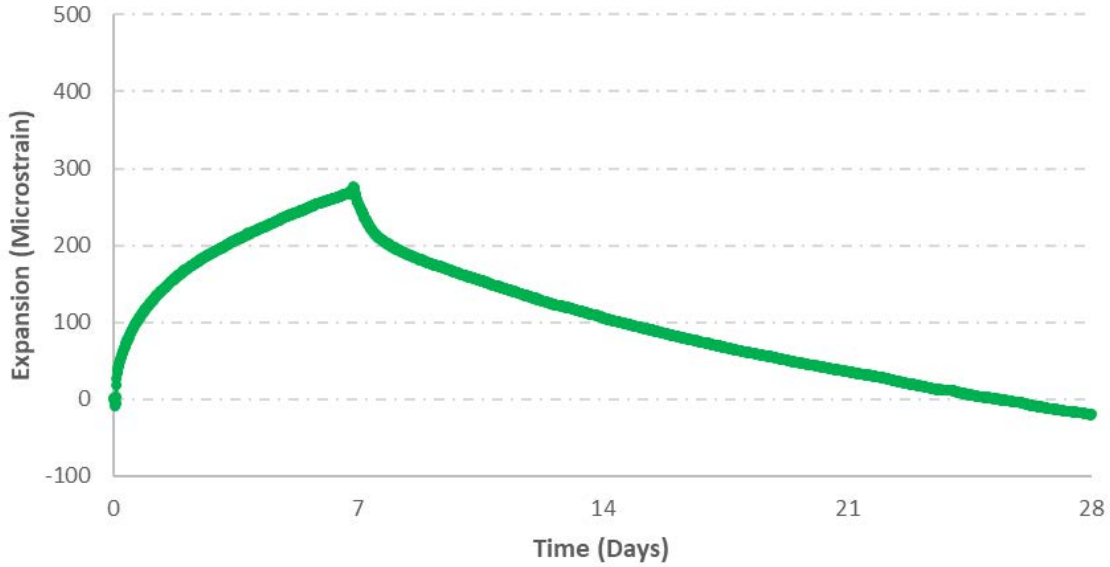

Figure 56: Restrained Column Expansion Results (5/8" Restraint Rods, 21% Komponent)

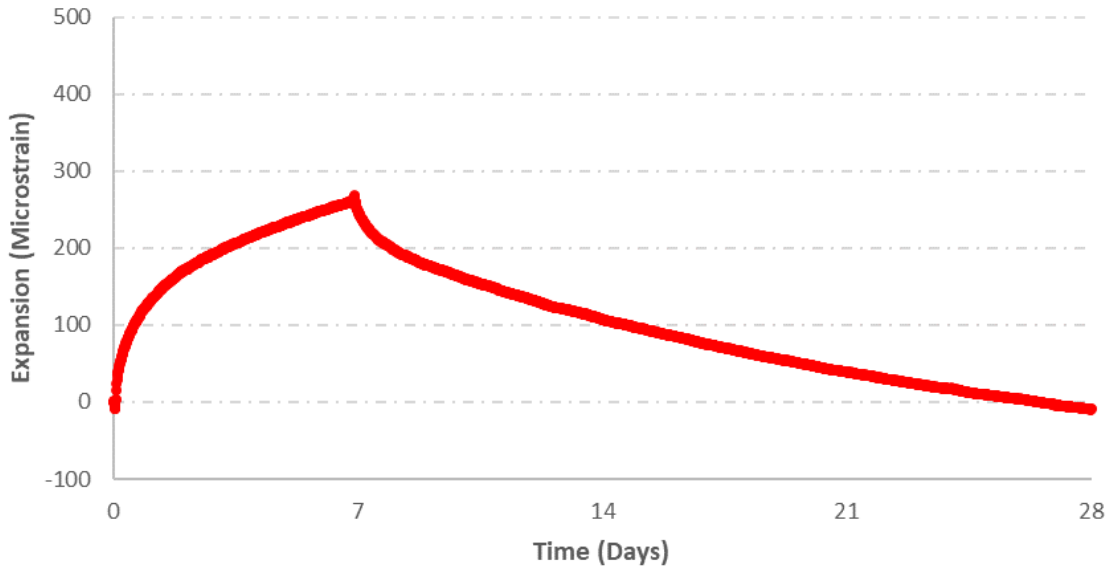

Figure 57: Restrained Column Expansion Results (3/4" Restraint Rods, 21% Komponent)

4.6 Restrained Column Load Development

4.6.1 15% Replacement - Cured with Cardboard Forms in Place

This section presents the load development results for the restrained columns, using the first curing alternative, with 15% Komponent®. The color coding system is the same as for the previous plots. The zero time for these plots corresponds to when the load cells were installed and began monitoring load, which was between 6-8 hours after casting.

It was originally intended to focus this discussion on the load development of the 15% and 17% columns cast with the second curing alternative (the sprinkler system), so that the results could be compared with the 19% and 21% columns, which were only cast with the second curing alternative. Unfortunately, however, the load development data for the 15% and 17% columns, cast with the sprinkler system, was permanently lost due to the data files being corrupted because of an unknown

malfunction of the Somat data acquisition system.

Therefore, the only data available for the 15% and 17% restrained column load development data is that from the first curing alternative, where the cardboard jackets remained in place for the duration of the tests. This load development data is shown for the 15% columns in Figures 58-60

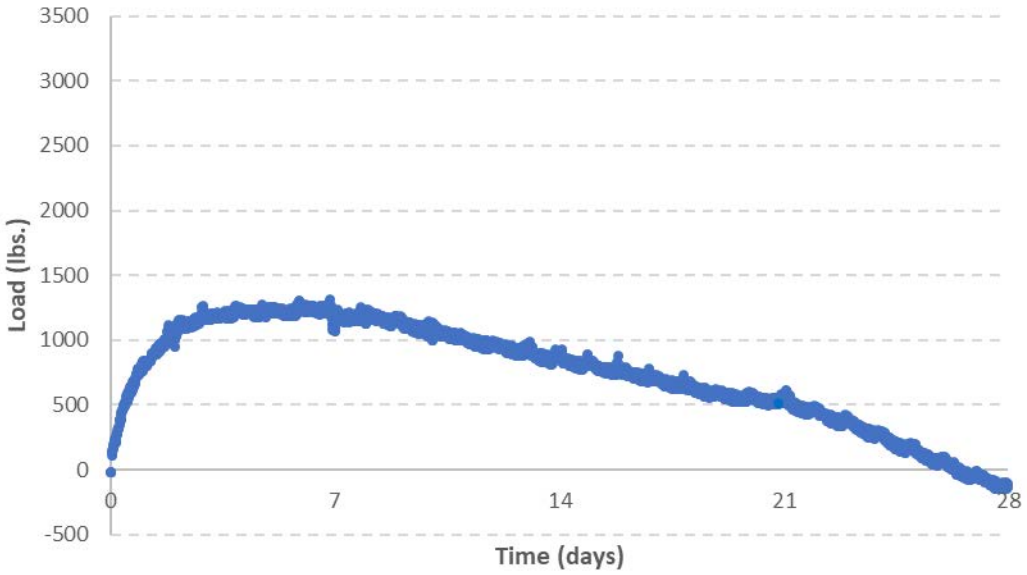

Figure 58: Restrained Column Load Development Results (1/2" Restraint Rods, 15% Komponent)

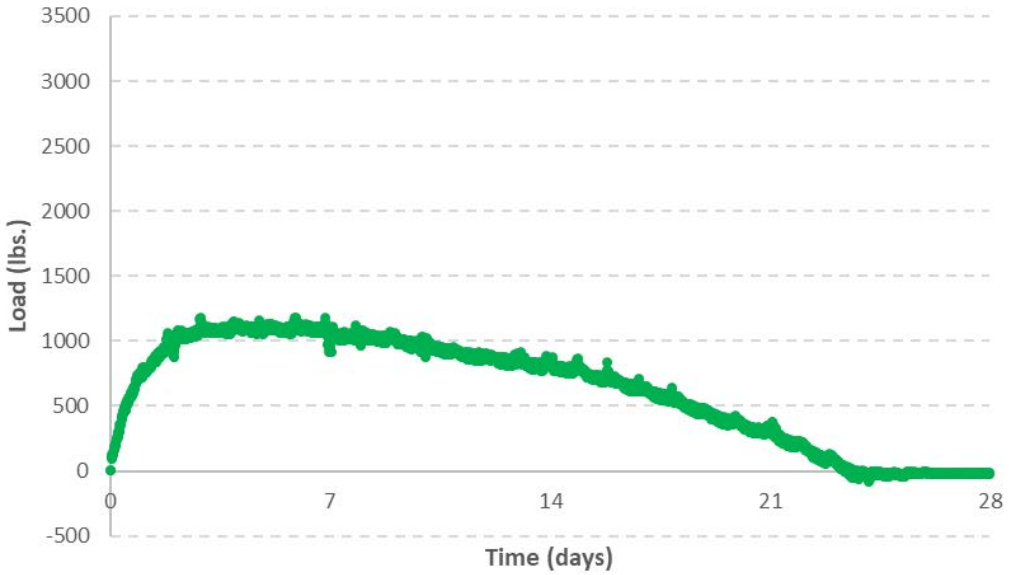

Figure 59: Restrained Column Load Development Results (5/8" Restraint Rods, 15% Komponent)

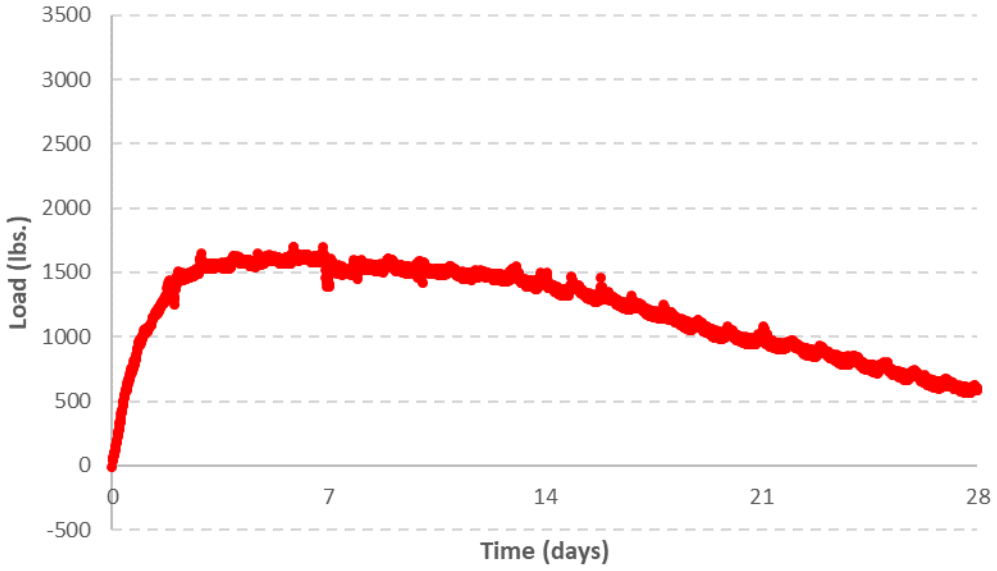

Figure 60: Restrained Column Load Development Results (3/4" Restraint Rods, 15% Komponent)

4.6.2 17% Replacement - Cured with Cardboard Forms in Place

This section presents the load development results for the restrained columns, using the first curing alternative, with 17% Komponent®. The color coding system is the same as for the previous plots. The zero time for these plots corresponds to when the load cells were installed and began monitoring load, which was between 6-8 hours after casting. Figures 61-63 show the data for the 17% restrained column load development data, from the first curing alternative, where the cardboard jackets remained in place for the duration of the tests.

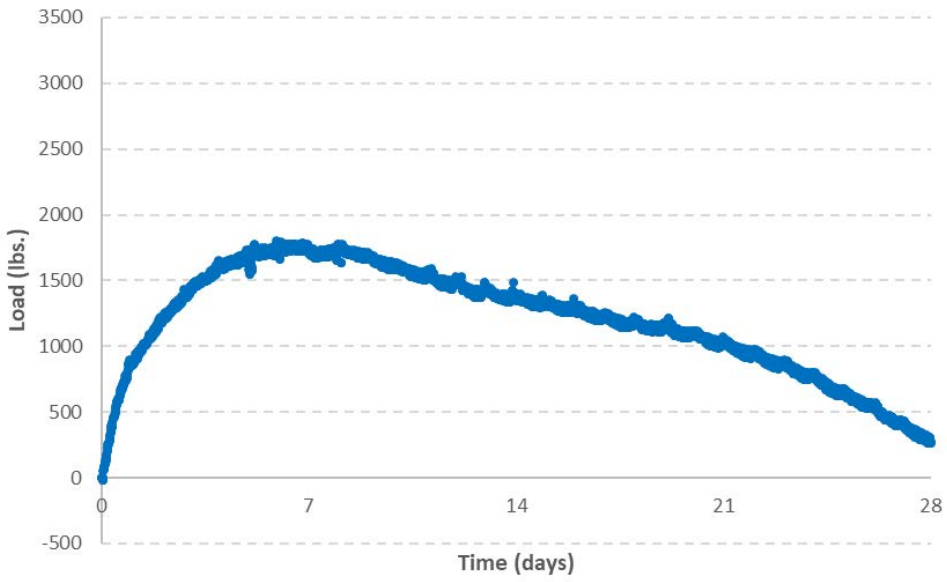

Figure 61: Restrained Column Load Development Results (1/2" Restraint Rods, 17% Komponent)

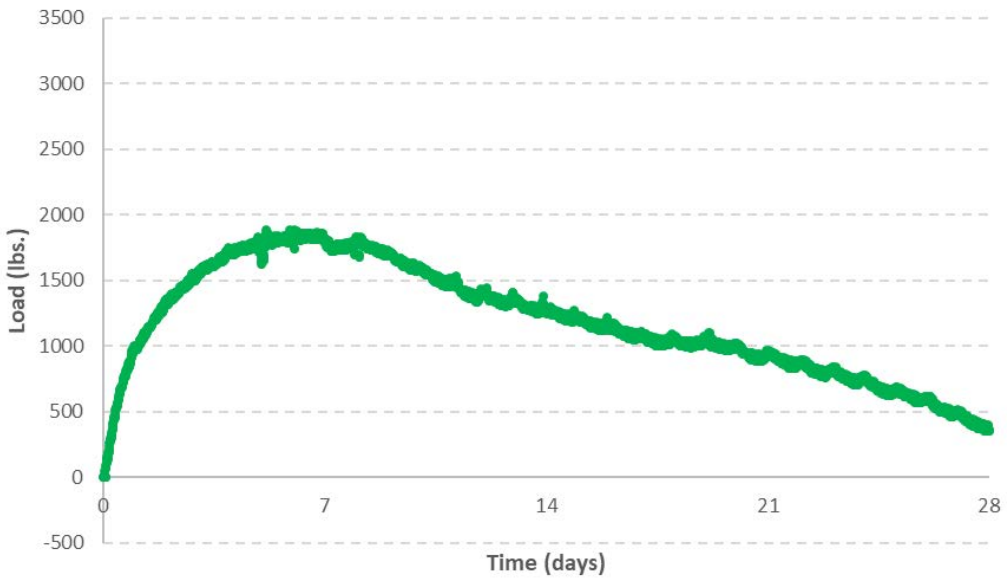

Figure 62: Restrained Column Load Development Results (5/8" Restraint Rods, 17% Komponent)

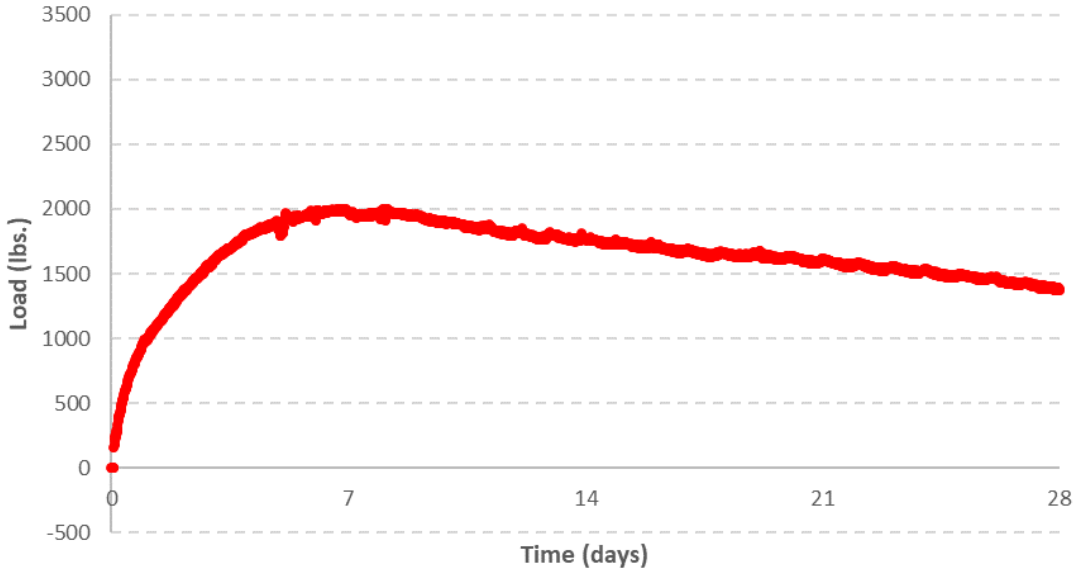

Figure 63: Restrained Column Load Development Results (3/4" Restraint Rods, 17% Komponent)

4.6.3 19% Replacement - Cured with Sprinkler System

This section presents the load development results for the restrained columns, using the second curing alternative, with 19% Komponent®. The color coding system is the same as for the previous plots. The zero time for these plots corresponds to when the load cells were installed and began monitoring load, which was between 6-8 hours after casting.

For the 19% replacement columns, the shrinkage was aggressive enough that after between 16 and 18 days, the load registered by the load cells was very nearly zero. Due to the bond that existed between the concrete column and the gypsum cement leveling compound used to cap the column (and due to the bond between the leveling compound and the reaction plate on the bottom of the load cells), the concrete column was firmly bonded to the reaction plate of the load cell. Therefore, as the concrete continued to shrink, this bond caused a tensile load to develop, and the load cells began to register negative load. At a certain point, however, as this tensile load increased, it overcame the bond strength of the capping compound, and the capping compound lost contact with the steel reaction plate of the load cell. This caused the load registered by the load cell to suddenly snap back to zero. Figures 64-66 show the load development graphs for the 19% restrained columns. These plots stop at around 24 days, because that is the point where the load comes to equilibrium near zero.

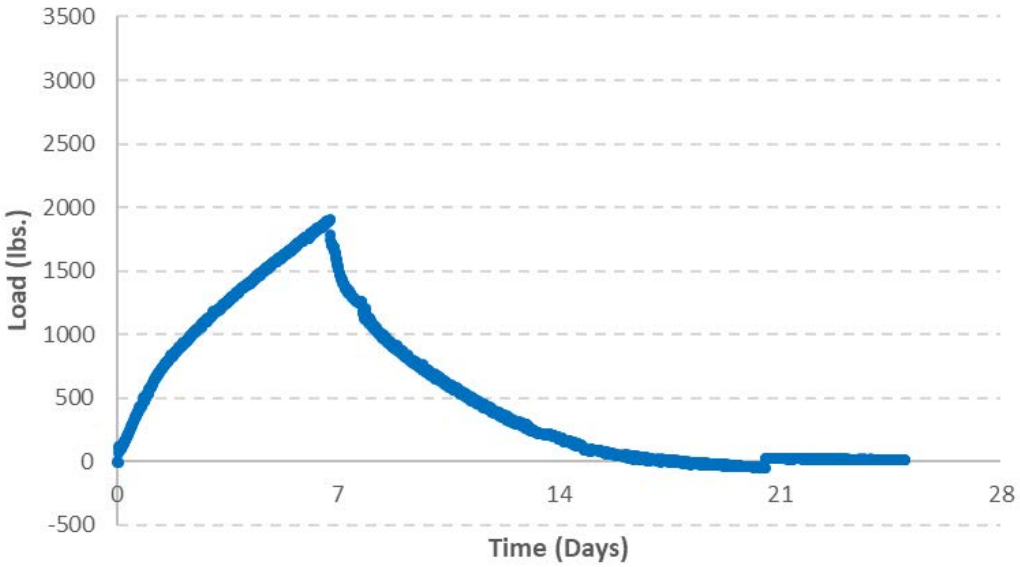

Figure 64: Restrained Column Load Development Results (1/2" Restraint Rods, 19% Komponent)

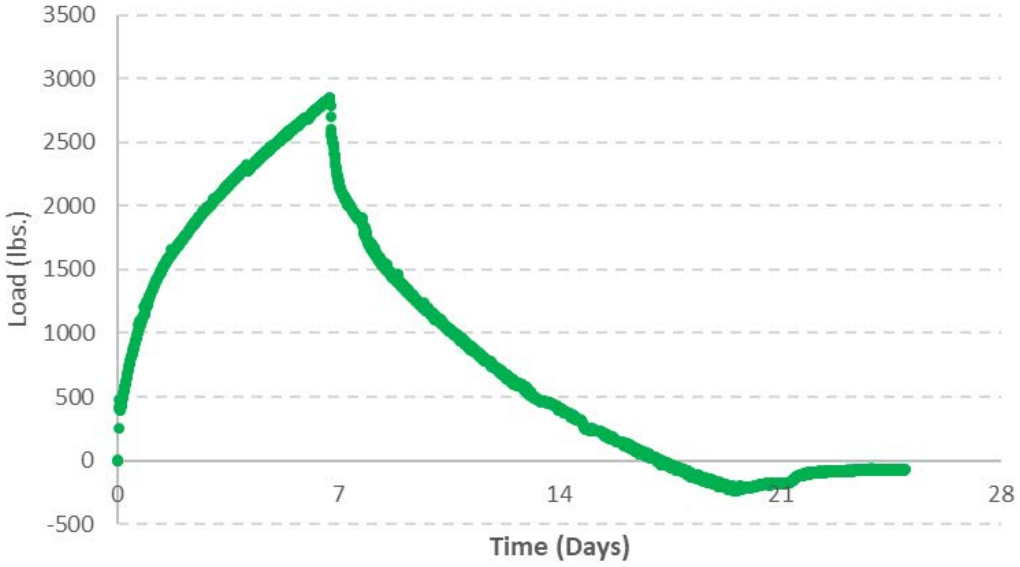

Figure 65: Restrained Column Load Development Results (5/8" Restraint Rods, 19% Komponent)

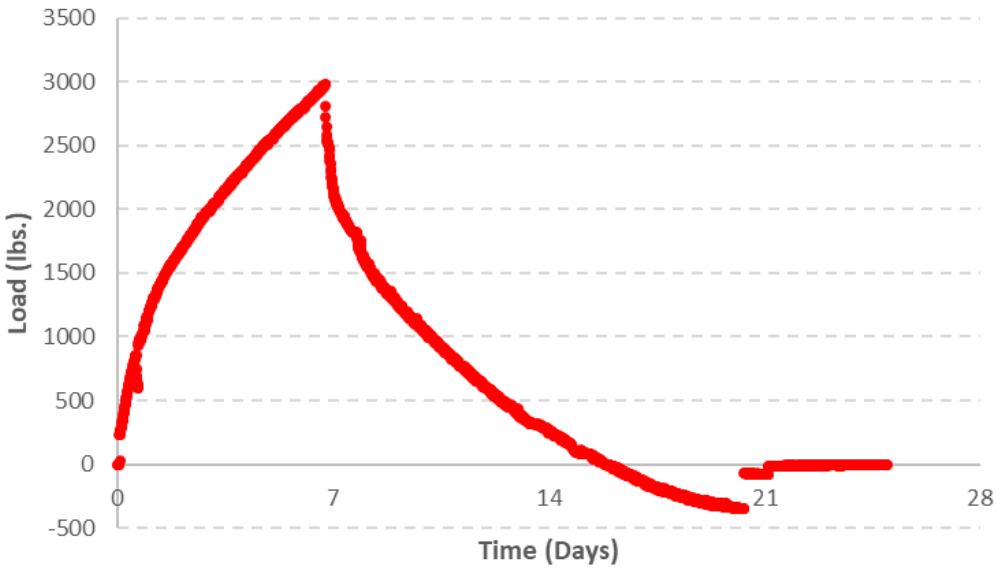

Figure 66: Restrained Column Load Development Results (3/4" Restraint Rods, 19% Komponent)

4.6.4 21% Replacement - Cured with Sprinkler System

This section presents the load development results for the restrained columns, using the second curing alternative, with 21% Komponent®. The color coding system is the same as for the previous plots. The zero time for these plots corresponds to when the load cells were installed and began monitoring load, which was between 6-8 hours after casting.

For the 21% replacement columns, the shrinkage was not aggressive enough to cause any significant tension at the load cell interface, like there was for the 19% columns. Instead, the load returned to zero more gradually, and without exhibiting the jolt from tension back to zero that was observed for the 19% columns. Figures 67-69 show the load development graphs for the 21% restrained columns.

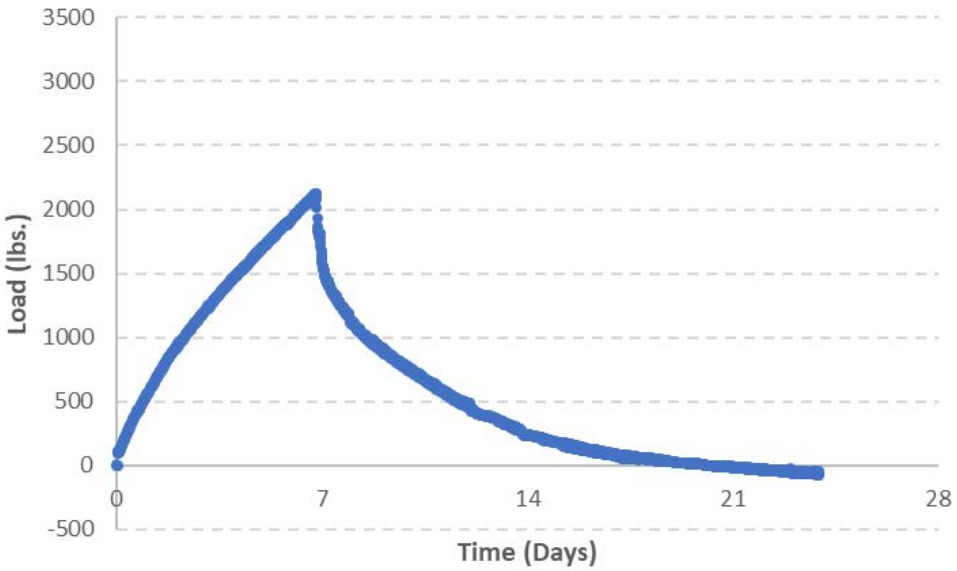

Figure 67: Restrained Column Load Development Results (1/2" Restraint Rods, 21% Komponent)

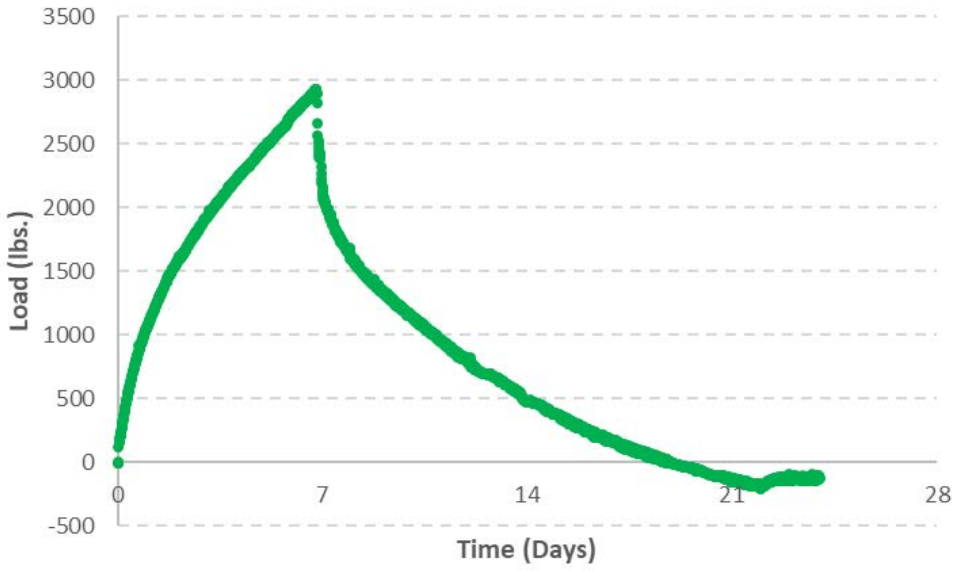

Figure 68: Restrained Column Load Development Results (5/8" Restraint Rods, 21% Komponent)

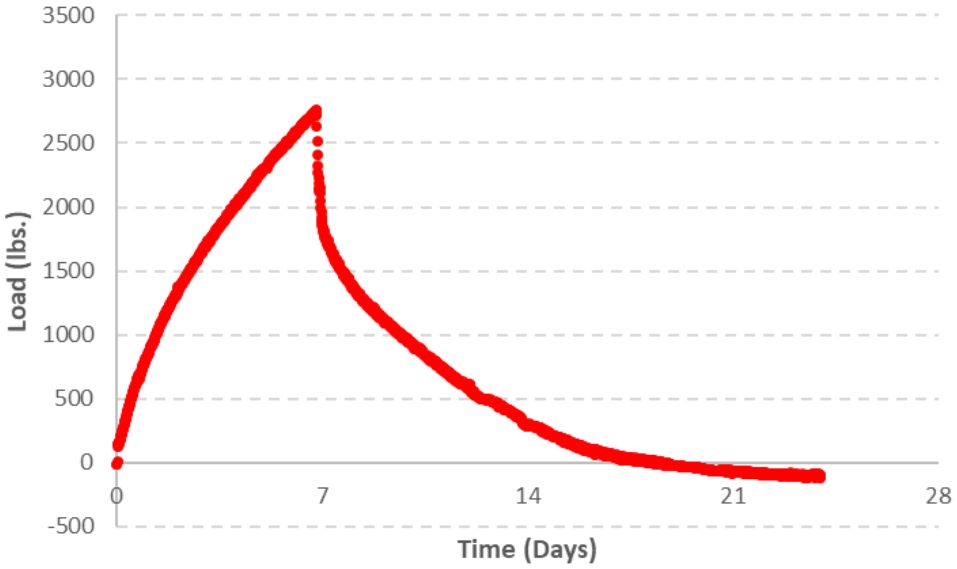

Figure 69: Restrained Column Load Development Results (3/4" Restraint Rods, 21% Komponent)

4.7 Compressive Cylinders

Figure 70 shows an overlay of the compressive strength data for the 4x8 cylinders, gathered for all four mix designs. The color-coding scheme for these curves is the same as for the previous figures.

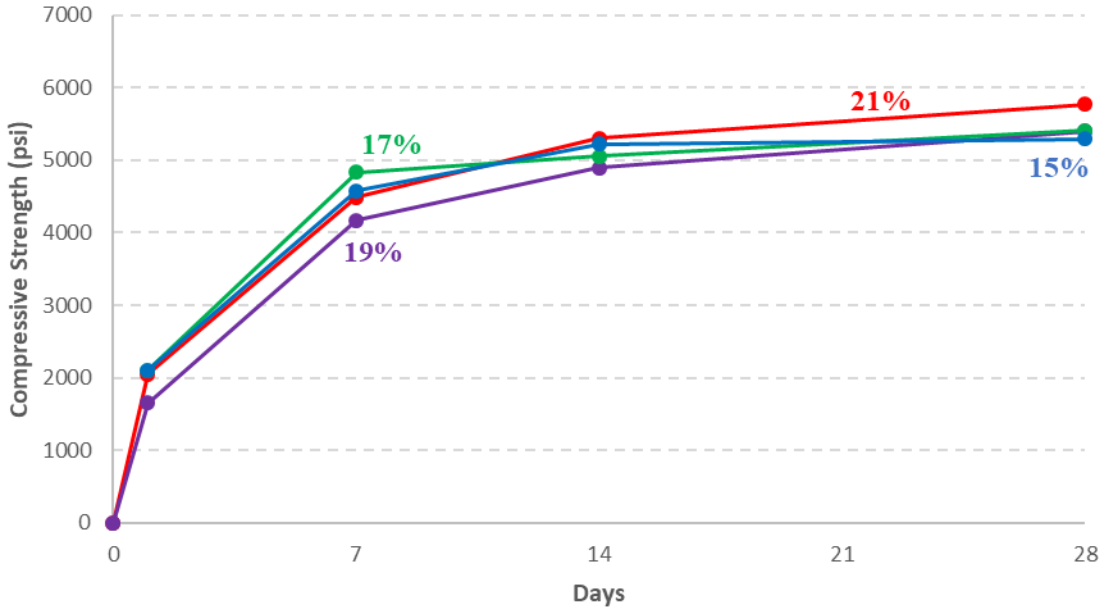

Figure 70: Compressive Strength Results

4.8 Fresh Properties

Table 6 summarizes the fresh property data for the 4 mixes that were used to cast the 15%, 17%, 19%, and 21% restrained columns with the second curing alternative.

Table 6: Fresh Properties for Restrained Columns

Fresh Properties	15% Replacement	17% Replacement	19% Replacement	21% Replacement
Temperature (^{0}F)	70	72	66	78
Slump (in.)	4 3/4	5	2 1/2	1 1/2
Entrapped Air (%)	1.5	-	1.2	1.4
Unit Weight (lb/ft^3)	147.6	147.2	146.2	147.3
Ambient Temperature (^{0}F)	48	64	36	41
Relative Humidity (%)	82	32	38	51

Chapter 5 – Discussion of Results

5.1 ASTM C157 Unrestrained Expansion

Figure 71 shows an overlay of the results for the ASTM C157 unrestrained expansion tests for all four mix designs. The color-coding scheme for these curves is the same as for the previous figures.

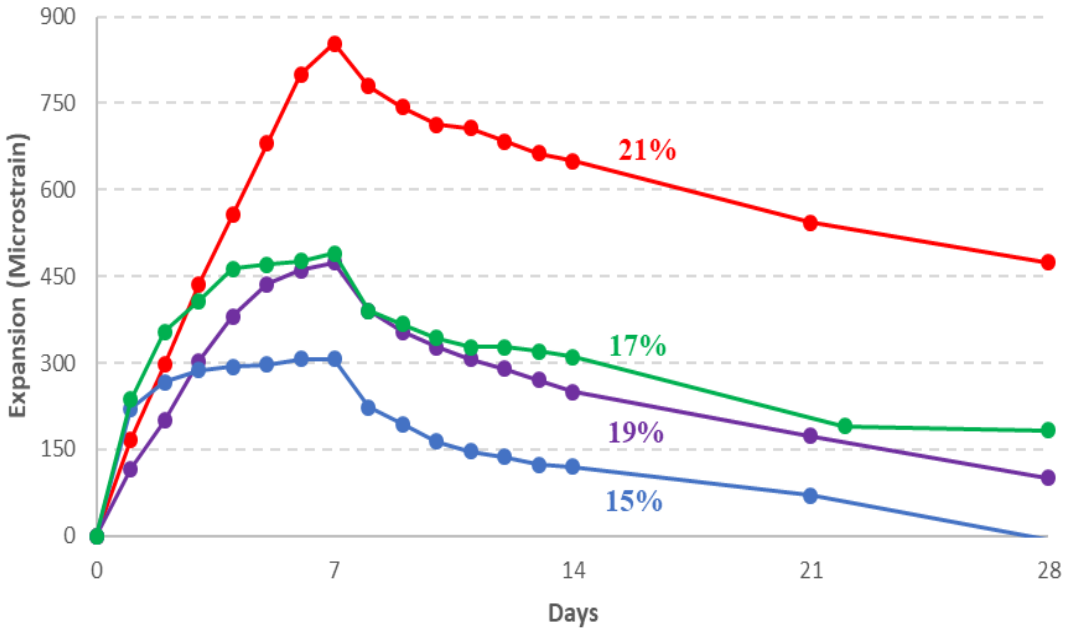

Figure 71: ASTM C157 Unrestrained Expansion Results

It can be observed that for these specimens, increased Komponent® results in a higher max expansion, as well as a steeper initial slope in the curve. On the whole, the slope of the descending portion of the curve is independent of the Komponent® content. One unexpected trend is that the 17% mix achieves a higher max expansion than the 19% mix. Between 0 and 7 days, the gap between those curves is significant, but between 7 and 10 days, the variation is within experimental error. The reason for this occurrence is unknown at this time. The sudden increase in the 17% curve from 22 days up to 28 days is because water cure was initiated for the restrained columns with the

misters during that time. This caused a humidity increase in the environmental chamber of around 30% for 7 days.

5.2 ASTM C878 Restrained Expansion

Figure 72 shows an overlay of the results for the ASTM C878 restrained expansion tests for all four mix designs. The color-coding scheme for these curves is the same as for the previous figures.

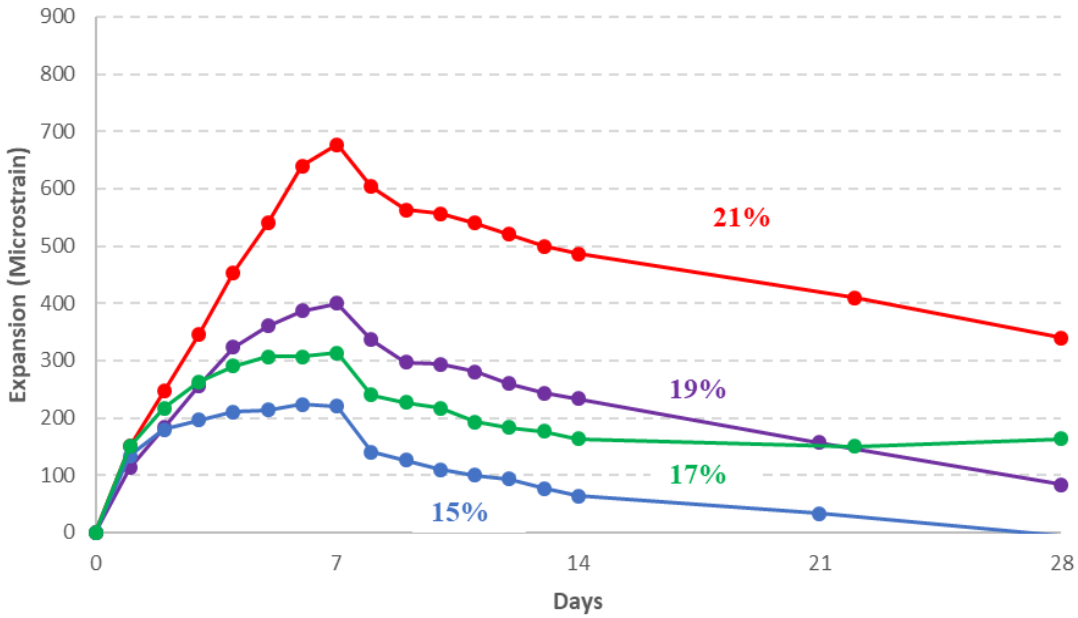

Figure 72: ASTM C878 Restrained Expansion Results

It can be observed that for these specimens, increased Komponent® resulted in higher max expansions, as well as steeper initial slopes in the curves. This behavior is identical to that of the C157 prisms. Overall, the slope of the descending portion of the curve is independent of the Komponent® content, except for the 17% curve, which was affected by the column curing. It is also worth noting that the shape of all four curves is similar to those in Figure 71, except that the max expansions have been driven down by 100-150 microstrain. This is due to the addition of the restraint of the C878 test.

Although the max expansion was reduced by a stiff boundary, shrinkage compensation was not hampered; all mixes except 15% remained in compression for the first 28 days, which is the most critical period for preventing drying shrinkage.

5.3 Unrestrained Expansion Cylinders

Figure 73 shows an overlay of the expansion data for the unrestrained 6”x12” cylinders, gathered for all four mix designs. The color-coding scheme for these curves is the same as for the previous figures.

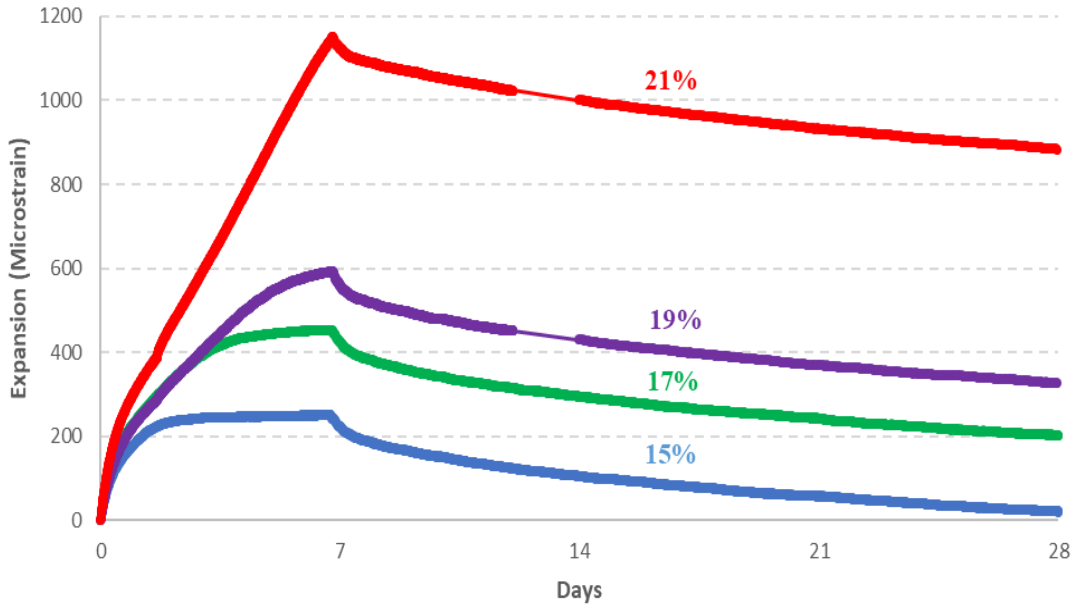

Figure 73: VWSG Unrestrained Expansion Cylinder Results

These curves follow the expected trend of increased percentages of Komponent® resulting in progressively higher maximum expansions. Additionally, there is a much larger increase in the max expansion between 19% and 21% compared to the differences between the other curves. This indicates that the increase in expansion may not linearly related to the percentage of Komponent®. Finally, it should be noted that although increased Komponent® results in the curve being steeper initially, the

slope of the curve in the shrinkage regime is nearly constant across all four mixes.

5.4 Restrained Expansion Cylinders

Figure 74 shows an overlay of the expansion data for the restrained 6”x12” cylinders, gathered for all four mix designs. The color-coding scheme for these curves is the same as for the previous figures.

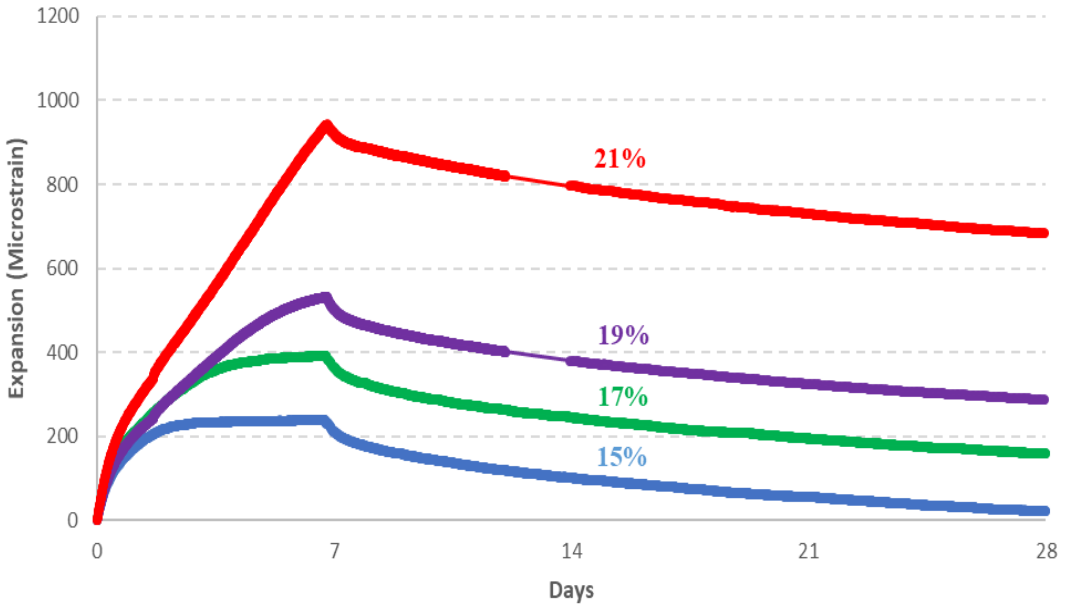

Figure 74: Restrained Expansion Cylinder Results

These curves also follow the expected trend of increased percentages of Komponent® resulting in progressively higher maximum expansions. Just like for the unrestrained 6”x12” cylinders, there is a much larger increase in the max expansion between 19% and 21% compared to the differences between the other curves. This further reinforces the idea that the increase in expansion may not be linearly related to the percentage of Komponent®. Finally, the trend of increased Komponent® resulting in the curve being steeper initially, but the slope of the curve in the shrinkage regime remaining nearly constant across all four mixes, is identical to the trend observed in

Figure 73.

5.5 Comparing Unrestrained Cylinders to ASTM C157 Prisms

The data from the expansion of both the 6”x12” cylinders and the ASTM prisms shows the result of immediate expansion, which reaches a maximum when the wet-cure is terminated at an age of 7 days, followed by a gradual trend of shrinkage. Additionally, increasing the percentage replacement of Komponent® increases the maximum expansion for any given type of specimen, and increasing the level of restraint slightly decreases the maximum expansion. Figure 75 shows a comparison of the unrestrained 6”x12” cylinder and the ASTM C157 test for a 15% replacement mix. The seemingly solid lines of data points represent the VWSG data from the cylinders, while the intermittent data points represent the data gathered from the ASTM tests.

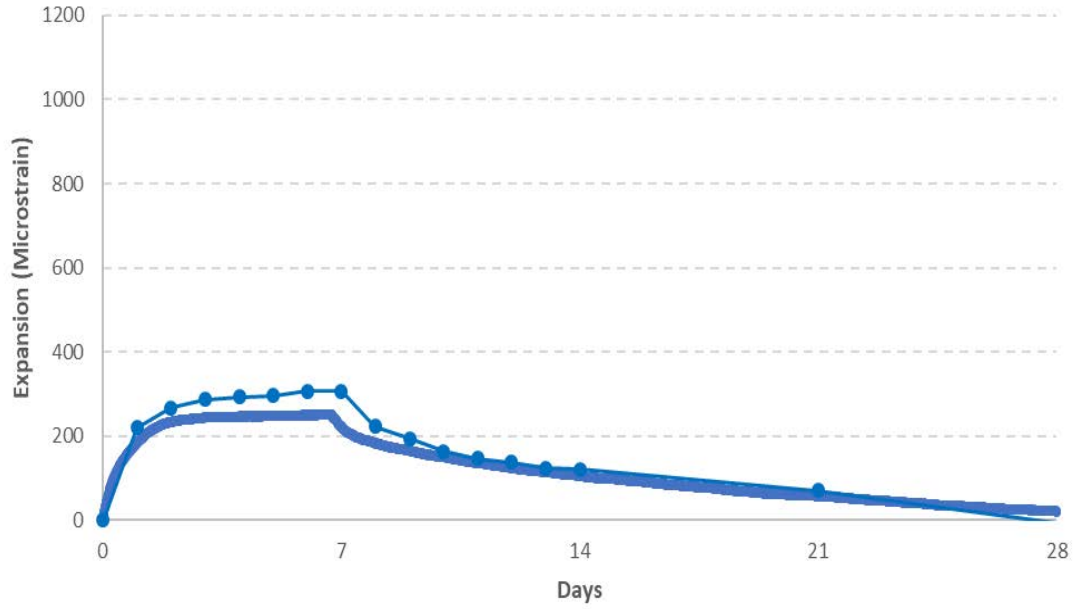

Figure 75: Overlay of Unrestrained Expansion Cylinder with ASTM C157 (15% Komponent®)

Figure 75 shows that the VWSG correlates well with the ASTM test. There is some slight spread between the curves at between 1-7 days, but as time progresses past

7 days, the curves converge and remained clustered together for the next 21 days.

Figure 76 shows a comparison of the unrestrained 6”x12” cylinder and the ASTM C157 test for the 17% replacement mix.

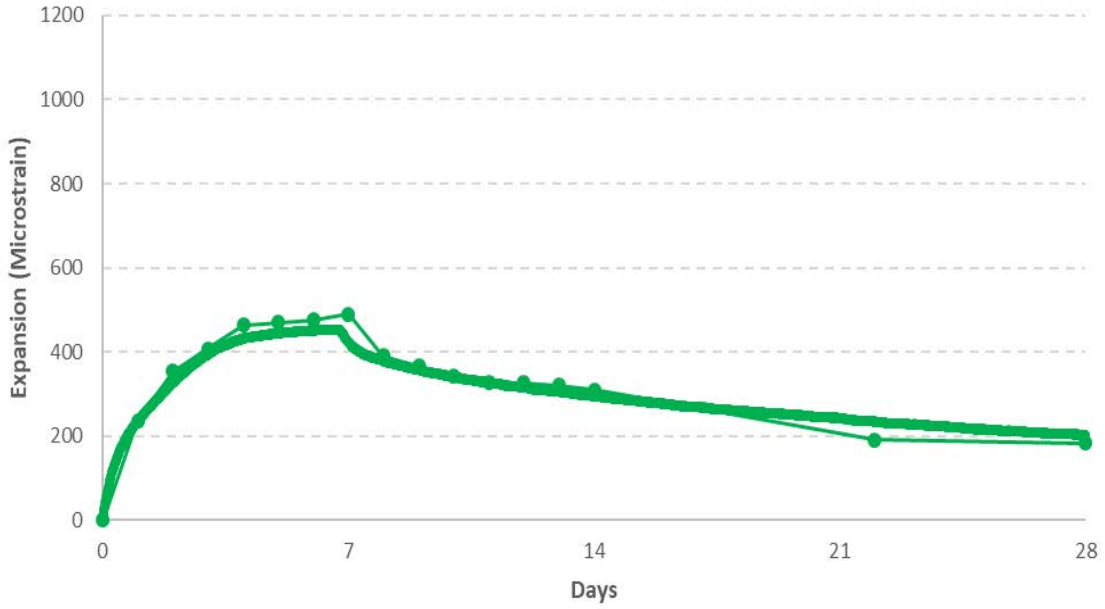

Figure 76: Overlay of Unrestrained Expansion Cylinder with ASTM C157 (17% Komponent®)

Figure 76 also shows excellent agreement between the VWSG and the ASTM test. In fact, for the 17% mix, there is actually less spread between the two curves than there is for the 15% mix. This correlation indicates that not only is the VWSG capturing the true behavior of the concrete’s expansion, it is also agreeing with the ASTM standard test. It is important, however, to note that this correlation is occurring for unrestrained specimens.

Figure 77 shows a comparison of the unrestrained 6”x12” cylinder and the ASTM C157 test for a 19% replacement mix.

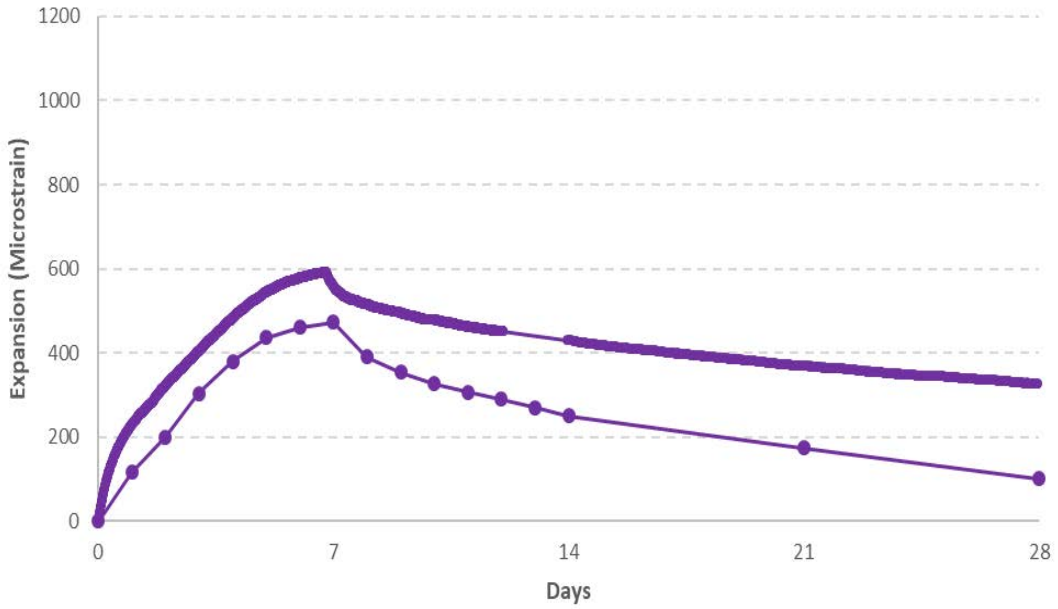

Figure 77: Overlay of Unrestrained Expansion Cylinder with ASTM C157 (19% Komponent®)

Figure 77 shows that at 19% replacement, the VWSG curves and ASTM curves are beginning to diverge. There is significant spread between the two curves across the entire 28 day time period. It is interesting to note, though, that despite the gap between the curves, they have very similar shapes. The only difference in shape comes after 7 days when shrinkage commences. At that point, the curve for the ASTM C157 specimens descends more steeply than the curve for the VWSG unrestrained cylinder.

Figure 78 shows a comparison of the unrestrained 6”x12” cylinder and the ASTM C157 test for a 21% replacement mix.

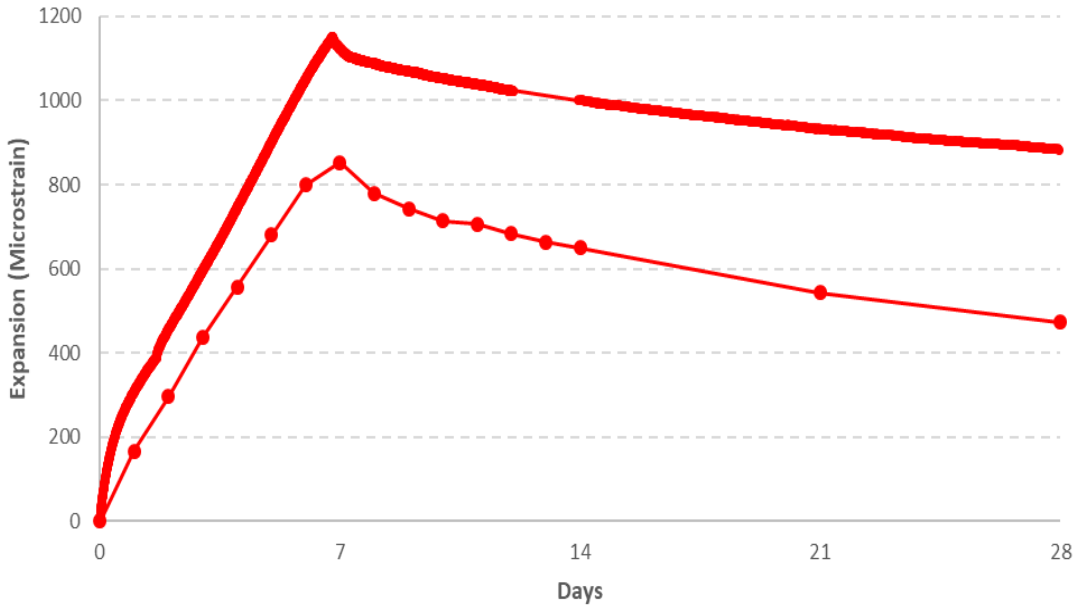

Figure 78: Overlay of Unrestrained Expansion Cylinder with ASTM C157 (21% Komponent®)

Figures 75 through 78 present some very meaningful trends. First of all, Figures 74 and 75 show that at relatively low percentage replacement, there is excellent agreement between the unrestrained cylinder with the VWSG and the ASTM C157 test; for the 15% and 17% mixes, there curves are essentially overlaid. As the replacement percentage becomes higher (Figures 76 and 77), the curves still mimic one another closely, but the maximum expansion shifts upward significantly for the VWSG data, compared to the ASTM C157 test. At 19% and 21% replacement, the slope of the curves diverges somewhat after 7 days, with the C157's experiencing more aggressive shrinkage. One final observation is that as the Komponent® content increases, the rate of expansion during the initial 7 days increases considerably.

Explaining these observations requires an understanding of the mechanism by which the Type K cement causes expansion. As mentioned in the literature review of this work, Type K cement creates expansion by utilizing ettringite crystals which

experience a volume increase when hydrated. It can be theorized, however, that before the volume increase of the ettringite crystals can lead to an increase in the gross dimensions of the specimen, they must partially fill the natural void spaces in the matrix of the concrete. The expansion of the shrinkage-compensating concrete can then be thought of as a two-stage process; (1) the ettringite crystals expand and partially bridge the void spaces in the concrete, and (2) the ettringite crystals continue to expand, causing the overall volume of the sample to increase. This theory may explain why reduced expansion is noted when lower percentages of Type K cement are used – more of the expansive potential of the Type K cement goes into filling void spaces, and there is less leftover to cause net expansion of the specimen.

Reviewing the data in Figures 74 through 77 in this light explains some of the observations. As the percentage of Komponent® is increased from 15% to 21%, the initial leg of the curve increases in slope rapidly because the void spaces in the concrete are filled much more rapidly, allowing more of the expansion of the ettringite crystals to contribute to dimensional growth of the specimens. There may be a possible explanation for the observed behavior of the 6”x12” cylinder specimens exhibiting a higher maximum expansion for greater percentages of Komponent®. A possibility is that the 6”x12” cylinders, which are larger than the 3”x3” C157 prisms, cause a size effect by which the total expansion is magnified at higher levels of Komponent® simply due to the higher volume of the sample. A second possibility may be researcher error, but this seems doubtful considering that this behavior has been replicated with the restrained 6”x12” cylinders and C878 specimens. A third possibility is that there is some unknown influence which is resulting in the increased discrepancy between max

expansions for the two specimen types at higher percentages of Komponent®. This would require future research to better understand.

The final observation from these comparisons was that the more rapid shrinkage is experienced by the ASTM C157 specimens, compared to the unrestrained 6”x12” specimens equipped with VWSG. This is primarily due to the fact that the C157 prisms have a much higher surface area to volume (SA/V) ratio than the 6”x12” cylinders; the larger surface area allows them to dry out faster after the wet-cure is terminated, causing them to shrink more aggressively. Table 7 shows a comparison of the SA/V ratio for the 4 types of small-scale length specimens. These calculations comprehend the reduced SA for the ends of the restrained specimens being covered.

Table 7: Comparison of SA/V Ratios for Length Change Specimens

Specimen	Surface Area (in^2)	Volume (in^3)	SA/V (in^{-1})
ASTM C157	153.00	101.25	1.51
ASTM C878	120.00	90.00	1.33
Unrestrained 6”x12”	254.47	339.29	0.75
Restrained 6”x12”	226.19	339.29	0.67

Close observation of Table 7 yields some notable results about how the geometric properties of these specimens may relate to the mechanical behavior of their expansion and shrinkage. First, the SA/V ratio for the C157 is almost exactly double that of the unrestrained 6”x12”, and the SA/V ratio for the C878 is exactly double that of the restrained 6”x12”. Second, when comparing the C157 to the C878, their SA/V ratios are different by 11.8%, and when comparing the unrestrained 6”x12” to the restrained one, their SA/V ratios are different by 11.1%.

5.6 Comparing Restrained Cylinders to ASTM C878 Prisms

In this section, the data for the 6”x12” cylinders equipped with VWSG is again compared to the ASTM standard test, but now when both are under a restrained condition (in other words comparing restrained 6”x12”’s to ASTM C878 specimens). Figure 79 shows the overlay of the VWSG data with the C878 data for the 15% replacement batch; as before, the ASTM data is the discrete points, while the VWSG data is the continuous curve.

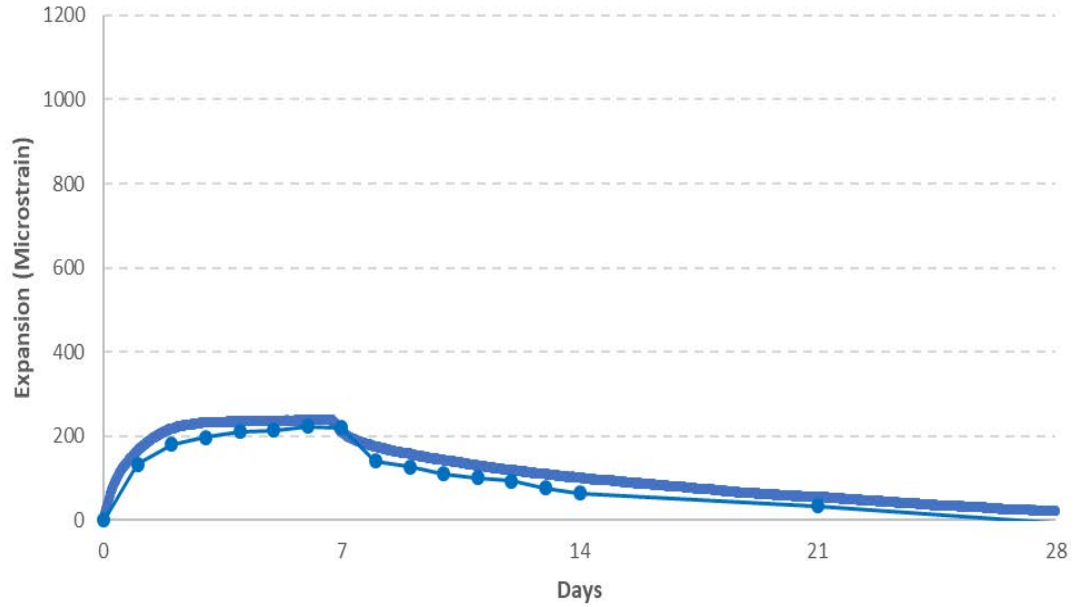

Figure 79: Overlay of Restrained Expansion Cylinder with ASTM C878 (15% Komponent®)

Figure 79 shows that for the 15% mix design, the expansion of the restrained 6”x12” measured with the VWSG correlates very closely with the readings taken for the ASTM C878 specimens. In addition, both specimens just reach zero strain, or in other words return to their original length, by an age of 28 days. Although shrinkage continues past 28 days, this axis boundary was chosen for these plots for the sake of

consistency.

Figure 80 shows the overlay of the VWSG data with the C878 data for the 17% replacement batch.

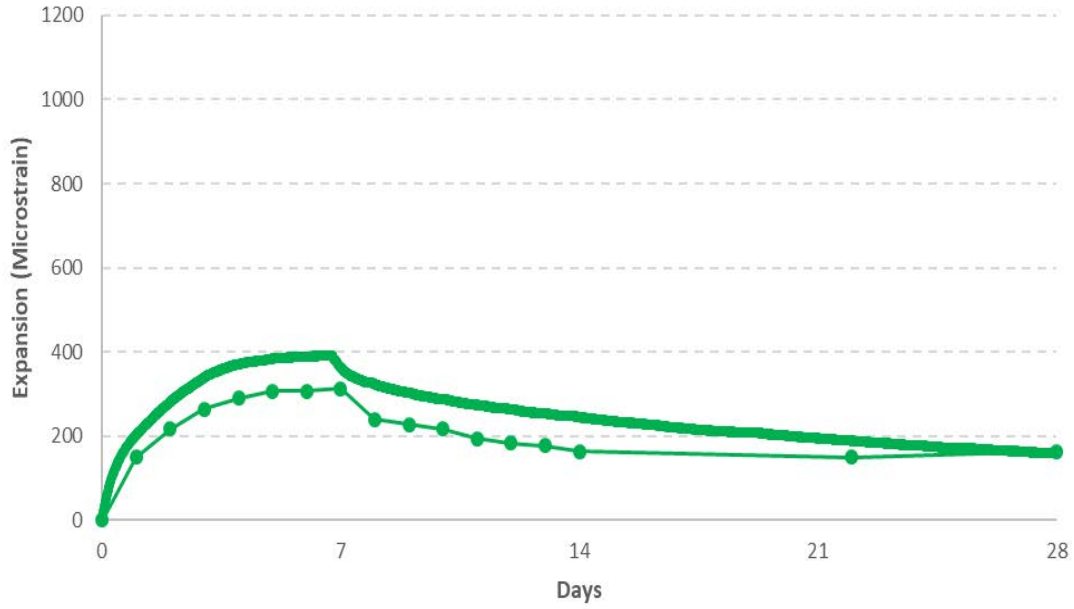

Figure 80: Overlay of Restrained Expansion Cylinder with ASTM C878 (17% Komponent®)

Figure 80 shows that for the 17% mix design, the expansion of the restrained 6”x12” measured with the VWSG correlates somewhat closely with the readings taken for the ASTM C878 specimens, although there is a noticeable gap between the two curves. This gap closes near the 28 day mark, but only because the C878 specimens began to expand again when they were exposed to moisture during the wet-cure period for a set of restrained columns.

Figure 81 shows the overlay of the VWSG data with the C878 data for the 19% replacement batch.

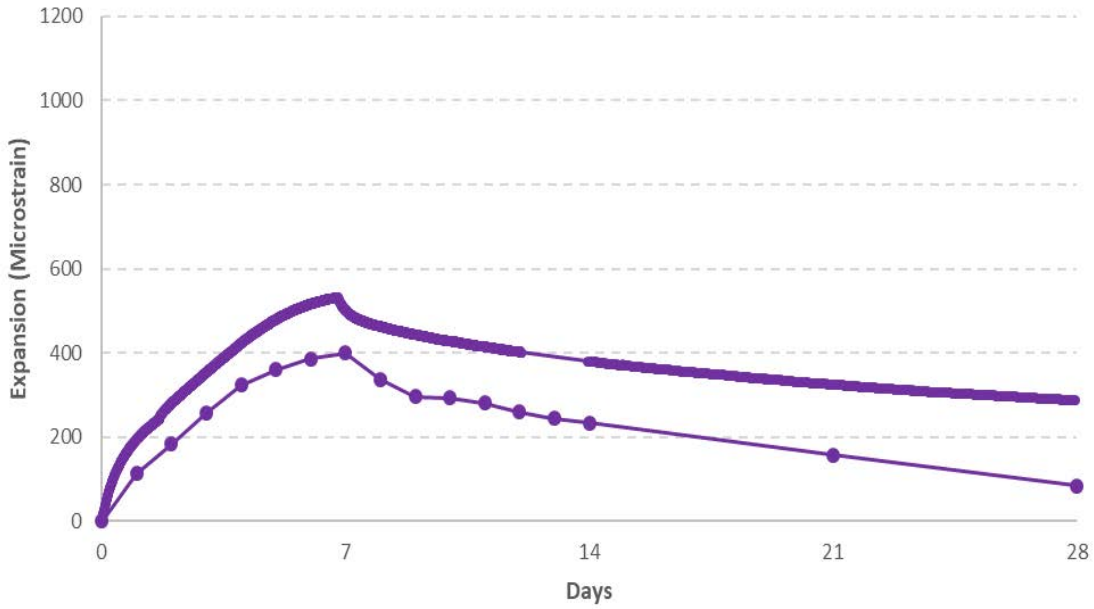

Figure 81: Overlay of Restrained Expansion Cylinder with ASTM C878 (19% Komponent®)

Figure 81 shows that for the 19% mix design, the difference between the expansion of the restrained 6”x12” and the ASTM C878 specimens is larger than for the 15% or 17% mixes. One other notable trend from Figure 81 is that after 7 days, the rate of shrinkage is more rapid for the C878 specimens than for the restrained 6”x12”. This is likely due to the SA/V ratio differences between these types of specimens.

Figure 82 shows the overlay of the VWSG data with the C878 data for the 21% replacement batch.

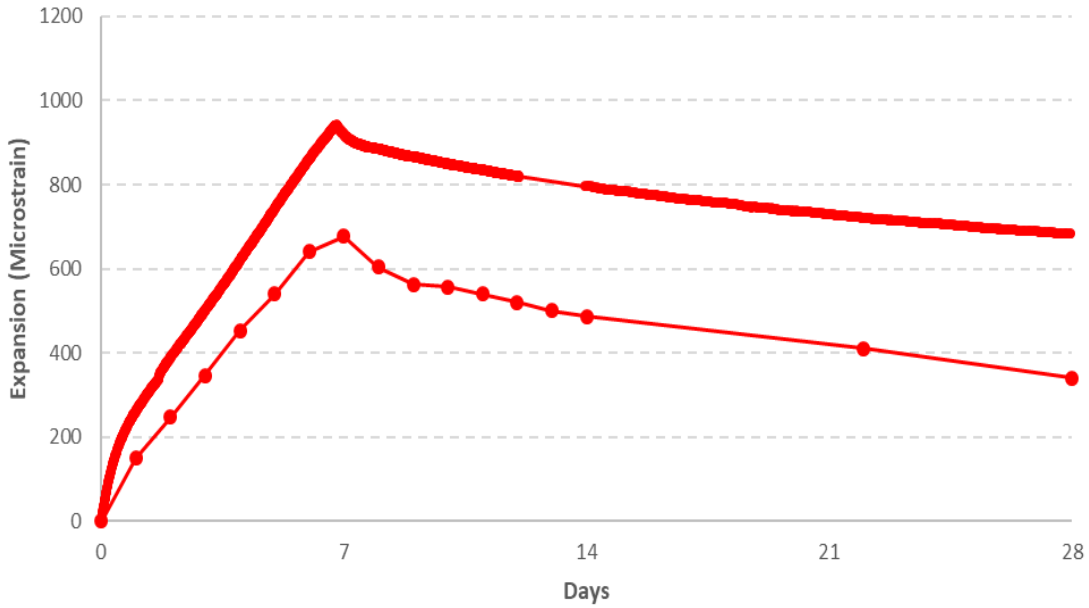

Figure 82: Overlay of Restrained Expansion Cylinder with ASTM C878 (21% Komponent®)

For the restrained specimens, the maximum expansion is lower than the corresponding unrestrained specimen for every percentage replacement. This could possibly support the two-stage expansion theory, because external restraint would drive more of the expansion into the internal void spaces, thus reducing the measured expansive strain. Second, the specimens with greater percentages of Komponent® are observed to have a steeper curve for the first 7 days of their life. Third, the SA/V ratio seems to have the effect of causing increased shrinkage; once wet cure ends, the ASTM prisms experience more aggressive shrinkage overall compared to the restrained cylinders. The 17% C878 specimen is an exception. At an age of 14 days, it rebounds from the shrinkage regime and begins to expand again. This was due to a major increase in humidity in the environmental chamber due to the activation of wet-cure on a set of restrained columns, a consequence of the curing alternative which was chosen (the continuous sprinkler system). This behavior was noted throughout the entirety of the

experiment – slight increases in humidity even weeks into curing caused an immediate recovery of positive strain.

The trend of the VWSG and the ASTM tests agreeing at lower percentage replacement mixes but deviating at higher ones was noted for the restrained specimens, similar to the unrestrained specimens. Since this behavior was identical, it can be reasonably inferred it is being driven by the same factors. There is one important difference, though. For the 21% Komponent mix, the difference in max expansion between the VWSG and ASTM test was less for the restrained specimens compared to the unrestrained ones. This behavior could possibly be explained as being the result of a combination of size effects coupled with the external restraint driving more of the expansion into the interior void spaces, which might cause the differential in maximum expansions to be driven down. More research would be needed, however, to determine the root cause of this behavior.

5.7 Comparing Expansion of Restrained Columns

5.7.1 Cured with Cardboard Forms in Place

Figures 83 and 84 show overlays of all the data gathered for the restrained expansion columns that were cured with the cardboard forms in place during the 7 day wet-cure period. The data in each plot is grouped by mix design, so that the effect of the variation of the stiffness of the restraint frame is evident. The color coding system is the same as all previous plots.

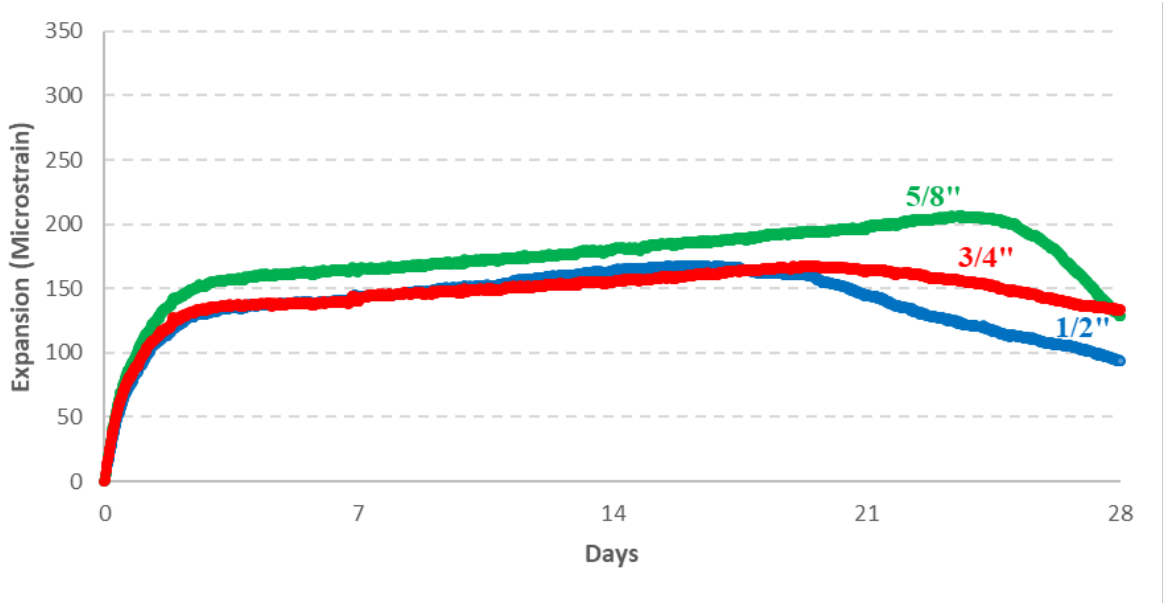

Figure 83: Restrained Column Expansion Results with Forms Left in Place (All Restraint Rods, 15% Komponent)

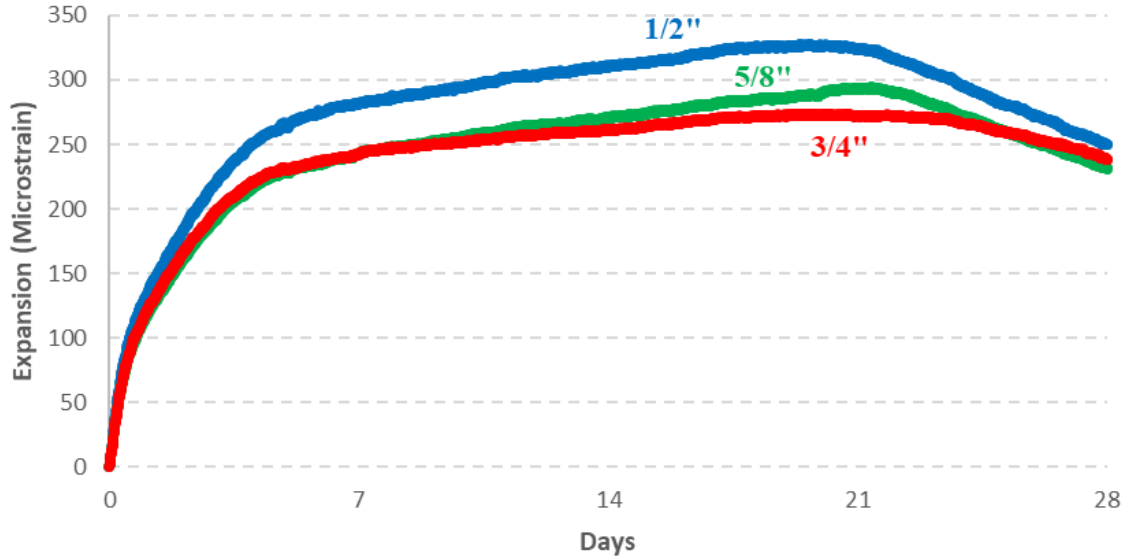

Figure 84: Restrained Column Expansion Results with Forms Left in Place (All Restraint Rods, 17% Komponent)

Type K SCC normally trends upward in a curvilinear manner for the first 7 days, at which point it reaches its maximum expansion when wet-cure is terminated. After the 7 day mark, the curve should begin to trend downwards again because drying occurs.

But the shrinkage region of the curve is typically far less aggressive than the initial expansion. It is clear from Figures 83 and 84 that leaving the cardboard forms on the restrained columns completely disrupted the trend defined by ASTM's C157 and C878, as well as VWSG cylinders. Because the forms were not removed when the water was drained out of the PVC jackets, and since the cardboard remained wet for days after this point, the concrete continued to gradually hydrate well past the intended wet cure period. One reason that the cardboard forms remained moist was because the drain on the PVC jacket was installed one inch from the bottom of the column. This left a small reservoir of water at the base which was continually wicked up by the cardboard. This resulted in three unintended consequences:

(1) The peak expansion did not occur at an age of 7 days. Due to the continued hydration, the maximum expansion varied between ages from around 20 days to 25 days.

(2) Because the cardboard forms dried slowly, the concrete columns also dried exceptionally slowly. Thus, there was no well-defined "peak" where the expansion regime ended and shrinkage commenced. The curve formed a somewhat flat elongated hump.

(3) Because the concrete bonded intimately to the cardboard form, an unintended and unrealistic source of restraint was added to the specimen. Instead of experiencing external restraint concentrically at its end only, each column now essentially experienced a continuous "skin friction" of sorts around its entire circumference. This disturbed the data by providing resistance that reduced the rate at which the column shrank (because it was

bonded to the cardboard, which does not shrink in the same manner concrete does – see Figures 83 and 84).

For these reasons, it was decided that the first curing alternative did not accurately isolate the variables of interest and no longer acted as an analog to a slab-on-slab interaction in the manner it was originally intended. Therefore, the restrained columns with 15% and 17% Komponent® mixes were repeated using the second curing alternative, which was also used for all the other remaining restrained columns.

5.7.2 Cured with Sprinkler System

This section shows overlays of all the data gathered for the expansion of the restrained columns, that were cured with the sprinkler system during the 7 day wet-cure period. The data is presented with plots comparing the columns both on the basis of the stiffness of the restraint system (for a given mix design) and on the basis of the percentage of Komponent® replacement in the mix (for a given restraint stiffness). As is standard in this work, when comparing mix designs, red represents ¾" rods, green 5/8" rods, and blue ½" rods. When comparing restraint conditions, red represents 21% replacement, purple 19% replacement, green 17% replacement, and blue 15% replacement. Figure 85 shows the overlay of the VWSG data for all restraint levels for the 15% restrained columns.

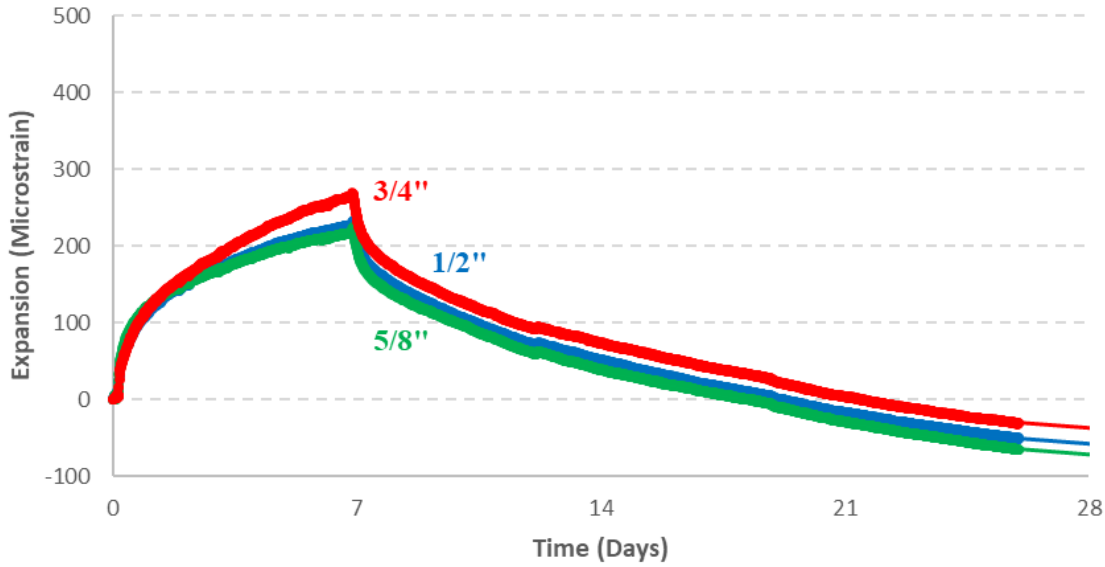

Figure 85: Restrained Column Expansion Results with Sprinkler Curing (All Restraint Rods, 15% Komponent)

In Figure 85, the curves are not stacked in a discernable order, but they are clustered very tightly together. In other words, there is very little difference apparent between the expansion resulting from restraint frames of drastically different stiffness. This indicates that at a very low level of Komponent® replacement, all three boundary conditions are too stiff for significant differences in expansion to be observed between restraint stiffness levels.

Figure 86 shows the overlay of the VWSG data for all restraint levels for the 17% restrained columns.

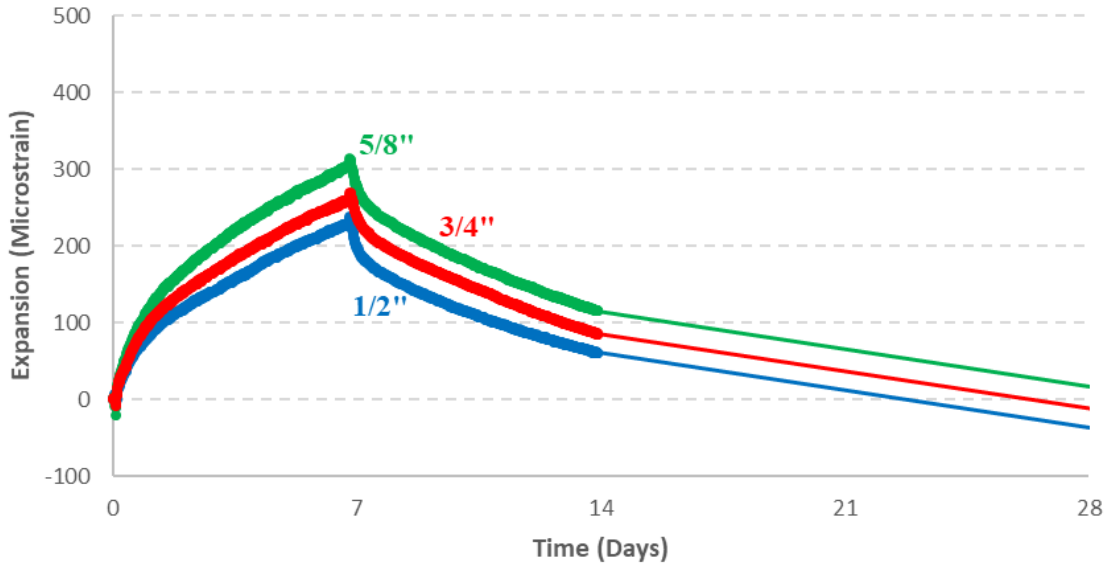

Figure 86: Restrained Column Expansion Results with Sprinkler Curing (All Restraint Rods, 17% Komponent)

In Figure 86, the curves are still not stacked in a discernable order. Instead of the ½" curve showing the highest expansion, followed by the ⅝" and finally the ¾", the ⅝" and ¾" curves both lie higher than the ½" curve. The reason for this discrepancy is not known at this time, although it might have something to do with the gypsum cement capping compound. This product was used to create a level bearing surface for the load cell. This compound generally set fairly fast; by the time that the final columns were being capped, the first column's leveling compound was usually set firmly. However, in an effort to commence wet-cure in as timely a manner as possible, the sprinkler system was turned on immediately after the capping of the last column. This was the case for both the 15% and 17% columns cast with the sprinkler system. It was discovered late in this research that if the water was turned on too soon, and the compound on the columns capped last was too soft, the running water further delayed the gypsum cement from setting. This delay could possibly last for hours. The gypsum cement still being soft

allowed free expansion of the column, with almost no restraint being exerted on it by the frame or by the capping compound. Importantly, the order used when casting the columns always went from lowest restraint to highest restraint for each mix, because that was the order the frames were placed in. Thus, the ½" column was always cast first, followed by the ⅝" and ¾" columns. The entire capping process took around 5-10 minutes. This means that by the time the water came on, the leveling compound for the ½" column had been set for at least 15 minutes, but for the other two restraint frames, the compound had been there 10 minutes or less, and may not have been completely set. This means the ⅝" and especially the ¾" columns would have the opportunity to expand more than the ½" columns, because they were expanding into the soft medium of the capping compound instead of a more rigid boundary condition. This is especially impactful at such an early age, because that is when the system is the most sensitive to disturbances. These facts may help explain Figures 84 and 85, and may be the most likely factors that resulted in the observed trend of the ⅝" and ¾" curves showing higher expansion, relative to the ½" curve.

Finally, Figure 86 shows more spread between the curves than Figure 85 did. This also helps to reinforce the idea that higher Komponent® mixes provide more potential for extra expansion, which serves to cause greater differences in expansion for boundary conditions with different stiffness.

Figure 87 shows the overlay of the VWSG data for all restraint levels for the 19% restrained columns. For the 19% and 21% columns, the issue with the gypsum cement leveling compound had been discovered, and more care was taken to allow the capping compound to set on all the columns before proceeding to turn on the water

system.

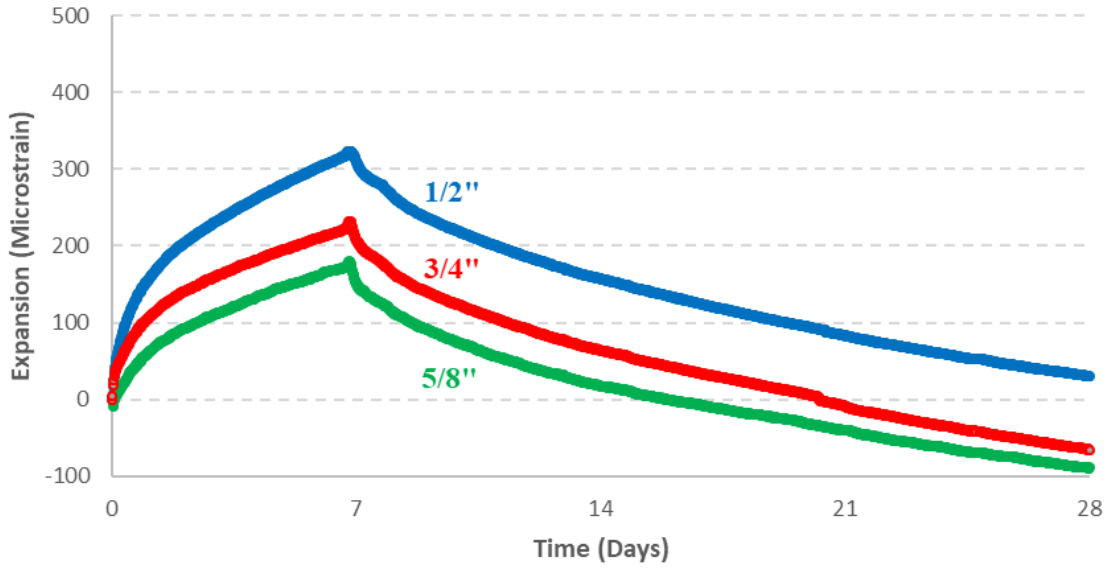

Figure 87: Restrained Column Expansion Results with Sprinkler Curing (All Restraint Rods, 19% Komponent)

Figure 87 shows two very important trends. First, at 19% replacement, the range of data between the curves at any given time is even greater than at 17% replacement. Second, once care was taken where the leveling compound was concerned, the ordering of the trends is much closer to what would be expected according to the principles of engineering mechanics; the ½" curve reaches an expansion nearly 100 microstrain higher than the next curve. Although the ¾" curve is still higher than the ⅝" curve, these curves are only separated by about 30 microstrain, less than 1/3 of the gap between the top two curves. At 7 days, there is a 92 microstrain gap between the ½" and ¾" curves, and by 14 days, that gap is equal to 94 microstrain. This means that the ¾" curve is descending slightly more steeply and thus is shrinking slightly faster than the columns restrained by the ½" rods. Similarly, at 7 days, there is a 53 microstrain gap between the ¾" curve and the ⅝" curve. By 14 days, that gap has been reduced to 47

microstrain, which indicates that the column restrained by the ¾" rods is shrinking slightly more than the other two columns. This would tend to support the conclusion that stiffer external restraint causes more aggressive shrinkage, but it must be understood that, according to this data, it is by a very slight margin. The reason that the ¾" curve still shows higher expansion than the ⅝ curve is not known at this time. The age and manner in which the columns are capped could be contributing factors, but this would require future research to determine.

Figure 88 shows the overlay of the VWSG data for all restraint levels for the 21% restrained columns.

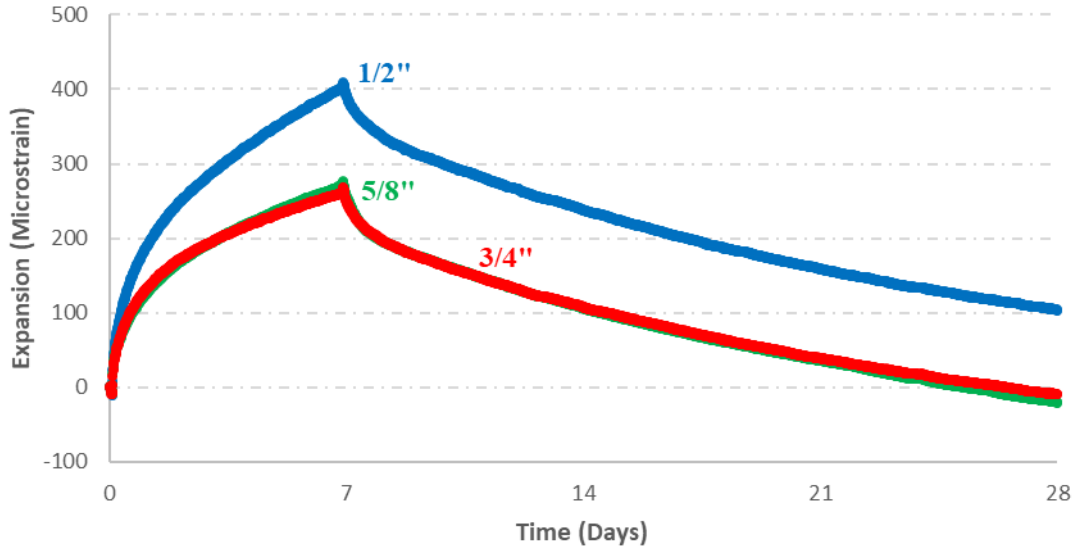

Figure 88: Restrained Column Expansion Results with Sprinkler Curing (All Restraint Rods, 21% Komponent)

Figure 88 shows the greatest differential in maximum expansion between the ½" frame and the other frames, of between 132 and 140 microstrain. This spread is once again greater than the spread associated with the next highest replacement mix design. Interestingly, for the 21% replacement mix, the columns associated with the ⅝" and ¾" frames are almost exactly the same, with the ⅝" curve only 7 microstrain higher at

exactly 7 days. This is the first mix for the restrained columns that displays the expected ordering of the trends, though, the two higher restraints are practically at the same level of expansion. For the purpose of comparing trends relating to the maximum expansions of the restrained columns at 7 days, as well as the spread between the curves as a function of both restraint level and mix design, Table 8 presents expansion data gathered from Figures 85-88 at both 7 and 14 days.

Table 8: Comparison of Variation Between Column Expansion Curves

	15%			17%		
Spread between curves	***1/2"-5/8"***	***1/2"-3/4"***	***5/8"-3/4"***	***1/2"-5/8"***	***1/2"-3/4"***	***5/8"-3/4"***
7 day spread	8	36	44	76	31	45
14 day spread	12	23	35	55	25	30
Average spread	10	29	39	65	28	37

	19%			21%		
Spread between curves	***1/2"-5/8"***	***1/2"-3/4"***	***5/8"-3/4"***	***1/2"-5/8"***	***1/2"-3/4"***	***5/8"-3/4"***
7 day spread	144	92	53	133	140	7
14 day spread	140	94	47	131	131	1
Average spread	142	93	50	132	135	4

Table 8 shows that, in general, the most consistent trend is that the spread between the ½" curve and the other two curves, ¾" and ⅝", always increases with increasing Komponent®. At 15%, the spread is 8 and 36 microstrain between the ½" / ⅝" and ½" / ¾" curves, respectively. At 17%, those gaps increase to 76 and 31 microstrain, at 19% they increase to 145 and 92 microstrain, and at 21% they increase to 133 and 140 microstrain. This same trend holds true when comparing the spread between the ⅝" curve and the other two curves, up until 21%, where instead of gapping, the ⅝" and ¾" curves are essentially overlaid. This means that, for the most part, increasing Komponent® not only increases peak expansion, but also increases the

spread between the expansion of columns at the same levels of external restraint. This indicates that this may be a non-linear system, because if the system were linear, increasing the Komponent® content would increase the expansion of all three columns uniformly, and the spread therefore would not vary.

Figure 89 shows the overlay of the VWSG data for all mix designs, for the restrained columns in the frames with 1/2” restraint rods.

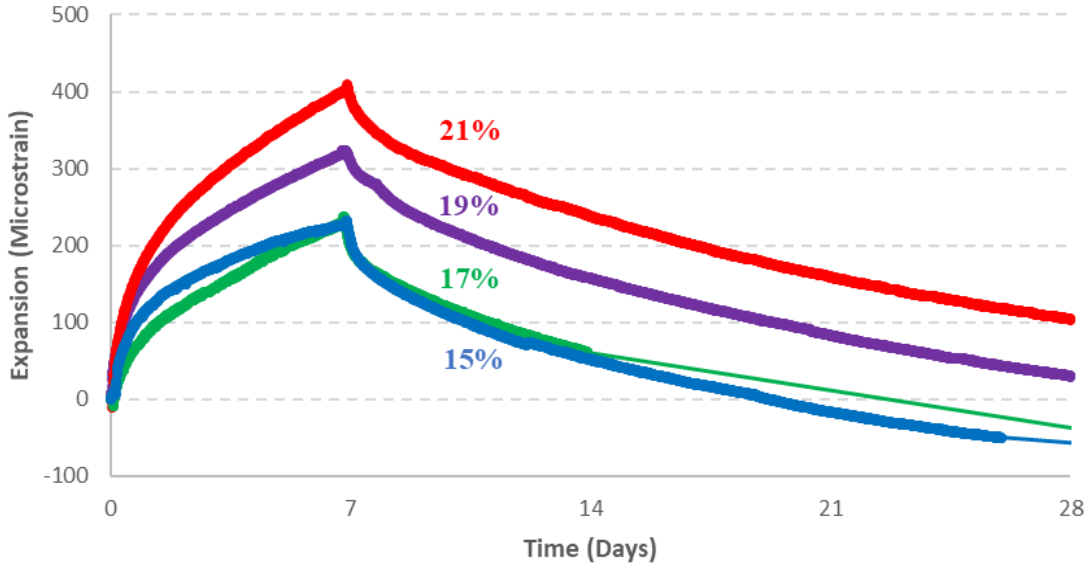

Figure 89: Restrained Column Expansion Results with Sprinkler Curing (1/2" Restraint Rods, All Mix Designs)

When comparing the columns by mix design instead of restraint level, the trend matches the behavior expected according to mechanics almost perfectly. The 21% mix exhibits the highest expansion, followed by the 19% and finally the 17% and 15%, which lie very close to one another. At 7 days, the spread between 21% and 19% is 85 microstrain, the spread between 19% and 17% is 86 microstrain, and the spread between 17% and 15% is 6 microstrain. Additionally, based on the spread later in time, it is apparent that curves remain nearly parallel, meaning that they are shrinking due to

drying at around the same rate. This data may further support the theory that somewhere above 17% Komponent®, a saturation point is reached where enough of the voids fill up that any additional expansion results in significant spread between the peak length change of the members from different mixes. To determine whether this is the case, more mixes would need to be conducted with percentage replacements at a finer increment above 17%.

It is also interesting to note that in Figure 89, there is a marked change in slope of all 4 curves at around 2 days, where the slope decreases significantly, and the curves begin to round off more. The reason for this abrupt change in slope is not known for certain, but it may have to do with the chemistry of the concrete. The hydration of Type K cement produces both ettringite and belite. It is possible that the initial more rapid expansion is motivated by ettringite production, while the remaining expansion is fueled by production of belite. This mechanism is not known for certain, however.

Figure 90 shows the overlay of the VWSG data for all mix designs, for the restrained columns in the frames with 5/8” restraint rods.

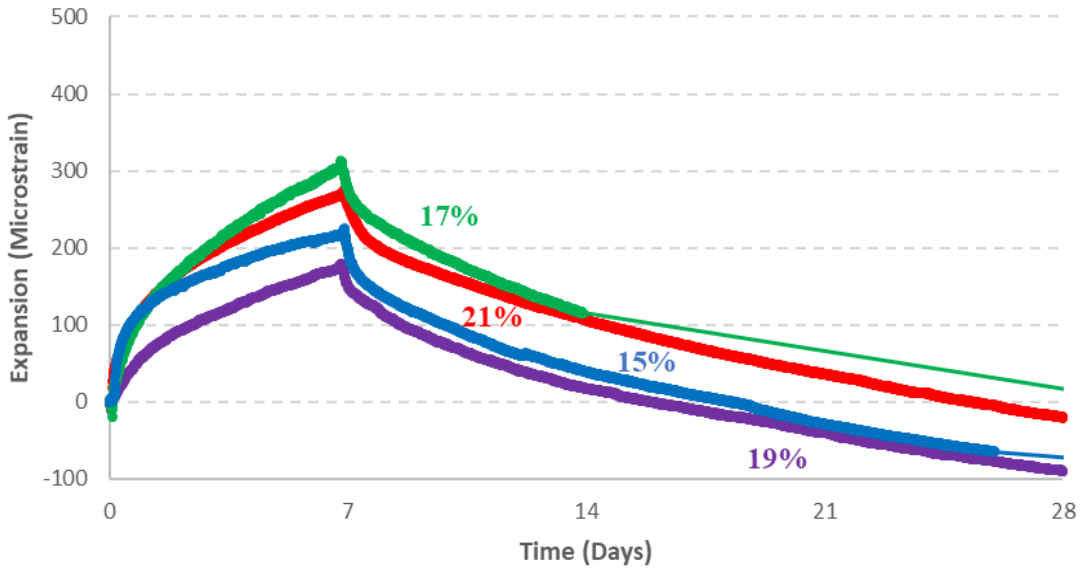

Figure 90: Restrained Column Expansion Results with Sprinkler Curing (5/8" Restraint Rods, All Mix Designs)

In Figure 90, the trends do not fit the ordering that would be expected based on mechanics, but it should be noted that the spread between these curves is significantly reduced compared to Figure 89. In other words, a substantial increase in the stiffness of the restraint frame causes the differences in expansion due to the mix designs to be greatly reduced. In this case, there is a total spread, from the highest curve to the lowest curve, of 134.6 microstrain. This is 42 microstrain less than the total spread from the ½" restraint, which was 176.5 microstrain (see Figure 89). Just like in Figure 89, there is a sudden shift in the slope of the curves at between 2 and 3 days, where the curves round off and the rate of expansion drops somewhat. This may have to do with a change between the production of ettringite and belite.

Figure 91 shows the overlay of the VWSG data for all mix designs, for the restrained columns in the frames with ¾" restraint rods.

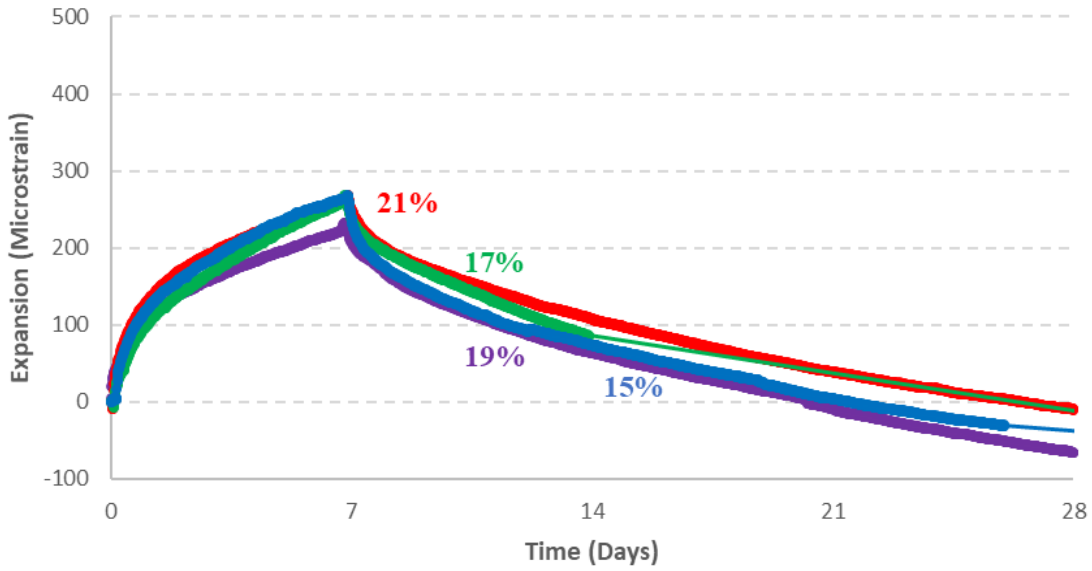

Figure 91: Restrained Column Expansion Results with Sprinkler Curing (3/4" Restraint Rods, All Mix Designs)

In Figure 91, which shows the column expansion data at the highest level of restraint, the curves for all 4 mix designs are, for all practical purposes, on top of one another. At 7 days, the total spread between the curves with the highest and lowest Komponent® is only 37 microstrain, and three of the curves (21%, 17%, and 15%) fall within 0.50 microstrain of one another at that time. Considering that VWSG can only measure to an accuracy of 1 microstrain, this indicates that, within the accurate range of these instruments, three of the four curves hit exactly the same peak expansion. The level of spread in peak expansion due to the increased percentage of Komponent® has been almost completely eradicated because of the extremely stiff boundary condition. One observation worth noting, however, is that despite the stiffness of the frame, which is 44% higher than a mature slab, a peak expansion of around 270 microstrain is still reached, and for the 21% mix, 0 strain is not reached until 28 days. This means that for the 21% mix design, shrinkage is completely eliminated until after full design strength

has been reached. This is partly due to the fact that although all four mixes have little spread at 7 days, the 21% mix shows a shallower slope in the shrinkage regime. This indicates that one advantage of increased Komponent® may be less rapid shrinkage, not just higher peak expansion. Table 9 shows a compilation of the spread values between the curves for Figures 89-91.

Table 9: Comparison of Variation Between Column Expansion Curves (Constant Restraint)

	1/2"			5/8"		
Spread between curves	***15% - 17%***	***17% - 19%***	***19% - 21%***	***15% - 17%***	***17% - 19%***	***19% - 21%***
7 day spread	6	86	85	89	-135	97
14 day spread	10	96	81	77	-99	90
Average spread	8	91	83	83	-117	93

	3/4"		
Spread between curves	***15% - 17%***	***17% - 19%***	***19% - 21%***
7 day spread	1	-37	37
14 day spread	12	-22	44
Average spread	6	-30	40

Table 9 reinforces the observation that the ¾" restraint frames result in, by far, the tightest grouping among the four mix designs. For the ⅝" and ½" restraint frames, the 19% and 21% mixes generally result in greater spreads than the 15% and 17% mixes.

5.8 Comparing Load Development of Restrained Columns

This section compares the load development registered by the load cells for the restrained columns with the various mix designs. The color coding system is the same as for all previous figures. The data presented for the 15% and 17% mixes is from the curing system where the jackets remained in place; this is due to the fact that the data

for these mixes, cast with the curing alternative 2, was lost when the data acquisition system failed. Figure 92 shows the load development data for the 15% restrained columns.

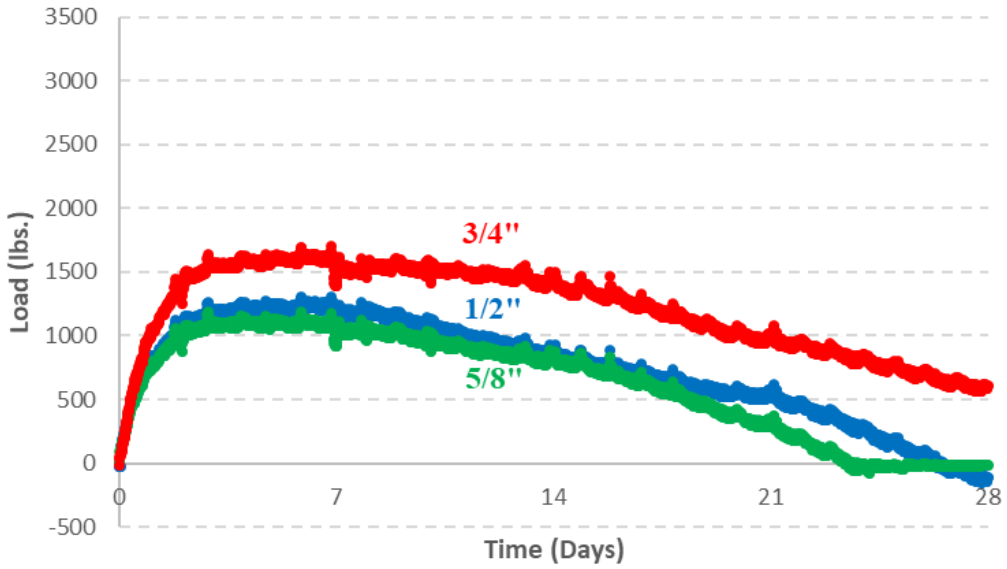

Figure 92: Restrained Column Load Development Results (All Restraint Rods, 15% Komponent)

The waves that appear on the curve in Figure 92 are due to diurnal temperature variations; note that there are 7 peaks in every 7 day time period. Because the insulation of the environmental chamber is imperfect, the daily temperature fluctuations cause noise in the data as the temperature of the water in the PVC jackets varies. As expected according to the principles of engineering mechanics, the ¾" restraint results in the highest load achieved, at around 1600 lbs. The ½" and ⅝" restraints produce less load, at around 1000-1250 lbs. Therefore, the spread between the ¾" curve and the other two curves is around 250 lbs for the ½" curve and 500 lbs for the ⅝" curve. It would be expected that the ⅝" restraint would produce more load than the ½" restraint, according to engineering mechanics. This trend was most likely disrupted by the jackets interfering with the true behavior of the specimens. Figure 93 shows the load

development data for the 17% restrained columns.

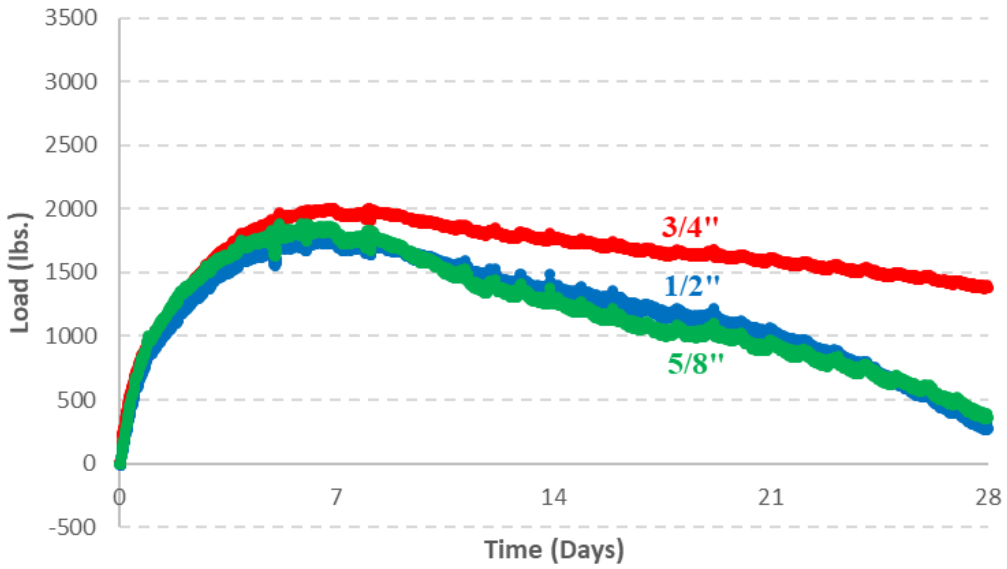

Figure 93: Restrained Column Load Development Results (All Restraint Rods, 17% Komponent)

As expected, the ¾" restraint results in the highest load achieved, at around 2000 lbs. The ½" and ⅝" restraints produce less load, at around 1700-1800 lbs. So at 7 days, the total spread between the curves is around 300 lbs, but by 28 days, this disparity has widened to around 1000 lbs. Again, the trend of the ⅝" curve not lying completely above the ½" curve was most likely disrupted by the jackets interfering with the true behavior of the specimens. In both Figures 92 and 93, the presence of the jackets changes the true behavior of the SCC material. Under normal circumstances, the load should peak sharply around 7 days, and then rapidly begin to decrease after that time. Because of the jackets however, three fundamental changes occur:

(1) The magnitude of peak expansion is affected by the extra restraint provided by the cardboard jacket

(2) The cardboard holds water, allowing hydration past 7 days, which in turn helps maintain load

(3) The cardboard form provides restraint against shrinkage, which also reduces the rate at which the load decreases

Figure 94 shows the load development data for the 19% restrained columns. These were cured using the sprinkler system, and therefore, they give a clearer representation of the expected material behavior.

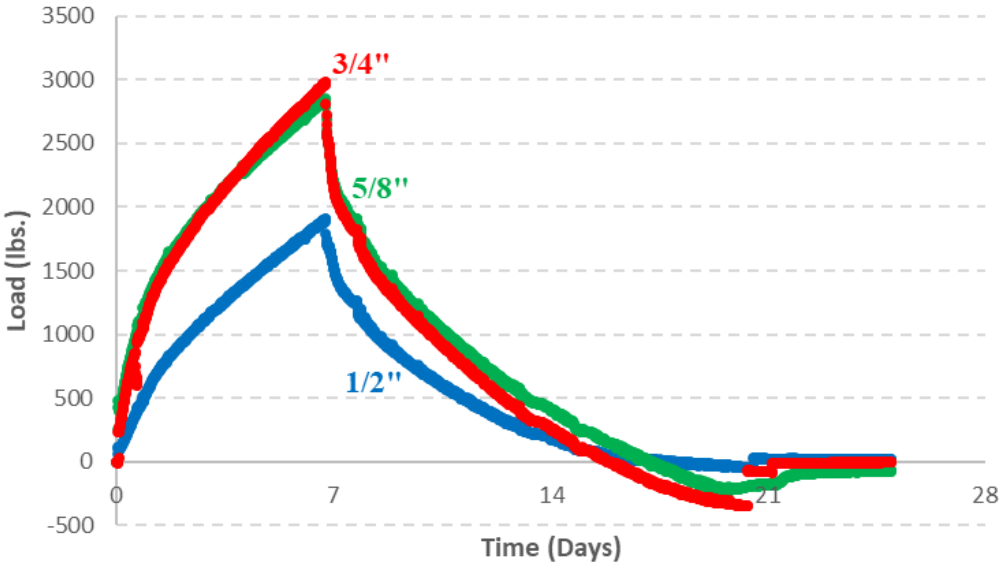

Figure 94: Restrained Column Load Development Results (All Restraint Rods, 19% Komponent)

In this case, the ¾" and 5/8" restraint frames reach very nearly the same peak loads, around 3000 lbs, with the ¾" slightly higher. The ½" curve is much lower, reaching a peak load of less than 2000 lbs. At 7 days, there is a 48 lb. difference between the ¾" and ⅝" curves, but a 673 lb. difference between the ⅝" curve and the ½" curve. By the time that the first curve reaches zero load, which is the ¾" restraint at around 16 days, the spread between the three curves is only 150 lbs. Therefore, the ¾"

frame reaches the highest load development, but it is also the curve which descends and loses load the most rapidly. Clearly, the lack of the interference of the jackets provides a smoother curve, with a peak at 7 days, and an immediate decrease in load from that point forward.

Figure 95 shows the load development data for the 21% restrained columns. These were also cured using the sprinkler system, and therefore, they also give a clearer representation of the appropriate material behavior.

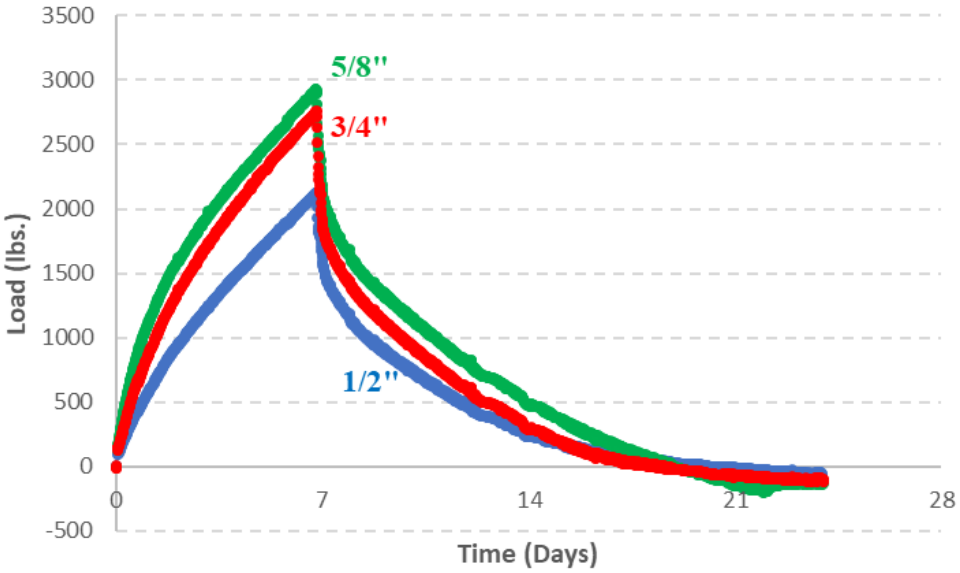

Figure 95: Restrained Column Load Development Results (All Restraint Rods, 21% Komponent)

Again, the ¾" and ⅝" restraint frames reach very nearly the same peak loads, this time between 2800-3000 lbs, with the ⅝" slightly higher. The ½" curve is much lower, reaching a peak load of just over 2000 lbs. At 7 days, the spread between the ⅝" and ¾" restraint curves is 170 lbs, and the spread between the ⅝" and the ½" curves is 804 lbs. At between 18 and 19 days, the ¾" curve reaches zero load, while the ½" curve is at around 40 lbs and the ⅝" curve is at approximately 30 lbs. It is also clear that the

behavior of these curves is very similar to the behavior of the 19% curves, because they were cured in the same manner.

Figures 96-98 compare the 15% and 17% columns, cast with the first curing system, to the 19% and 21% columns, cast with the second curing system. Note the difference in the shape of the curves; the 15% and 17% curves are more elongate due to the jackets restraining their shrinkage, and/or the wicking action of the cardboard keeping the columns moist. Figure 96 displays the load development for the ½" restraint frames, with all 4 mix designs.

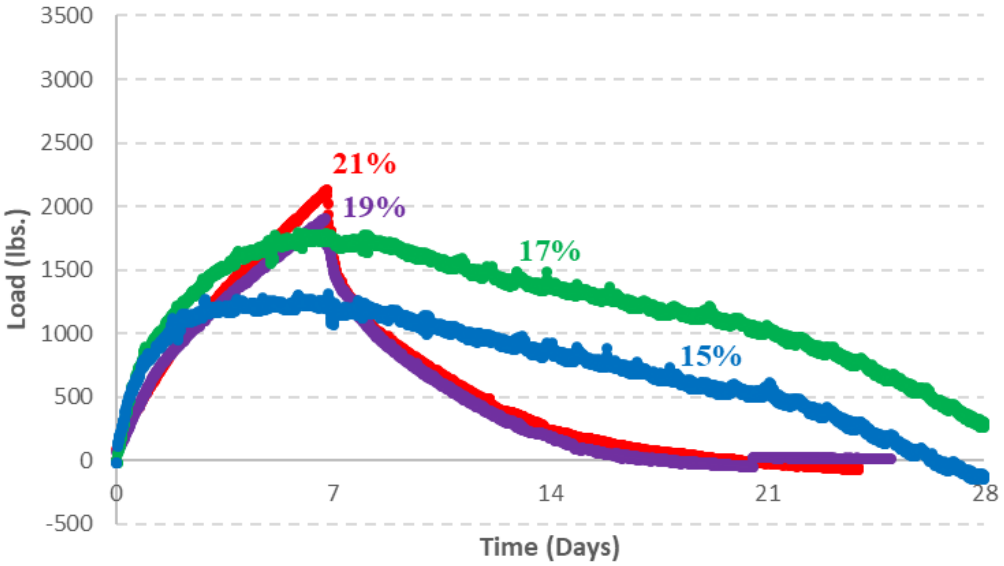

Figure 96: Restrained Column Load Development Results (1/2" Restraint Rods, All Mix Designs)

In Figure 96, the curves are layered in the exact order that would be predicted by engineering mechanics; 15% through 21% in increasing order, where the 15% curve reaches a maximum of around 1250 lbs, and the 21% curve reaches a maximum of around 2100 lbs. It is also apparent from Figure 96 that the first curing alternative was a failure due to the different curves produced for the 15% and 17% columns.

Figure 97 displays the load development for the ⅝” restraint frames, with all 4 mix designs.

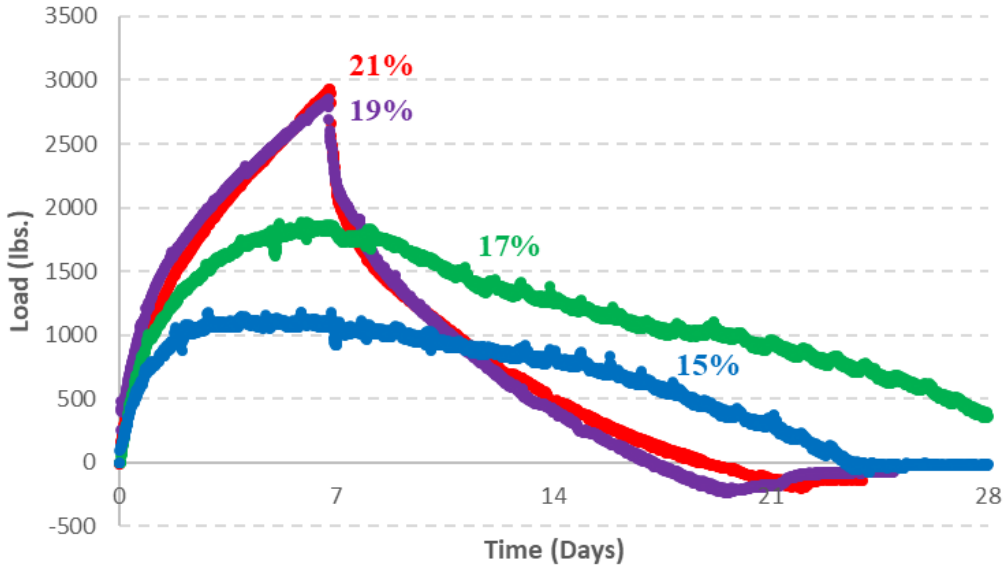

Figure 97: Restrained Column Load Development Results (5/8" Restraint Rods, All Mix Designs)

In Figure 97, the curves are still layered in the order predicted by mechanics, except for the fact that the 19% and 21% curves have approximately the same maximum load of around 2800-2900 lbs. The 17% and 15% curves accordingly follow in the expected order, lower than the 19% and 21% curves.

Figure 98 displays the load development for the ¾” restraint frames, with all 4 mix designs.

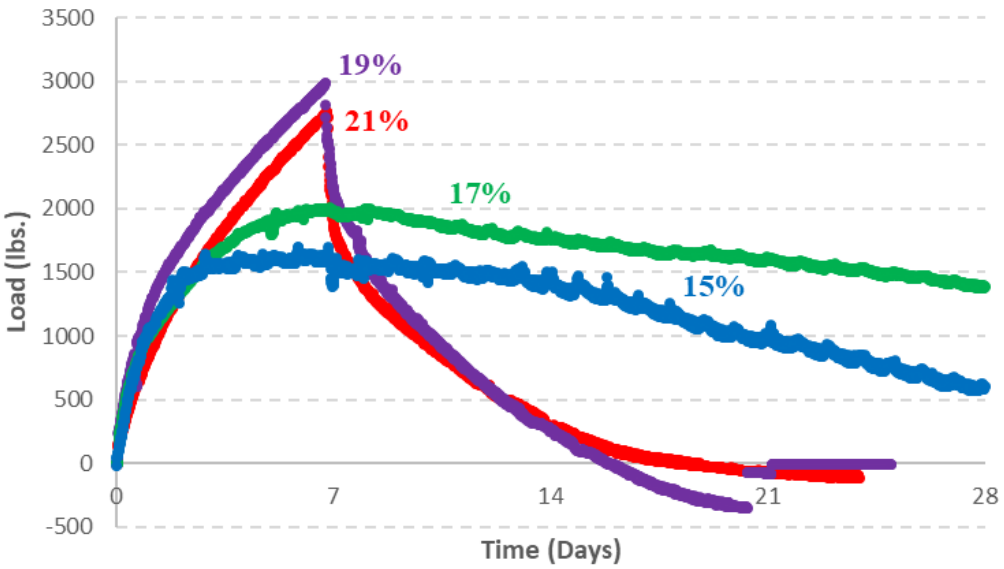

Figure 98: Restrained Column Load Development Results (3/4" Restraint Rods, All Mix Designs)

In Figure 98, the curves are mostly layered in the expected order, except for the fact that the 19% curve actually lies higher than the 21% curve, but only by a slight margin. The 19% curve just reaches 3000 lbs, while the 21% curve comes up shy of that mark, around 2750 lbs. After that, the 17% and 15% curves fall in the expected order, layered underneath the 19% and 21% curves.

5.9 Analyzing Self-Induced Stress-Strain Behavior

Shrinkage-compensating concrete made with Type K cement naturally expands when saturated during the curing process, because the hydration reaction fuels the growth of ettringite crystals within the concrete matrix. In this experiment, the restrained columns were equipped with VWSG's embedded in order to measure the strain caused by this expansive behavior. Additionally, the restraint frames were equipped with load cells so that the force caused by this expansive behavior could be quantified. Gathering both of these datasets simultaneously created an extremely unique

scenario. The material expanding against a passive restraint system was also creating an axial stress on itself. Since both load and strain data was being gathered, it was possible to plot the stress-strain curves induced by the material itself. This is an extremely rare phenomenon. With the exception of some preliminary work done by Seth Roswurm in 2013, to the best of the author's knowledge, there has never been any in-depth study of the stress-strain relationship of a concrete material which is being loaded by the reaction caused by its own growth.

A significant amount of data reduction had to occur in order to plot the stress versus the strain. The VWSG's collected strain data on a set interval, which was set to 15 minutes for these experiments. This provided excellent fidelity in the data, without producing an excessive amount of data. The Somat data logger used for the load cells had a sampling frequency of 0.1 Hz, or 1 reading every 10 seconds. Since the load cells ran for the same time period as the VWSG's, at a sampling rate of at least 0.1 Hz, the Somat produced roughly two orders of magnitude more data points than the VWSG did. For the 19% and 21% replacement batches, the sampling rate was set to 1 Hz, resulting in over two million data points being collected for each dataset within the testing period. In order for a meaningful stress-strain curve to be plotted, every strain data point must be paired with a stress data point that occurred at the same time step. This required a computer program that could selectively weed out the unwanted load values and pare down the dataset to load values occurring every 15 minutes, so that they could be matched up with the strain values from the VWSG. Initially, this was done using a macro script in Excel's VBA which stepped through the dataset, deleting the unwanted data points. This method was eventually deemed infeasible because it took nearly 10

hours to run through a third of the data from one set of columns. Because of this massive time requirement, the VBA code was scrapped and a simple set of Matlab commands was used to extract the desired values from the larger data set. Matlab performed this operation much more efficiently and significantly reduced the time requirement for the data reduction process.

Once the data had been reduced, load values and strain values could be matched up on the same time intervals and plotted versus one another to create the self-induced stress-strain curves.

5.9.1 15% and 17% Replacement

In order to produce meaningful stress-strain data, it was very important that the mechanical behavior of the concrete be interfered with as little as possible. For this reason, the primary curing system of soaking the columns with sprinklers was the only means used in this experiment that would reduce the interference with the columns enough to produce clean stress-strain data. Unfortunately, the corruption of the load data for the 15% and 17% mixes made it impossible to plot stress-strain data for these mixes.

5.9.2 19% Replacement

Figures 99-102 present the stress-strain curves for the restrained columns cast with 19% Komponent®. The color coding follows the previously established convention.

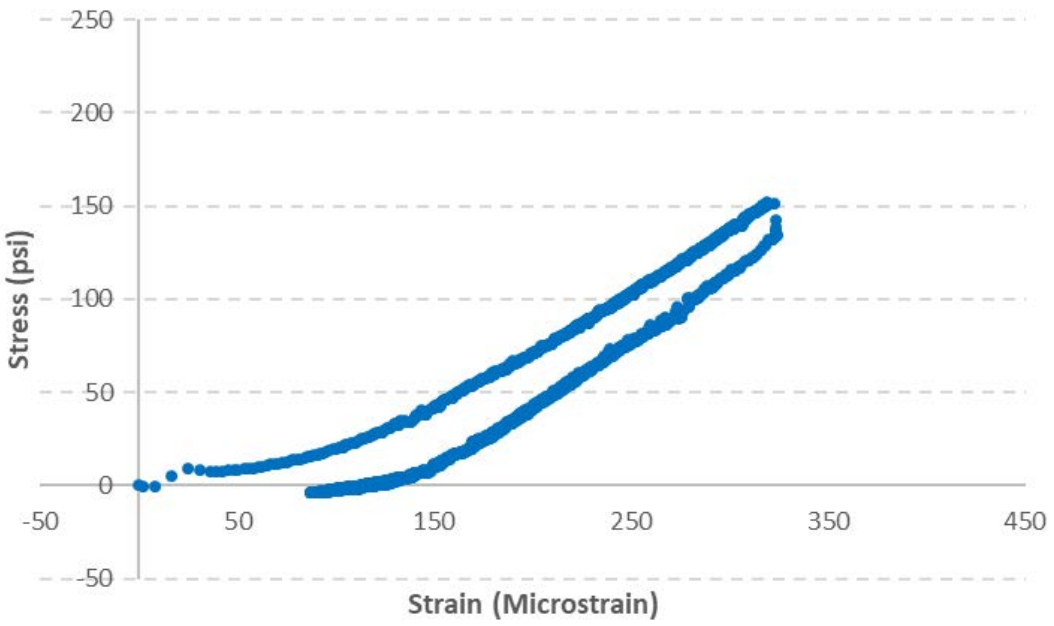

Figure 99: Restrained Column Stress-Strain Curve (1/2" Restraint Rods, 19% Komponent)

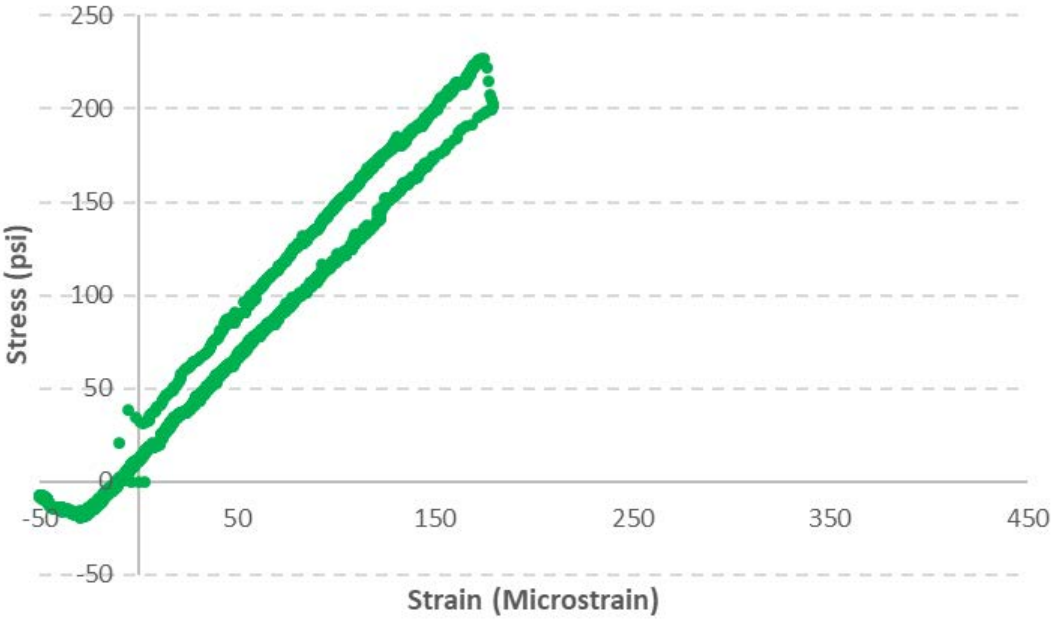

Figure 100: Restrained Column Stress-Strain Curve (5/8" Restraint Rods, 19% Komponent)

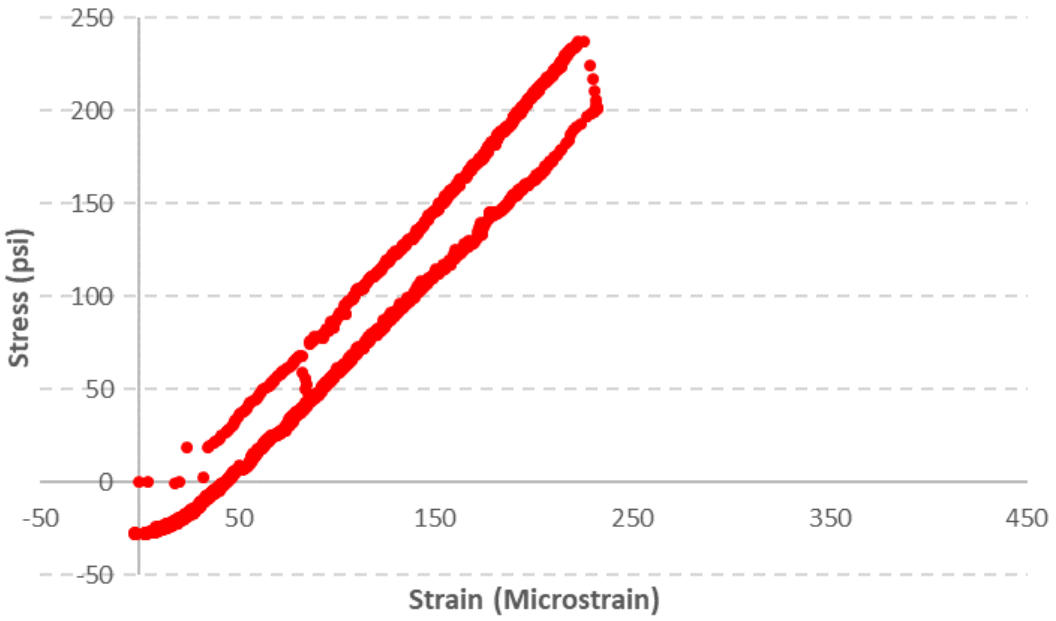

Figure 101: Restrained Column Stress-Strain Curve (3/4" Restraint Rods, 19% Komponent)

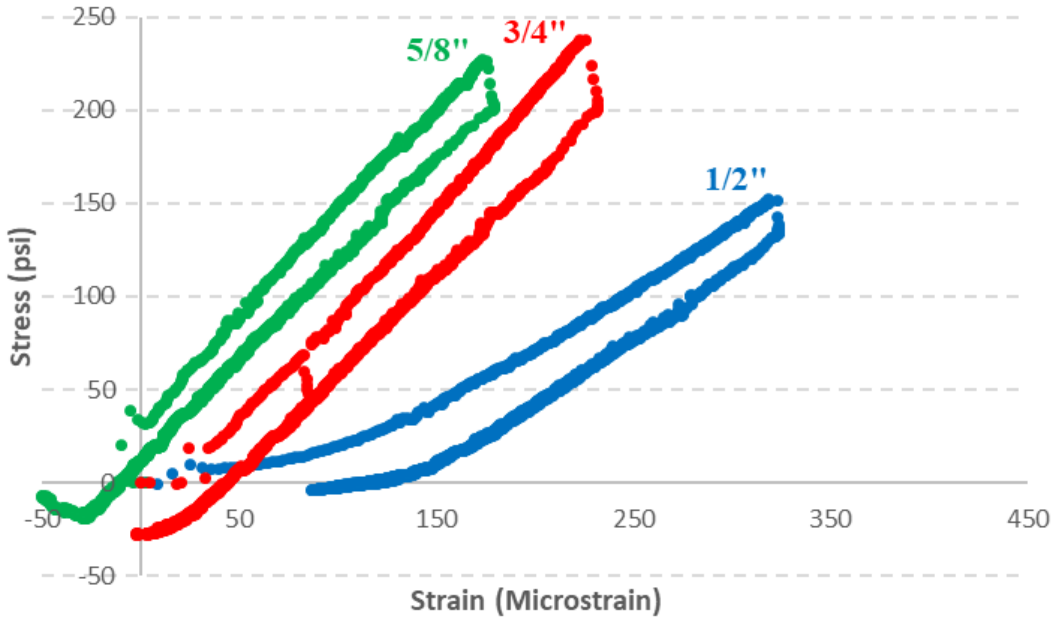

Figure 102: Restrained Column Stress-Strain Curves (All Restraint Rods, 19% Komponent)

Figure 102 shows a direct comparison of the three stress-strain curves for the

19% mix, at the three levels of restraint of the columns. The curve associated with the column in the ½" restraint frame is clearly shallower than the other two curves. This makes sense, because that means that it is reaching a higher strain at a lower stress, which is expected for a softer boundary condition. The other two stiffer frames have stress-strain curves with slopes that are nearly the same. Those curves also have hooks near the bottom, where negative stresses were induced as the columns shrank, due to the bond between the tops of the columns and the load cells. It is worth pointing out that the stress-strain curve for the 5/8" restraint frame may be incorrect at early age. Note that in Figure 100, the first strain reading is at 40 psi with zero strain, even though all pre-compression loads were kept near zero.

5.9.3 21% Replacement

Figures 103-106 present the stress-strain curves for the restrained columns cast with 21% Komponent®. The color coding follows the previously established convention.

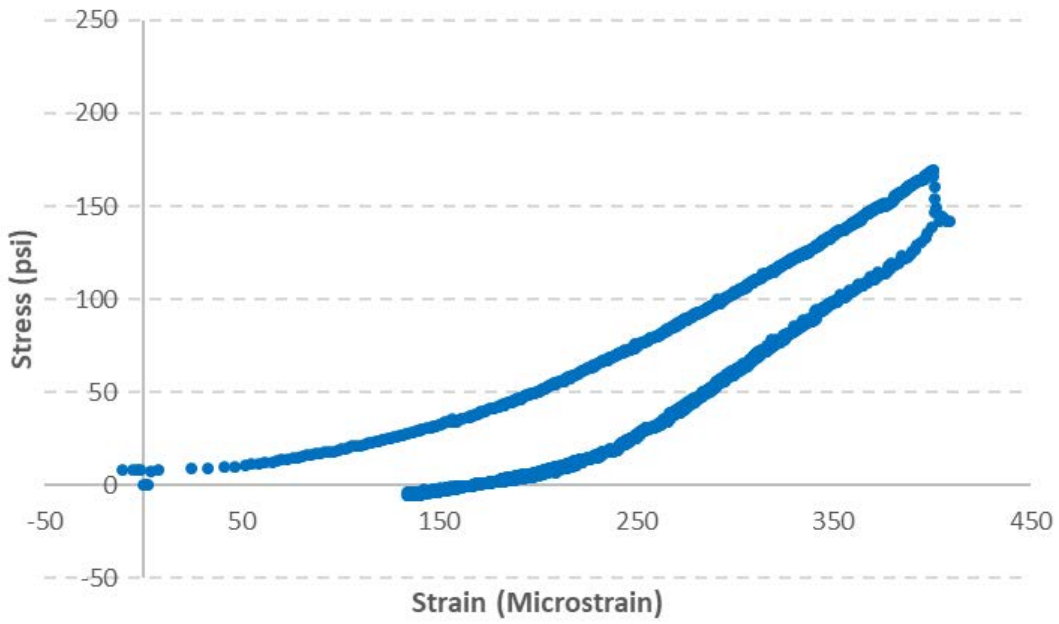

Figure 103: Restrained Column Stress-Strain Curve (1/2" Restraint Rods, 21% Komponent)

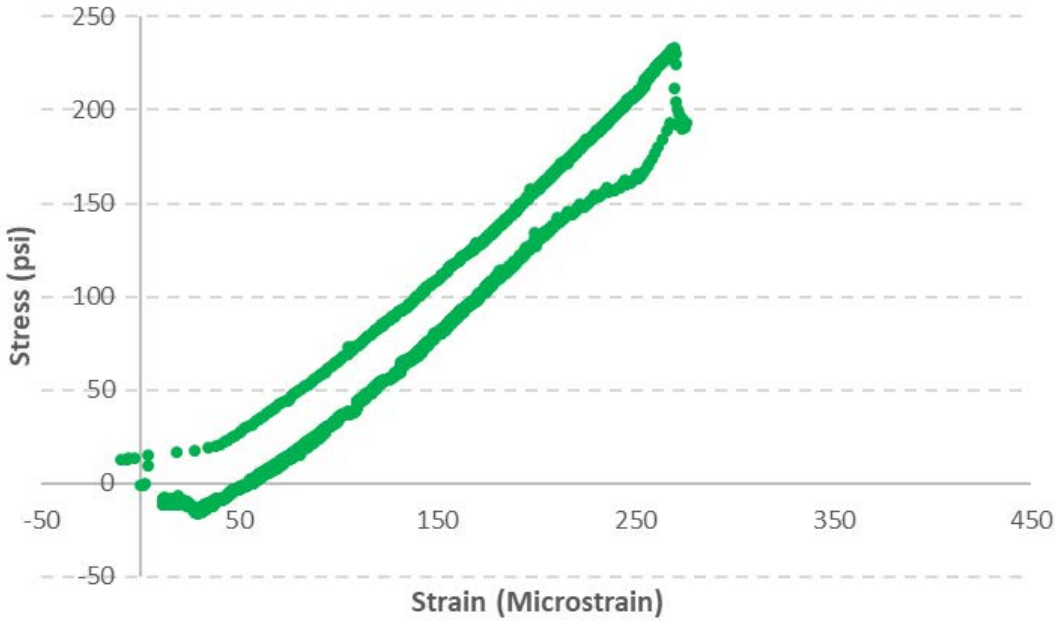

Figure 104: Restrained Column Stress-Strain Curve (5/8" Restraint Rods, 21% Komponent)

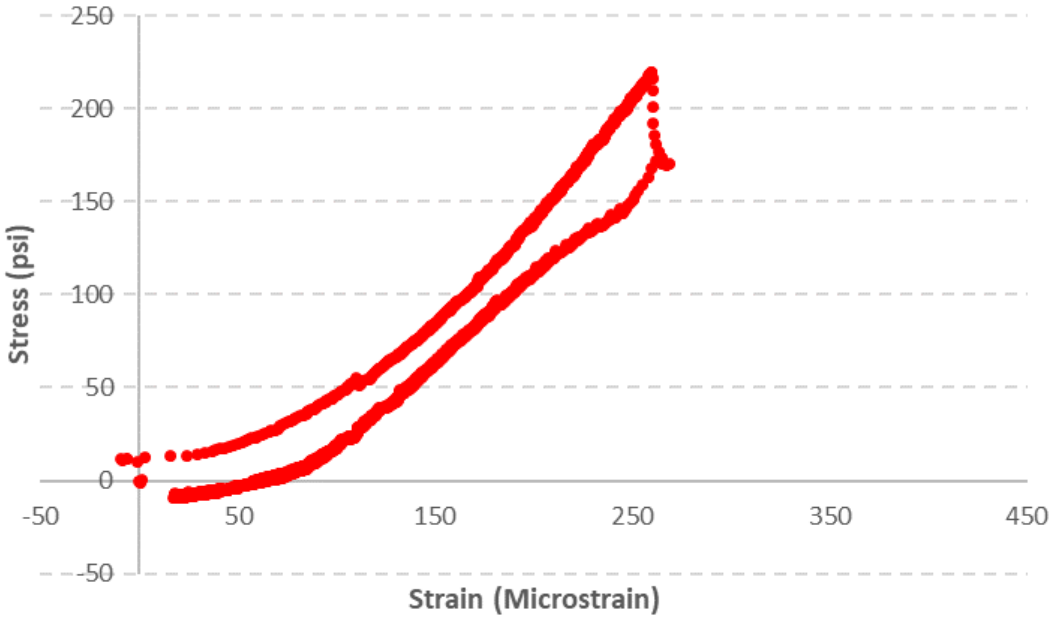

Figure 105: Restrained Column Stress-Strain Curve (3/4" Restraint Rods, 21% Komponent)

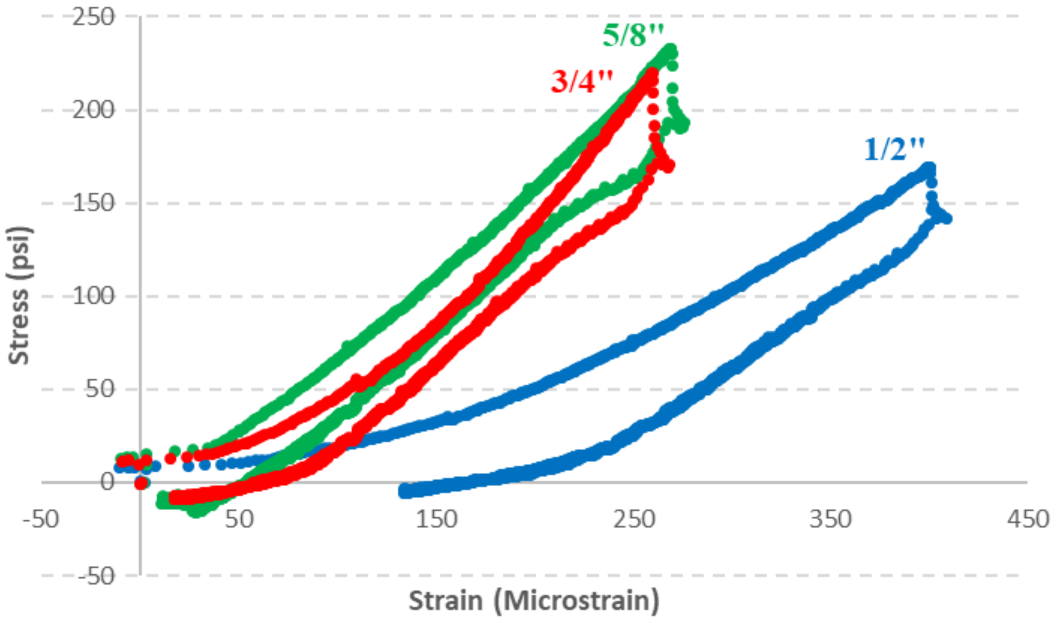

Figure 106: Restrained Column Stress-Strain Curves (All Restraint Rods, 21% Komponent)

Figure 106 shows a direct comparison of the three stress-strain curves for the 21% mix, at the three levels of restraint of the columns. The curve associated with the column in the ½" restraint frame is clearly shallower than the other two curves, just like for the 19% columns. In this case the slope of the ¾" curve is slightly steeper than the ⅝" curve. Again, this is reasonable, because the ¾" restraint frame is stiffer, which means that more stress should be developed at a relatively low strain. Since slope equals rise over run (or change in stress over change in strain), this results in a larger (or steeper) slope. Additionally, in Figure 106, it appears that the ½" curve encloses much more area than the ⅝" curve, which in turn appears to enclose more area than the ¾" curve. These areas were not quantified, however, due to the uncertain nature of whether that information would be useful.

5.9.4 Overlaid Curves by Level of Restraint

Figures 107 through 109 compare the stress-strain curves for the two mixes for a given level of restraint. Only the 19% and 21% mixes can be compared, as explained in section 5.7.1.

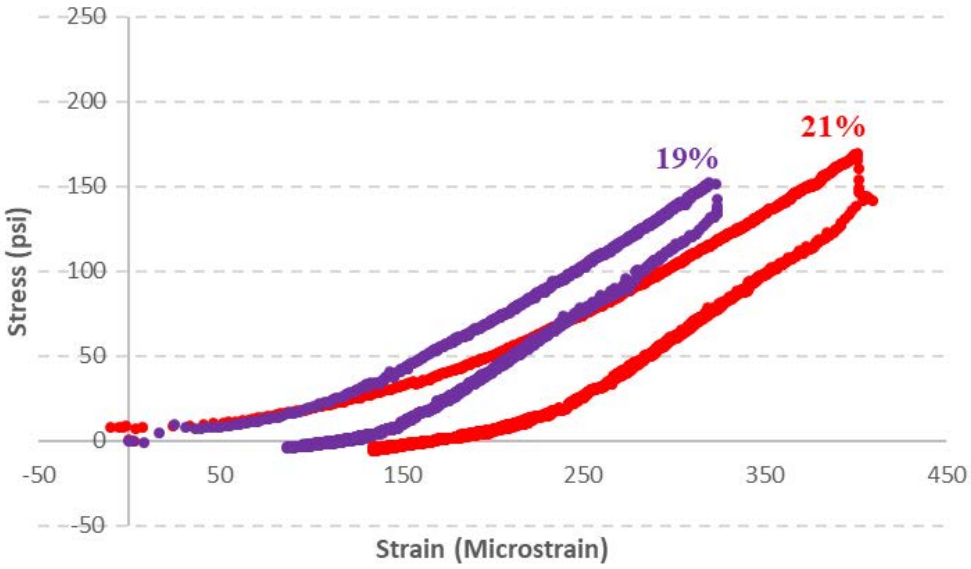

Figure 107: Restrained Column Stress-Strain Curves (1/2" Restraint Rods, 19% and 21% Komponent)

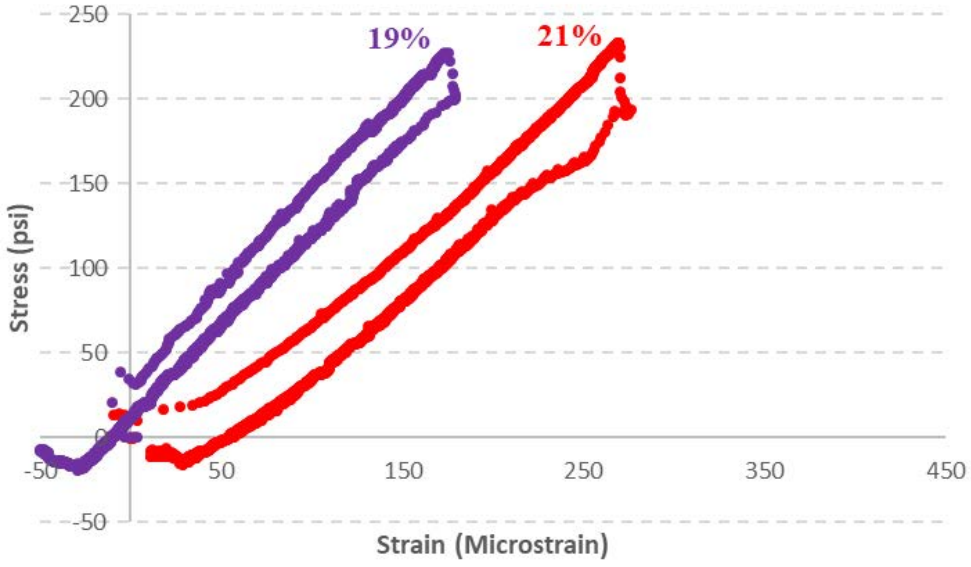

Figure 108: Restrained Column Stress-Strain Curves (5/8" Restraint Rods, 19% and 21% Komponent)

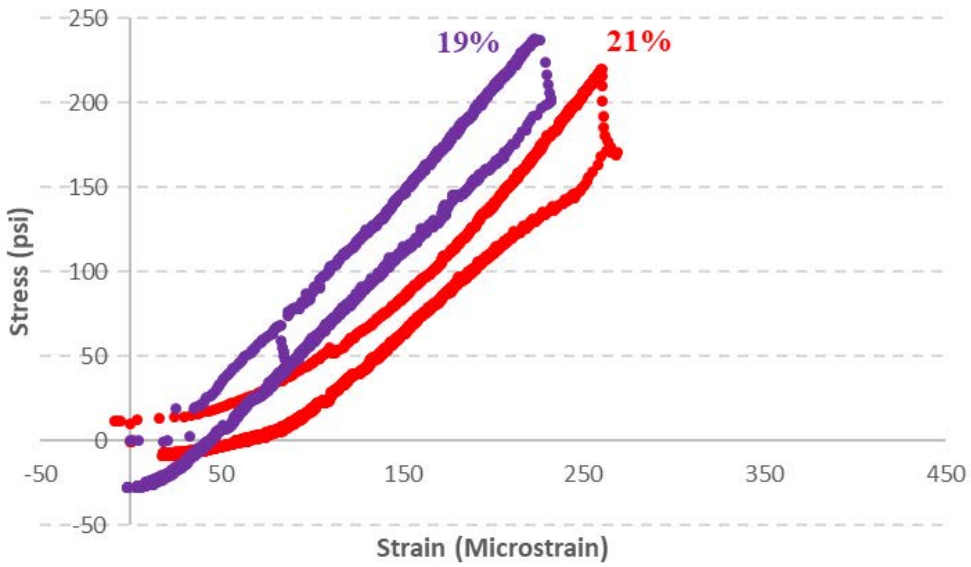

Figure 109: Restrained Column Stress-Strain Curves (3/4" Restraint Rods, 19% and 21% Komponent)

One interesting observation to make concerning Figures 107 - 109 is that, surprisingly, the 21% curves are in general less steep than the 19% curves. This is because the 19% and 21% curves attain approximately the same stress in each case, yet the 21% curves reliably attain that maximum stress at a far greater strain, compared to the 19% curves. This indicates that, perhaps, the effects of the restraint stiffness and the expansive potential of the concrete on the resulting strain in the concrete and reaction at the boundary condition are de-coupled to a certain extent. In other words, it is possible that the stiffness of the external restraint is the dominating influence on the load development behavior, while the expansive potential of the concrete (which is based upon the Komponent® content of the mix) is the dominating influence on the maximum length change of the specimen.

5.9.5 Meaning of Stress-Strain Curves

The stress-strain curves produced during this research raise many questions about the material behavior of shrinkage-compensating concrete, but the meaning of these results is still quite inconclusive. A stress-strain curve for a material generally shows an increase in stress for each incremental increase in strain during loading, and the curve then turns and tends towards zero stress during unloading. The path that the curve takes during unloading, however, depends on whether that material is linear-elastic (or on whether it is a material that has been loaded past its linear-elastic range). According to Hooke's Law, a linear-elastic material has a stress-strain curve that returns along the original path it was loaded on, and it returns to the strain it originally started at. If the material is loaded past its linear-elastic range, the unloading portion of the curve follows a parallel but offset path back to zero stress, and it does not return to zero strain. This offset produces an enclosed area, and the curve is referred to as a hysteresis loop. In engineering mechanics, the area enclosed by this curve is a measure of how much energy the material absorbed, due to the work done on it by the external load that caused the material to deform. This behavior indicates that this Type K SCC is behaving in an elastic but non-linear manner.

In this case, however, the meaning of the area enclosed by these self-induced hysteresis loops is much less clear. This is because the force that is acting on the specimen is not truly an external force; it is nothing more that the reaction of the frame, which is being caused by the expansion of the material itself. Thus, any energy that the material is absorbing is energy that was released when the material expanded, which intuitively makes very little sense. Therefore, the meaning of the area enclosed by these

loops, as it pertains to the expansion mechanism, is unclear at this time.

5.10 Overall Shrinkage Compensation

This research set out with the intent of determining whether Type K SCC can completely negate the effects of early age drying shrinkage. Specifically, this research set out to identify a mix design that could completely eliminate early age drying shrinkage, given realistic levels of external restraint due to the boundary conditions, and given realistic curing methods. In this context, "early-age" would refer to behaviors or effects that impact the concrete before it reaches its design strength.

After the first curing system was discarded due to inaccuracies and difficulties that have been previously described, it was determined that removing the column forms and curing the concrete with water sprayed from misters resulted in data that better represented the true behavior of the material. Additionally, this curing system is realistic, because it is very straightforward, feasible, and commonplace, for concrete to be water-cured in the field by simply soaking it continuously with soaker hose, misters, or soaked burlap or blankets.

Another goal was to identify a mix design that could offset early age drying shrinkage under a realistic boundary condition. Although many specimen types were studied in this experiment, the only ones that accurately depict the stiff external restraint that SCC would face in the field are the restrained columns with four ⅝" diameter rods. Of the 4 mix designs tested, the one that successfully prevented shrinkage for a full 28 days was the mix with 21% Komponent® replacement. Refer to Figure 57, which shows that the 21% mix did not return to its original length (net zero strain) until between 27 and 28 days under the highest degree of restraint, which is even 44% higher

than the theoretical midpoint of stiffness.

This means that for the 21% mix under realistic levels of restraint or higher, no tensile stress occurs due to shrinkage strain for the first 28 days. This essentially means that this mix design will prevent the concrete from cracking due to early age drying shrinkage (if early age is defined to be 28 days or younger). To put this in perspective, the following equation can be used to obtain a conservative estimate of the tensile strength of a concrete specimen, based on its modulus of rupture (MOR):

$$\boldsymbol{f_r = 7.5\lambda\sqrt{(f'_c)}} \qquad \text{(Equation 2: ACI 318-14)}$$

where,

f_r = modulus of rupture (psi)

λ = lightweight factor (unitless – 1.0 for normal weight concrete)

f'_c = compressive strength of concrete (psi)

From Figure 71, the 28 day compressive strength of the 21% mix was 5770 psi. Since SCC is normal weight concrete, $\lambda = 1.0$, and:

$$\boldsymbol{f_r = 7.5 * 1.0 * \sqrt{5770\ psi} = 570\ \text{psi}}$$

Therefore, the 28-day tensile strength of the 21% mix would conservatively be set at 570 psi. According to Figure 70, the lowest stress that was measured within the 28 day testing period was -9.5 psi, which is 9.5 psi in tension. In other words, the shrinkage of the concrete had produced a tensile stress on the concrete of just 9.5 psi in the early age period, which is less than 2% of the conservatively estimated tensile capacity. Therefore, it can be concluded that even under realistic boundary conditions, the right

SCC mix design can fully compensate for the effects of early age drying shrinkage, especially considering that mix designs higher than 21% Komponent® replacement can also be utilized, which is recommended as a future research topic.

5.11 Performance of VWSG

Overall, the VWSG's in this research were used with a good deal of success. The data showed good agreement between the 6"x12" cylinders equipped with VWSG and the ASTM prisms when it comes to small-scale material characterization. At this time, the divergence between the two at higher percentages of Komponent® cannot be explained with absolute certainty, but, on the whole, the VWSG equipped cylinders produced more smooth, reliable data than the ASTM prisms, and they did so without the chance for the user error and bias inherent to taking manual measurements. The only drawback to the use of the VWSG was the fact that the instruments can occasionally glitch, causing the partial or complete loss of the data associated with that particular specimen. This fact makes redundancy in instrumentation helpful when it is possible, and it also means that great care should be taken when handling, installing, and casting concrete around these gages. For the most part, these glitches, which are typically caused by either temporarily running out of battery or filling up the memory capacity of the data logger, only caused brief gaps in the data. These gaps were not an issue, since, once the data logger restarted, the curves pick up where they left off and the missing data can be replaced with a straight line connecting the known data points.

The process of reducing the data from the VWSG was fairly straightforward. All VWSG data was corrected for temperature, according to the variation in temperature in the concrete relative to the initial reading. This correction was performed because of the

difference in the coefficient of thermal expansion (CTE) between the concrete and the wire in the VWSG. Because all specimens were cured in the environmental chamber, however, where the temperature stayed very constant, this correction had a minimal effect. Additionally, all strain data was zeroed to the time that final set occurred in the concrete, which, for these mix designs, was consistently around 6 hours after the time of the first water being added to the concrete during mixing. This 6 hour mark also coincided with the time that the water cure was initiated. By zeroing the VWSG data to the final set mark, a consistent starting point was obtained that could be used for proper comparison of all the specimens in this research.

5.12 Comparisons with Previous Research

The first goal of this research was to improve upon the experiments that Dr. Chris Ramseyer and Seth Roswurm performed in 2013. For this reason, the results from the restrained columns from this research are compared to those from the 2013 experiments here. Figure 110 shows the expansion data for the 15% Komponent® restrained columns from Seth Roswurm's 2013 research.

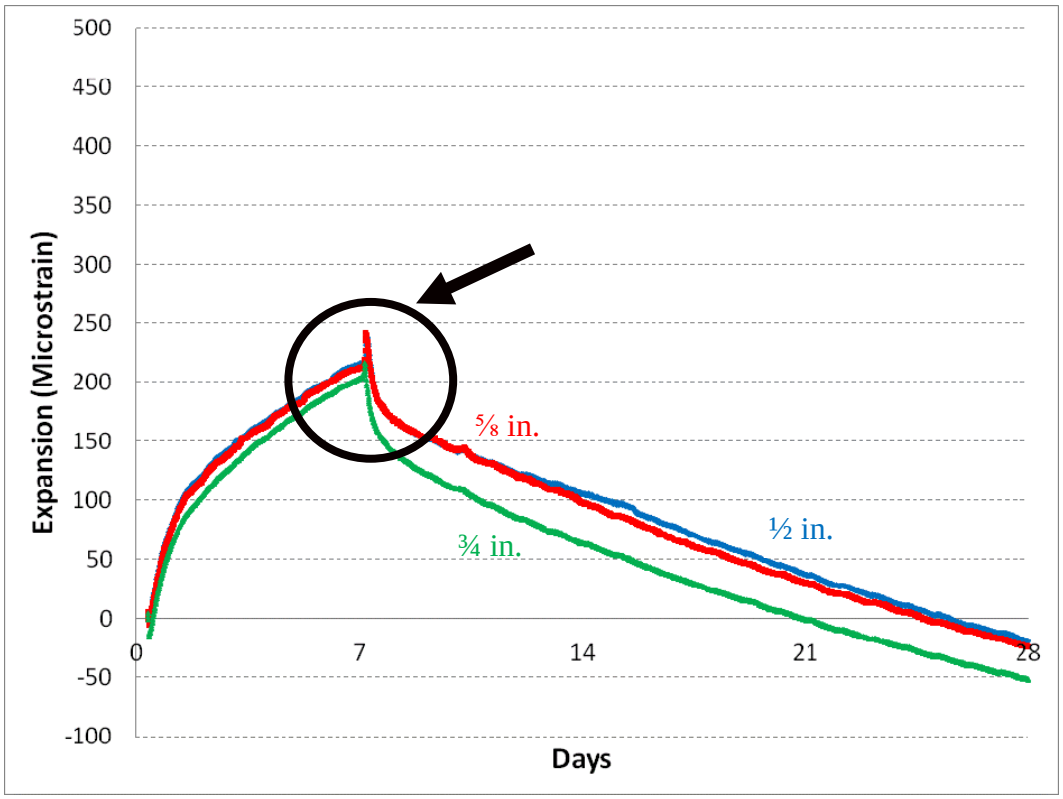

Figure 110: 15% Komponent Column Expansion Results (Seth Roswurm, 2013)

Of particular interest from Figure 110 is the unusual spike in expansion at 7 days, highlighted with the circle and arrow. This behavior cannot be explained according to the mechanical properties of the material, since expansion ceases with the termination of wet cure. Instead, because this time correlates to the removal of the cardboard forms, it is likely that the forms were providing restraint against expansion, and when they were removed there was an elastic response by the column. Figure 111 shows the expansion data for the 15% Komponent® restrained columns from this research, cured with misters.

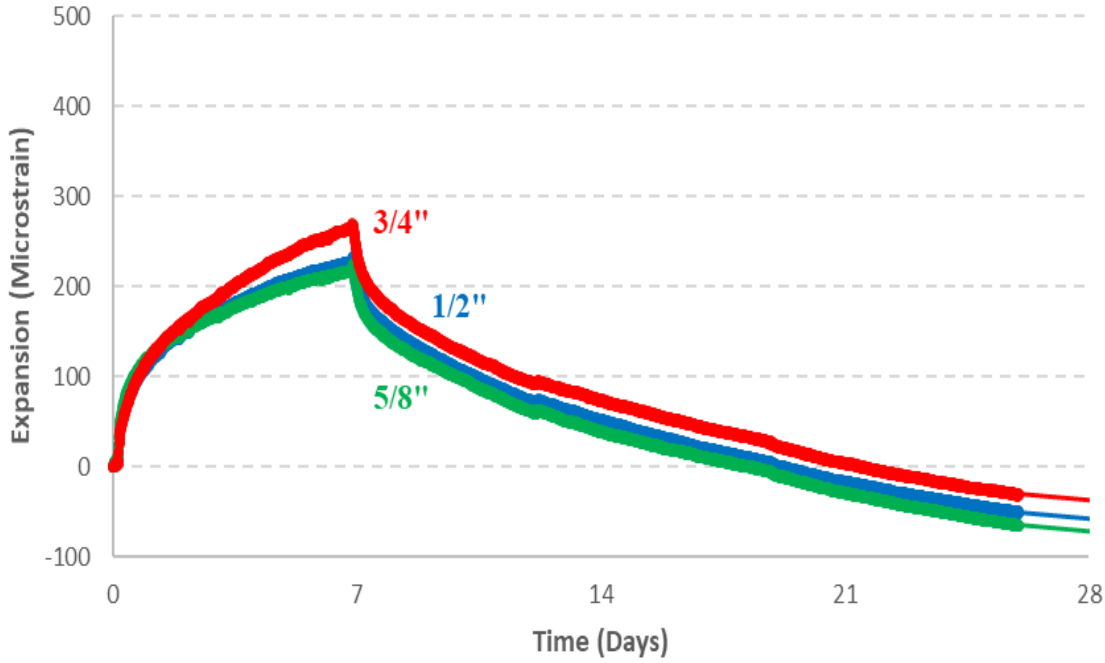

Figure 111: Restrained Column Expansion Results with Sprinkler Curing (All Restraint Rods, 15% Komponent)

In Figure 111, there is a smooth trend of expansion, followed by immediate shrinkage. This stands in contrast to Figure 110, where each column experiences expansions as high as 50 microstrain due to the release of restraint when de-molded. Therefore, this research has improved the restrained column test by eliminating a source of disturbance in the data.

The next improvement made in this research has to do with the effect of the curing system on the load development data. Figure 112 shows the load development data for the 15% Komponent® restrained columns from Seth Roswurm's 2013 research.

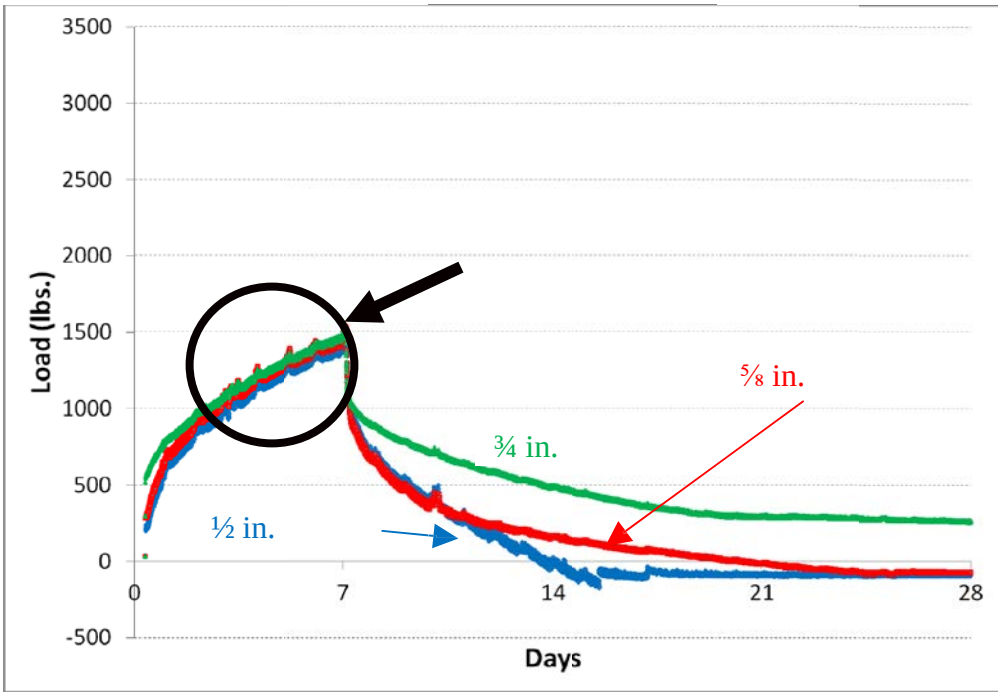

Figure 112: 15% Komponent Column Load Results (Seth Roswurm, 2013)

Of particular interest from Figure 112 are the undulations in the load curves between 0 and 7 days, highlighted with the circle and arrow. This behavior was due to the fact that since the columns were cured with a reservoir of water around the columns, the diurnal temperature variations were enough to cause slight variations in the registered load. For the ½" and ⅝" restraints, there are 7 such undulations in the first week, or one per day. Figure 113 shows the load data for the 19% Komponent® restrained columns from this research, cured with misters.

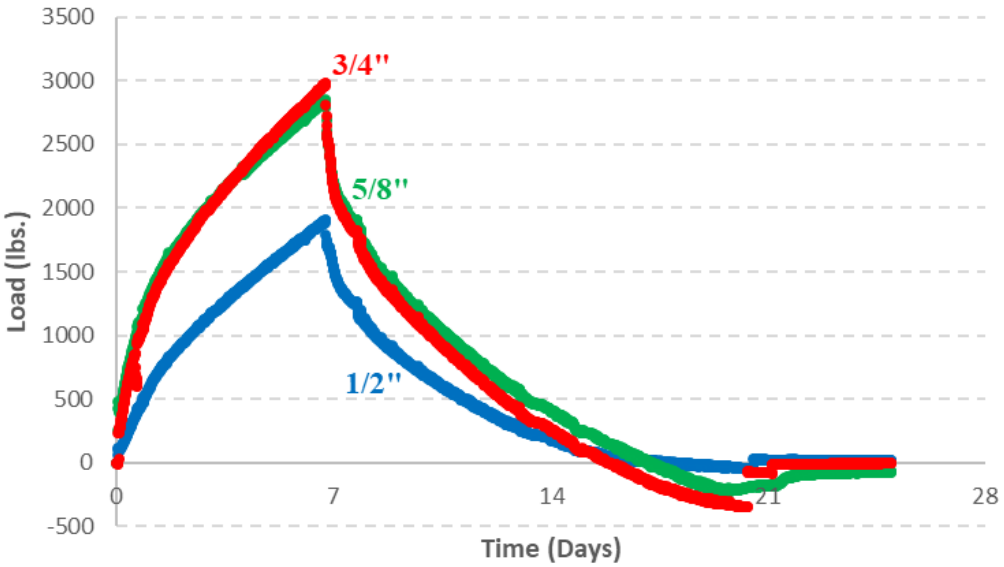

Figure 113: Restrained Column Load Development Results (All Restraint Rods, 19% Komponent)

In Figure 113, the load development curves are much smoother than those from Figure 112. This has to do with the sprinkler-based curing system. Since water was constantly coming from the tap with constant temperature around 60 degrees Fahrenheit, the temperature of the concrete stayed much more constant, and the diurnal undulations in the data were resolved.

The last improvement made in this research has to do with the observed patterns in the stress-strain data. Figure 114 shows the stress-strain data for the 30% Komponent® restrained columns from Seth Roswurm's 2013 research.

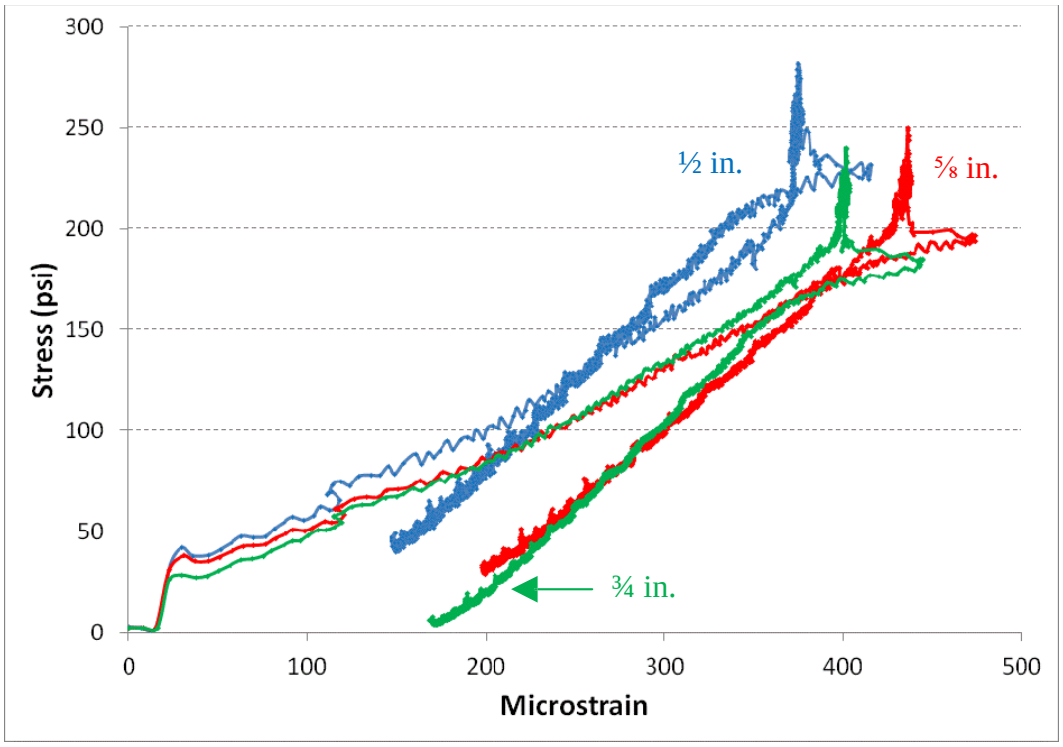

Figure 114: 30% Komponent Stress-Strain Results (Seth Roswurm, 2013)

It can be seen in Figure 114 that the stress-strain curves produced in these experiments were extremely non-linear, especially near the max expansions, when the specimens were disturbed during de-molding. Additionally, the ½" and ⅝" curves cross themselves on the unloading portion of the curve. This behavior is likely incorrect, because this theoretically would indicate that the system is producing energy. Under most circumstances, this behavior should not occur. Figure 115 shows the stress-strain data for the 21% Komponent® restrained columns from this research, cured with misters.

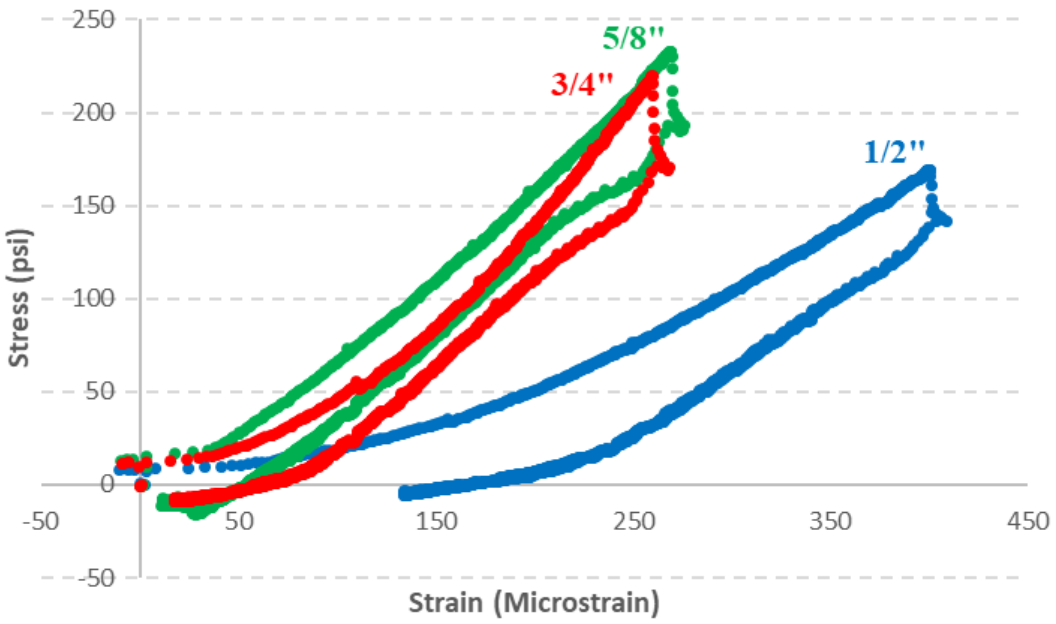

Figure 115: Restrained Column Stress-Strain Curves (All Restraint Rods, 21% Komponent)

In Figure 115, the stress-strain curves are much smoother than those from Figure 114, and the loading and unloading portions are individually much less ragged. Also, the portion of the curve where the transition occurs between loading and unloading does not experience the same disturbances as Figure 114, because there was no need for de-molding and jostling the columns. Finally, in Figure 115, none of the curves cross over themselves, meaning that another discrepancy in Ramseyer and Roswurm's 2013 work has been successfully addressed.

Chapter 6 – Summary

6.1 Conclusions

This research covered a broad range of both unrestrained and restrained SCC specimens, cast with 4 distinct mix designs. This research scope has provided an abundance of data that allows trends to be compared based on specimen type, restraint condition, or the percentage of Komponent® used in the mix design. Analyzing this data has resulted in the following conclusions:

(1) The concrete expands during wet-cure, reaching its highest level of expansion at 7 days, before the wet-cure is terminated. After that, the concrete begins to shrink. This is true for all specimen types and mix designs, except for the columns whose jackets were intentionally not removed.

(2) Utilizing a mix design with a higher percentage of Komponent® replacing Portland cement generally results in higher degrees of peak expansion and therefore less shrinkage at a given time in the future, when comparing similar specimens.

(3) Unrestrained specimens (whether ASTM prisms or 6”x12” cylinders) exhibit higher peak expansions and less shrinkage at any given time than their restrained counterparts.

(4) For the restrained columns, the lowest degree of restraint (those frames restrained by four ½” rods) reliably corresponded to the highest degree of expansion, the least aggressive shrinkage, and the lowest degree of load development, when compared to columns cast with the same mix design

with the other degrees of restraint. This fact held true once the capping compound issue was identified and efforts were made to remediate it, which included the 19% and 21% columns.

(5) The VWSG instruments were crucial to this experiment, they performed well, and it is recommended that their advantages continue to be leveraged for improving both future research and full-scale instrumentation of concrete structures in the field.

(6) Early-age drying shrinkage can be adequately offset using a mix with 21% Komponent, if early-age is defined to be behaviors or effects occurring before the concrete reaches design strength. This is based on the fact that the 21% mix, subjected to the highest restraint stiffness (four ¾" steel rods), experiences positive strain for the first 28 days.

(7) The meaning/usefulness of the stress-strain curves produced in these experiments, as it pertains to the material behavior of Type K SCC, are not fully understood at this time. The only definite conclusion is that the data suggests that this material behaves in a non-linear, elastic manner.

6.2 Recommendations for Future Work

6.2.1 Porosity Experiments

One topic that requires future work is studying the porosity of Type K SCC specimens cast with Komponent®, in order to get a feel for how the ettringite growth affects the porosity of the concrete matrix. This might also shed light on the expansion mechanism and help determine whether the idea of a two-stage expansion process is accurate.

Concrete naturally has many void spaces within its volume because the fine aggregate, coarse aggregate, and cement particles do not pack together perfectly; those void spaces in turn serve to make concrete a porous material. As mentioned previously, SCC achieves its purpose by expanding due to the hydration of ettringite crystals. Before the expansion of the ettringite contributes to the entire mass of concrete gaining length, it stands to reason that many of the ettringite crystals would expand into and fill the void spaces in the concrete. This idea is the basis of the two-stage expansion mechanism theory. In order to confirm this idea, however, further research needs to be conducted concerning the porosity of SCC specimens. It is recommended that this work involve testing the porosity of plain concrete samples as a control, and then testing an array of SCC samples that range in Komponent® content from 15% to 21%, which were the mixes used in this experiment. It is expected that the control sample would exhibit the highest porosity, indicating that it had the most void spaces, and that the SCC specimens would exhibit lower porosities. In addition, it would be expected that as the percentage of Komponent® increased, that the porosity would correspondingly decrease, due to the fact that the higher percentage mixes would produce more ettringite

and therefore have the potential to fill more of the void spaces.

6.2.2 Restrained Column Protocol

A protocol has been established according to this experiment for testing SCC under a realistic, passive restraint system. The following approaches were used for executing the restrained column tests in these experiments, and they are recommended if these tests are to be repeated in the future:

(1) Utilize 4” diameter, removable PVC forms. In this experiment, the PVC form was split longitudinally, and the two halves were held together with 6 stainless steel hose clamps. The inside of the forms was lubricated so that the clamps could be removed, and the PVC forms were easily slipped off when set was achieved.

(2) Utilize a micro-mister system to cure the columns. Although constantly spraying water causes a local humidity increase that can affect other specimens, misters are a preferred alternative due to reduced disturbance to the columns.

(3) Install load cells carefully to eliminate pre-compression loads. Great care must be taken to install the testing heads so that they are in contact with the columns without exerting a compressive load on them. The presence of the capping compound helped provide a cushion whereby contact was achieved without loading the column.

(4) Allow the capping compound to set for at least 1 hour prior to initiating water cure to prevent impact on strain or load measurement.

6.2.3 Restrained Columns with Other Mix Designs

Another topic that requires future attention is repeating the restrained column tests with more mix design alternatives that include higher percentages of Komponent®. Although the conclusions drawn from this research are based on a significant amount of data, they only cover a narrow band of potential mix designs. It is possible that continuing to increase the percentage of Komponent® to 23%, 25%, 27%, and 29% would show a change in the observed trends. Another adjustment that could be made to the mix design to expand this work into further research would involve the water to cement (W/C) ratio. In this research, every mix design utilized a 0.50 W/C ratio. This value actually represents the higher end of commonly used W/C ratios, which, for Portland cement based concretes, means that strength will be reduced, and shrinkage will be exacerbated. Therefore, any or all of these tests could be repeated at lower W/C ratios. This could be helpful for the following reasons:

(1) For many applications, high early compressive strengths are desirable, which is possible at lower W/C ratios. Therefore, any data characterizing how this material behaves at lower W/C ratios might be helpful.

(2) Normal concrete experiences more severe shrinkage for higher W/C ratios. Thus, it is possible that if the specimens in this research were cast at lower W/C ratios they too would experience less shrinkage. If so, then a mix design with the same percentage of Komponent® would provide more sufficient shrinkage compensation over time, if it were cast at a lower W/C ratio.

(3) Concrete durability is often superior when the concrete has a lower W/C ratio, protecting it from delayed ettringite formation, sulfate attack, and other issues. Therefore, it is important to understand how SCC specimens act under restraint when they have a low W/C ratio.

6.2.4 Restrained Columns with Chemical Prestress

Another topic that would be an excellent topic for future research would involve casting restrained columns at high percentages of Komponent® with steel fibers in the mix. The purpose of this experiment would be to investigate whether the presence of steel fibers coupled with high expansion in the concrete could produce enough of a chemical prestressing effect to prevent the rapid loss of expansion after the wet-cure is terminated. Essentially, these fibers will be stretched when the chemical prestress is applied (due to the concrete's expansion), as the concrete is placed in compression. But as the concrete tries to shrink after 7 days, the stress will be stored in the fibers, which will serve to maintain compression in the concrete. As mentioned in the literature review, a concept similar to this was used at the Rockford Airport, but the chemical prestress was only relied upon to provide compression in the transverse direction; in the longitudinal direction, the joints were either kept (just at a wider spacing) or mechanical post-tensioning was used to keep the concrete in compression. By further investigating chemical prestressed concrete with steel fibers, in an externally restrained condition, it could be feasible to rely only upon the expansion of the material to prestress the concrete, which would eliminate the need for costly and time consuming post-tensioning equipment and labor.

Chemical prestressed concrete of this sort, on a large scale, would be of special

usefulness in the residential concrete slab and foundation industry. Post-tensioning of residential slabs is a common means of securing them against cracking due to both shrinkage and applied loads, but it can be slow and expensive. The slab must be formed up with the ducts in place, and after the concrete is cast, the cables must be jacked, which cannot occur until the concrete has made strength. Care must be taken to either completely grout or fully de-bond the strands, and if the duct becomes damaged before casting the slab, it may interfere with tensioning the strand. Also, special equipment and expertise is required to tension the strands. Chemically prestressed concrete made with expansive Type K cement and fibers, however, might present a much more efficient system for residential slabs.

References

"ACI 223, Standard Practice for the Use of Shrinkage-Compensating Concrete," American Concrete Institute, Farmington Hills, MI.

"ACI 318-14, Building Code Requirements for Structural Concrete," American Concrete Institute, Farmington Hills, MI.

"ASTM Standard C138 Standard Test Method for Density (Unit Weight), Yield, and Air Content (Gravimetric) of Concrete," ASTM International, West Conshohocken, PA.

"ASTM Standard C143 Standard Test Method for Slump of Hydraulic-Cement Concrete," ASTM International, West Conshohocken, PA.

"ASTM Standard C157 Standard Test Method for Length Change of Hardened Hydraulic-Cement Mortar and Concrete," ASTM International, West Conshohocken, PA.

"ASTM Standard C192 Standard Practice for Making and Curing Concrete Test Specimens in the Laboratory," ASTM International, West Conshohocken, PA.

"ASTM Standard C231 Standard Test Method for Air Content of Freshly Mixed Concrete by the Pressure Method," ASTM International, West Conshohocken, PA.

"ASTM Standard C566 Standard Test Method for Total Evaporable Moisture Content of Aggregate by Drying," ASTM International, West Conshohocken, PA.

"ASTM Standard C878 Standard Test Method for Restrained Expansion of Shrinkage-Compensating Concrete," ASTM International, West Conshohocken, PA.

Chusid, M., "1,200-Foot Post-Tensioned Slab with Type K Cement Cleared for Take-off", PTI Journal, December 2006.

Crawford, Murphy, & Tilly, Inc., "Constructability Report; Prestressed, Fibrous Concrete Pavement, Greater Rockford Airport, IL", U.S. Army Corps of Engineers and the U.S. DOT FAA, May 1995.

Eskildsen, S., Jones, M., Richardson, J., "No More Pour Strips," Concrete International, Vol. 31, No. 10, October 2009, pp. 42-47.

Hanson, J.A., Elstner, R.C., Clore, R.H., "The Role of Shrinkage Compensating Cement in Reduction of Cracking of Concrete," ACI Special Publication, Vol. 38, No. 12, 1973, pp. 251-272.

Herrin, S. and Naughton, J., "10 Year Performance of Innovative Pavements, Greater Rockford Airport", Airfield Pavements Specialty Conference, September 2003.

Moffat, B.S., “Shrinkage Compensating Concrete: An Investigative Study,” Metropolis and Beyond, Structures Congress, April 2005, American Society of Civil Engineers, Reston VA.

National Weather Service, “Weather Observations for the Past Three Days – Norman/Max Westheimer,” National Oceanic and Atmospheric Administration, Norman OK, <http://forecast.weather.gov/MapClick.php?lat=35.2208&lon=-97.4466#.WkvQ3ExFxEw>

Phillips, M.V., Ramey, G.E., Pittman, D.W., “Bridge Deck Construction Using Type K Cement,” Journal of Bridge Engineering, Vol. 2, No. 4, November 1997, pp. 176-182.

Pittman, D.W., Ramey, G.E., Webster, G., Carden, A., “Laboratory Evaluation of Concrete Mixture Designs Employing Type I and Type K Cement,” Journal of Materials in Civil Engineering, Vol. 11, No. 2, May 1999, pp. 144-150.

Ramseyer, C., Personal Conversations, University of Oklahoma, March 13, 2018.

Richardson, D., Tung, Y., Tobias, D., Hindi, R., “An Experimental Study of Bridge Deck Cracking using Type K-Cement,” Construction and Building Materials, Vol. 52, February 2014, pp. 366-374.

Roswurm, S.M., “Investigation of the Mechanical Behavior of Type K Shrinkage Compensating Concrete under Various Forms of Mechanical Restraint,” Thesis, The University of Oklahoma, 2013.

Russell, H.G., “Design of Shrinkage Compensating Concrete Slabs,” Klein Symposium on Expansive Cement Concretes, Special Publication Vol. 38, January 1973, pp. 193-226.

Appendix A – Fresh Data and Mix Quantities

A.1 15% Replacement Mix

A.1.1 First Batch (Curing Alternative No. 1)

15% Komp. Batch Test: My Research 8/2/2016

w/cm =	0.5		Sand % water =	3.457	start 9:24 AM
PC =	493	type I	Rock % water =	0.686	batch 9:25 AM
RS =	0				stop 9:34 AM
Komp =	87				
FA =	0				

Sand SG:	2.63	SSD=	0.70	b/bo =	0.65	Fineness Modulus = 2.5
Rock SG:	2.68	SSD=	0.86	DRUW =	101.0	
H2O SG=	1.0					
C SG=	3.15					
RS SG=	2.88					
Komp SG	2.88					
FA SG=	2.58					

Moisture Content

Sand :	Wt (lb)		
Pan	0.49	Mc =	3.457
Pan + wet Sand	4.68		
Pan + dry Sand	4.54		
Aggregates :			
Pan	0.58	Mc =	0.686
Pan + wet Agg	6.45		
Pan + dry Agg	6.41		

	Theoretical Weight	Volume
Portland Cement	493.0	2.51
Rapid Set Cement	0	0.00
Komponent	87	0.48
Fly Ash	0	0.00
Water	290.0	4.65
Rock	1772.6	10.60
Air Entrapped 2%	0.0	0.54
DCI-chemical part	0.0	0.00
Sand	1349.2	8.22
Sum	3991.70969	27

		1 yd	4.25	cu ft		
Portland Cement		493.0	77.60	lb		
Rapid Set Cement		0.0	0.00	lb		
Komponent		87.0	13.69	lb		
Fly Ash		0.0	0.00	lb		
Coarse Aggregate, #67		1784.7	280.93	lb		
Fine Aggregate, Dover Sand		1395.8	219.71	lb		
Water		254.6	40.08	lb		
Air Ent. Admixture	oz	0.0	0.00	ml		
Citric Acid Retarder	lb	0.0	0.00	lb		
Glenium (MRWR)	oz	0.0	0.00	ml	oz/cwt	0.00
DCI (Accel w/ water)	oz	0.0	0.00	ml	oz/cwt	0.00

Concrete Temperature	76 F
Air Temperature	82 F
Humidity	55%
Air Content	1.10%
Slump	5"
Unit Weight Pot Empty	7.76
Unit Weight Pot Full	44.31

Expected Unit Wt		147.84
Measured	36.55	146.20
Difference	%	1.11

Figure 116: Fresh Data and Mix Quantities for 15% Replacement, Mix #1

A.1.2 Second Batch (Curing Alternative No. 2)

15% Komp. Batch Test: My Research 3/25/2017

w/cm =	0.5		Sand % water =	1.818	start 10:49 AM
PC =	493	type I	Rock % water =	0.219	batch 10:52 AM
RS =	0				stop 10:54 AM
Komp =	87				
FA =	0				

Moisture Content

Sand :	Wt (lb)		
Pan	0.49	Mc =	1.818
Pan + wet Sand	4.41		
Pan + dry Sand	4.34		
Aggregates :			
Pan	0.53	Mc =	0.219
Pan + wet Agg	5.1		
Pan + dry Agg	5.09		

Sand SG:	2.63	SSD=	0.70	b/bo = 0.65	Fineness Modulus = 2.5
Rock SG:	2.68	SSD=	0.86	DRUW = 101.0	
H2O SG=	1.0				
C SG=	3.15				
RS SG=	2.88				
Komp SG	2.88				
FA SG=	2.58				

Theoretical	Weight	Volume
Portland Cement	493.0	2.51
Rapid Set Cement	0	0.00
Komponent	87	0.48
Fly Ash	0	0.00
Water	290.0	4.65
Rock	1772.6	10.60
Air Entrapped 2%	0.0	0.54
DCI-chemical part	0.0	0.00
Sand	1349.2	8.22
Sum	3991.70969	27

		1 yd	4.25	cu ft		
Portland Cement		493.0	77.60	lb		
Rapid Set Cement		0.0	0.00	lb		
Komponent		87.0	13.69	lb		
Fly Ash		0.0	0.00	lb		
Coarse Aggregate, #67		1776.4	279.62	lb		
Fine Aggregate, Dover Sand		1373.7	216.23	lb		
Water		286.0	45.02	lb		
Air Ent. Admixture	oz	0.0	0.00	ml		
Citric Acid Retarder	lb	0.0	0.00	lb		
Glenium (MRWR)	oz	0.0	0.00	ml	oz/cwt	0.00
DCI (Accel w/ water)	oz	0.0	0.00	ml	oz/cwt	0.00

Concrete Temperature	70 F
Air Temperature	48 F
Humidity	82%
Air Content	1.50%
Slump	4 3/4"
Unit Weight Pot Empty	7.76
Unit Weight Pot Full	44.66

Expected Unit Wt		147.84
Measured	36.9	147.60
Difference	%	0.16

Figure 117: Fresh Data and Mix Quantities for 15% Replacement, Mix #2

A.2 17% Replacement Mix

A.2.1 First Batch (Curing Alternative No. 1)

17% Komp. Batch Test: My Research 8/4/2016

w/cm =	0.5		Sand % water =	2.676	start 9:11 AM
PC =	481	type I	Rock % water =	0.358	batch 9:12 AM
RS =	0				stop 9:17 AM
Komp =	99				
FA =	0				

Sand SG=	2.63	SSD=	0.70	b/bo =	0.65	Fineness Modulus = 2.5
Rock SG=	2.68	SSD=	0.86	DRUW =	101.0	
H2O SG=	1.0					
C SG=	3.15					
RS SG=	2.88					
Komp SG	2.88					
FA SG=	2.58					

Moisture Content

Sand :	Wt (lb)		
Pan	0.58	Mc =	2.676
Pan + wet Sand	3.65		
Pan + dry Sand	3.57		
Aggregates :			
Pan	0.49	Mc =	0.358
Pan + wet Agg	3.29		
Pan + dry Agg	3.28		

Theoretical	Weight	Volume
Portland Cement	481.0	2.45
Rapid Set Cement	0	0.00
Komponent	99	0.55
Fly Ash	0	0.00
Water	290.0	4.65
Rock	1772.6	10.60
Air Entrapped 2%	0.0	0.54
DCI-chemical part	0.0	0.00
Sand	1348.2	8.22
Sum	3990.77041	27

		1 yd	4.25	cu ft		
Portland Cement		481.0	75.71	lb		
Rapid Set Cement		0.0	0.00	lb		
Komponent		99.0	15.58	lb		
Fly Ash		0.0	0.00	lb		
Coarse Aggregate, #67		1778.9	280.01	lb		
Fine Aggregate, Dover Sand		1384.3	217.90	lb		
Water		271.6	42.75	lb		
Air Ent. Admixture	oz	0.0	0.00	ml		
Citric Acid Retarder	lb	0.0	0.00	lb		
Glenium (MRWR)	oz	0.0	0.00	ml	oz/cwt	0.00
DCI (Accel w/ water)	oz	0.0	0.00	ml	oz/cwt	0.00

Concrete Temperature	80 F
Air Temperature	82 F
Humidity	66%
Air Content	1.30%
Slump	5 1/4"
Unit Weight Pot Empty	7.76
Unit Weight Pot Full	44.43

Expected Unit Wt		147.81
Measured	36.67 %	146.68
Difference		0.76

Figure 118: Fresh Data and Mix Quantities for 17% Replacement, Mix #1

A.2.2 Second Batch (Curing Alternative No. 2)

17% Komp. Batch Test: My Research 4/6/2017

w/cm =	0.5		Sand % water =	1.714	start 12:32 PM
PC =	481	type I	Rock % water =	0.273	batch 12:34 PM
RS =	0				stop 12:41 PM
Komp =	99				
FA =	0				

Sand SG:	2.63	SSD=	0.70	b/bo =	0.65	Fineness Modulus = 2.5
Rock SG:	2.68	SSD=	0.86	DRUW =	101.0	
H2O SG=	1.0					
C SG=	3.15					
RS SG=	2.88					
Komp SG	2.88					
FA SG=	2.58					

Moisture Content

Sand :	Wt (lb)		
Pan	0.39	Mc =	1.714
Pan + wet Sand	3.95		
Pan + dry Sand	3.89		
Aggregates :			
Pan	0.58	Mc =	0.273
Pan + wet Agg	4.25		
Pan + dry Agg	4.24		

Theoretical	Weight	Volume
Portland Cement	481.0	2.45
Rapid Set Cement	0	0.00
Komponent	99	0.55
Fly Ash	0	0.00
Water	290.0	4.65
Rock	1772.6	10.60
Air Entrapped 2%	0.0	0.54
DCI-chemical part	0.0	0.00
Sand	1348.2	8.22
Sum	3990.77041	27

		1 yd	4.25	cu ft		
Portland Cement		481.0	75.71	lb		
Rapid Set Cement		0.0	0.00	lb		
Komponent		99.0	15.58	lb		
Fly Ash		0.0	0.00	lb		
Coarse Aggregate, #67		1777.4	279.77	lb		
Fine Aggregate, Dover Sand		1371.3	215.86	lb		
Water		286.5	45.10	lb		
Air Ent. Admixture	oz	0.0	0.00	ml		
Citric Acid Retarder	lb	0.0	0.00	lb		
Glenium (MRWR)	oz	0.0	0.00	ml	oz/cwt	0.00
DCI (Accel w/ water)	oz	0.0	0.00	ml	oz/cwt	0.00

Concrete Temperature	72 F
Air Temperature	64 F
Humidity	32%
Air Content	N.A.
Slump	5 "
Unit Weight Pot Empty	7.76
Unit Weight Pot Full	44.55

Expected Unit Wt		147.81
Measured	36.79	147.16
Difference	%	0.44

Figure 119: Fresh Data and Mix Quantities for 17% Replacement, Mix #2

A.3 19% Replacement Mix

A.3.1 First Batch

19% Komp. Batch Test: My Research 7/10/2017

w/cm =	0.5		Sand % water =	1.452	start 8:26 AM
PC =	470	type I	Rock % water =	0.000	batch 8:36 AM
RS =	0				stop 9:04 AM
Komp =	110				
FA =	0				

Sand SG:	2.63	SSD=	0.70	b/bo =	0.65	Fineness Modulus = 2.5
Rock SG:	2.68	SSD=	0.86	DRUW =	101.0	
H2O SG=	1.0					
C SG=	3.15					
RS SG=	2.88					
Komp SG	2.88					
FA SG=	2.58					

Moisture Content

Sand :	Wt (lb)		
Pan	0.57	Mc =	1.452
Pan + wet Sand	5.46		
Pan + dry Sand	5.39		
Aggregates :			
Pan	0.49	Mc =	0.000
Pan + wet Agg	4.36		
Pan + dry Agg	4.36		

	Theoretical Weight	Volume
Portland Cement	470.0	2.39
Rapid Set Cement	0	0.00
Komponent	110	0.61
Fly Ash	0	0.00
Water	290.0	4.65
Rock	1772.6	10.60
Air Entrapped 2%	0.0	0.54
DCI-chemical part	0.0	0.00
Sand	1347.4	8.21
Sum	3989.9094	27

		1 yd	4.25	cu ft		
Portland Cement		470.0	73.98	lb		
Rapid Set Cement		0.0	0.00	lb		
Komponent		110.0	17.31	lb		
Fly Ash		0.0	0.00	lb		
Coarse Aggregate, #67		1772.6	279.01	lb		
Fine Aggregate, Dover Sand		1366.9	215.16	lb		
Water		295.0	46.43	lb		
Air Ent. Admixture	oz	0.0	0.00	ml		
Citric Acid Retarder	lb	0.0	0.00	lb		
Glenium (MRWR)	oz	0.0	0.00	ml	oz/cwt	0.00
DCI (Accel w/ water)	oz	0.0	0.00	ml	oz/cwt	0.00

Concrete Temperature	78 F
Air Temperature	77 F
Humidity	79%
Air Content	1.10%
Slump	4 1/2"
Unit Weight Pot Empty	7.76
Unit Weight Pot Full	44.32

Expected Unit Wt		147.77
Measured	36.56	146.24
Difference	%	1.04

Figure 120: Fresh Data and Mix Quantities for 19% Replacement, Mix #1

A.3.2 Second Batch

19% Komp. Batch Test: My Research 12/8/2017

w/cm =	0.5		Sand % water =	1.951	start 11:27 AM
PC =	470	type I	Rock % water =	0.226	batch 11:29 AM
RS =	0				stop 11:36 AM
Komp =	110				
FA =	0				

Sand SG:	2.63	SSD=	0.70	b/bo =	0.65	Fineness Modulus = 2.5
Rock SG:	2.68	SSD=	0.86	DRUW =	101.0	
H2O SG=	1.0					
C SG=	3.15					
RS SG=	2.88					
Komp SG	2.88					
FA SG=	2.58					

Moisture Content

Sand :	Wt (lb)		
Pan	0.49	Mc =	1.951
Pan + wet Sand	4.67		
Pan + dry Sand	4.59		
Aggregates :			
Pan	0.57	Mc =	0.226
Pan + wet Agg	5.01		
Pan + dry Agg	5.00		

Theoretical	Weight	Volume
Portland Cement	470.0	2.39
Rapid Set Cement	0	0.00
Komponent	110	0.61
Fly Ash	0	0.00
Water	290.0	4.65
Rock	1772.6	10.60
Air Entrapped 2%	0.0	0.54
DCI-chemical part	0.0	0.00
Sand	1347.4	8.21
Sum	3989.9094	27

		1 yd	3.5	cu ft		
Portland Cement		470.0	60.93	lb		
Rapid Set Cement		0.0	0.00	lb		
Komponent		110.0	14.26	lb		
Fly Ash		0.0	0.00	lb		
Coarse Aggregate, #67		1776.6	230.29	lb		
Fine Aggregate, Dover Sand		1373.6	178.07	lb		
Water		284.1	36.83	lb		
Air Ent. Admixture	oz	0.0	0.00	ml		
Citric Acid Retarder	lb	0.0	0.00	lb		
Glenium (MRWR)	oz	0.0	0.00	ml	oz/cwt	0.00
DCI (Accel w/ water)	oz	0.0	0.00	ml	oz/cwt	0.00

Concrete Temperature	66 F
Air Temperature	36F
Humidity	38%
Air Content	1.20%
Slump	2 1/2"
Unit Weight Pot Empty	7.76
Unit Weight Pot Full	44.3

Expected Unit Wt		147.77
Measured	36.54	146.16
Difference	%	1.09

Curing notes and mix comments

Note that although exterior temp was 36 F, batch was conducted in the highbay, where the temp was in the 50's

Figure 121: Fresh Data and Mix Quantities for 19% Replacement, Mix #2

A.4 21% Replacement Mix

A.4.1 First Batch

21% Komp. Batch Test: My Research 7/10/2017

w/cm =	0.5		Sand % water =	1.452	start	10:20 AM
PC =	458	type I	Rock % water =	0.000	batch	10:29 AM
RS =	0				stop	11:10 AM
Komp =	122					
FA =	0					

Sand SG:	2.63	SSD=	0.70	b/bo =	0.65	Fineness Modulus = 2.5
Rock SG:	2.68	SSD=	0.86	DRUW =	101.0	
H2O SG=	1.0					
C SG=	3.15					
RS SG=	2.88					
Komp SG	2.88					
FA SG=	2.58					

Moisture Content

	Wt (lb)		
Sand :			
Pan	0.57	Mc =	1.452
Pan + wet Sand	5.46		
Pan + dry Sand	5.39		
Aggregates :			
Pan	0.49	Mc =	0.000
Pan + wet Agg	4.36		
Pan + dry Agg	4.36		

	Theoretical Weight	Volume
Portland Cement	458.0	2.33
Rapid Set Cement	0	0.00
Komponent	122	0.68
Fly Ash	0	0.00
Water	290.0	4.65
Rock	1772.6	10.60
Air Entrapped 2%	0.0	0.54
DCI-chemical part	0.0	0.00
Sand	1346.4	8.20
Sum	3988.97011	27

		1 yd	4.25	cu ft		
Portland Cement		458.0	72.09	lb		
Rapid Set Cement		0.0	0.00	lb		
Komponent		122.0	19.20	lb		
Fly Ash		0.0	0.00	lb		
Coarse Aggregate, #67		1772.6	279.01	lb		
Fine Aggregate, Dover Sand		1366.0	215.01	lb		
Water		295.0	46.43	lb		
Air Ent. Admixture	oz	0.0	0.00	ml		
Citric Acid Retarder	lb	0.0	0.00	lb		
Glenium (MRWR)	oz	0.0	0.00	ml	oz/cwt	0.00
DCI (Accel w/ water)	oz	0.0	0.00	ml	oz/cwt	0.00

Concrete Temperature	78 F
Air Temperature	82 F
Humidity	66%
Air Content	1.10%
Slump	5"
Unit Weight Pot Empty	7.76
Unit Weight Pot Full	44.39

Expected Unit Wt			147.74
Measured	36.63		146.52
Difference		%	0.83

Figure 122: Fresh Data and Mix Quantities for 21% Replacement, Mix #1

A.4.2 Second Batch

21% Komp. Batch Test: My Research 12/9/2017

w/cm =	0.5		Sand % water =	1.951	start	9:48 AM
PC =	458	type I	Rock % water =	0.226	batch	9:52 AM
RS =	0				stop	10:00 AM
Komp =	122					
FA =	0					

Sand SG:	2.63	SSD=	0.70	b/bo = 0.65	Fineness Modulus = 2.5
Rock SG:	2.68	SSD=	0.86	DRUW = 101.0	
H2O SG=	1.0				
C SG=	3.15				
RS SG=	2.88				
Komp SG	2.88				
FA SG=	2.58				

Moisture Content

Sand :	Wt (lb)		
Pan	0.49	Mc =	1.951
Pan + wet Sand	4.67		
Pan + dry Sand	4.59		
Aggregates :			
Pan	0.57	Mc =	0.226
Pan + wet Agg	5.01		
Pan + dry Agg	5		

Theoretical	Weight	Volume
Portland Cement	458.0	2.33
Rapid Set Cement	0	0.00
Komponent	122	0.68
Fly Ash	0	0.00
Water	290.0	4.65
Rock	1772.6	10.60
Air Entrapped 2%	0.0	0.54
DCI-chemical part	0.0	0.00
Sand	1346.4	8.20
Sum	3988.97011	27

		1 yd	3.5	cu ft		
Portland Cement		458.0	59.37	lb		
Rapid Set Cement		0.0	0.00	lb		
Komponent		122.0	15.81	lb		
Fly Ash		0.0	0.00	lb		
Coarse Aggregate, #67		1776.6	230.29	lb		
Fine Aggregate, Dover Sand		1372.7	177.94	lb		
Water		284.1	36.83	lb		
Air Ent. Admixture	oz	0.0	0.00	ml		
Citric Acid Retarder	lb	0.0	0.00	lb		
Glenium (MRWR)	oz	0.0	0.00	ml	oz/cwt	0.00
DCI (Accel w/ water)	oz	0.0	0.00	ml	oz/cwt	0.00

Concrete Temperature	78 F
Air Temperature	41 F
Humidity	51%
Air Content	1.40%
Slump	1 1/2"
Unit Weight Pot Empty	7.76
Unit Weight Pot Full	44.59

Expected Unit Wt		147.74
Measured	36.83	147.32
Difference	%	0.28

Curing notes and mix comments

Note that although exterior temp was in the 40's, batch was conducted in the highbay, where the temp was in the 60's

Figure 123: Fresh Data and Mix Quantities for 21% Replacement, Mix #2

Appendix B – Strain Data for ASTM C878 and C157 Tests

Table 10: Manually Measured Length Change Data (15% Komponent)

Time	ASTM C878	ASTM C157
(days)	(microstrain)	(microstrain)
0	0.00	0.00
1	133.33	220.00
2	180.00	266.67
3	196.67	286.67
4	210.00	293.33
5	213.33	296.67
6	223.33	306.67
7	220.00	306.67
8	140.00	223.33
9	126.67	193.33
10	110.00	163.33
11	100.00	146.67
12	93.33	136.67
13	76.67	123.33
14	63.33	120.00
21	33.33	70.00
28	-6.67	-6.67
56	-70.00	-73.33
90	-230.00	-136.67
180	-283.33	-206.67
330	-326.67	-216.67

Table 11: Manually Measured Length Change Data (17% Komponent)

Time	ASTM C878	ASTM C157
(days)	(microstrain)	(microstrain)
0	0.00	0.00
1	150.00	236.67
2	216.67	353.33
3	263.33	406.67
4	290.00	463.33
5	306.67	470.00
6	306.67	476.67
7	313.33	490.00
8	240.00	390.00
9	226.67	366.67
10	216.67	343.33
11	193.33	326.67
12	183.33	326.67
13	176.67	320.00
14	163.33	310.00
21	150.00	190.00
28	163.33	183.33
56	100.00	80.00
90	-26.67	-6.67
180	-76.67	-60.00
330	-123.33	-90.00

Table 12: Manually Measured Length Change Data (19% Komponent)

Time	ASTM C878	ASTM C157
(days)	(microstrain)	(microstrain)
0	0.00	0.00
1	113.33	116.67
2	183.33	200.00
3	256.67	303.33
4	323.33	380.00
5	360.00	436.67
6	386.67	460.00
7	400.00	473.33
8	336.67	390.00
9	296.67	353.33
10	293.33	326.67
11	280.00	306.67
12	260.00	290.00
13	243.33	270.00
14	233.33	250.00
21	156.67	173.33
28	83.33	100.00
56	30.00	26.67
90	-	-
180	-113.33	-80.00
330	-	-

Table 13: Manually Measured Length Change Data (21% Komponent)

Time	ASTM C878	ASTM C157
(days)	(microstrain)	(microstrain)
0	0.00	0.00
1	150.00	166.67
2	246.67	296.67
3	346.67	436.67
4	453.33	556.67
5	540.00	680.00
6	640.00	800.00
7	676.67	853.33
8	603.33	780.00
9	563.33	743.33
10	556.67	713.33
11	540.00	706.67
12	520.00	683.33
13	500.00	663.33
14	486.67	650.00
21	410.00	543.33
28	340.00	473.33
56	273.33	383.33
90	-	-
180	140.00	296.67
330	-	-

Appendix C – 19% and 21% Restrained Columns (Invalidated Tests)

Several attempts were required before the restrained column tests for the 19% and 21% mixes were completed and ran successfully. This is largely due to the fact that setting up these tests is a fairly complex process, and that provides the potential for mishaps. The first attempt at casting the 19% and 21% restrained columns was performed in July 2017, the second was in September 2017, and the third and final (successful) attempt was in December 2017. The data from the successful attempt is presented in the body of the thesis. There is no data from the second attempt due to the fact that after the columns had been completely cast, and water-cured for 7 days, it was discovered that the data acquisition system had failed to begin recording strain. Therefore, the most crucial data for this test was lost, and there was no data to salvage.

The first attempt at the 19% and 21% restrained columns (July 2017), however, did produce data worth presenting. The issue with this trial was caused by the configuration of the sprinkler system for the wet cure process. The ¼" tubing used to feed the foggers on the columns was all run from a garden hose that connected to a single spigot on the north side of Fears Lab. Therefore, it was obviously critical that this spigot remain running throughout the first 7 days of the test. To prevent any confusion or risk damaging the test, signs were posted throughout the lab, on both the inside and outside of all exterior doors, and on and above the spigot itself, warning users not to turn off the spigot. Unfortunately, despite the signage, a little over 1 day into the test, this spigot was shut off by an unknown user. Because it occurred near the end of the business day, and the water cure was being checked each morning, this was not discovered until 8 o'clock the next morning. The data indicates that this caused an

interruption of between 16 and 17 hours in the water cure.

It is important to note that this issue by no means stopped or permanently damaged the ability of the concrete to serve its purpose in shrinkage-compensation; however, because this interruption occurred so early in the life of the concrete, the time in which Type K cement causes the most rapid rates of expansion, the concrete stopped hydrating, and therefore lost an unknown amount of its 7-day expansive potential. For this reason, it was not possible to compare any of this data to the other restrained columns, because the peak expansions were irreconcilably altered.

As expected, however, the expansion restarted as soon as water cure was restored, and as the figures below show, the ordering of the expected trends were not disturbed, since all 6 columns were affected equally. Figures 124 and 125 show the expansion data for the first attempt at the 19% and 21% restrained columns, respectively.

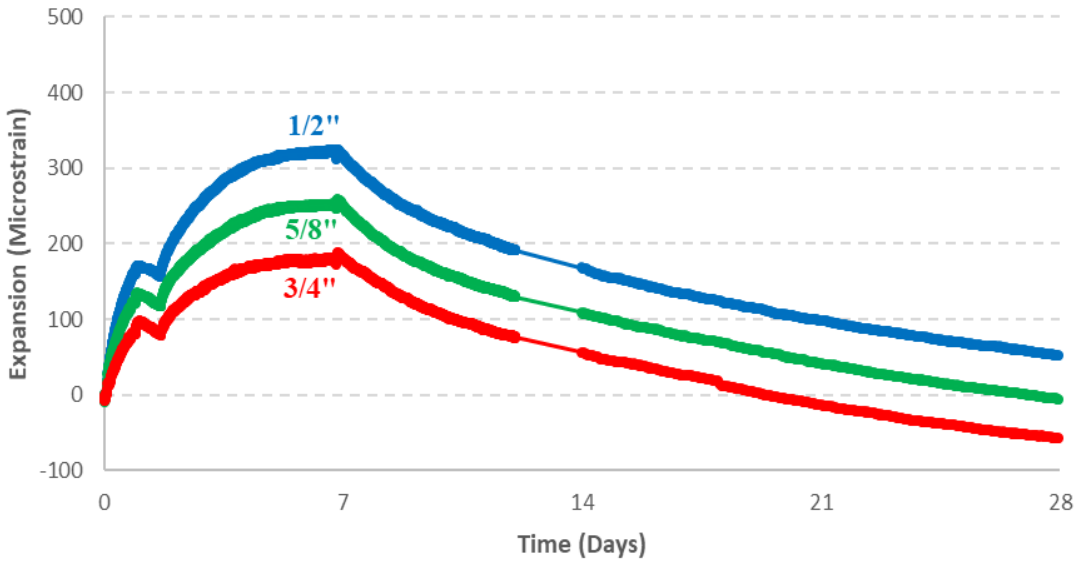

Figure 124: Restrained Column Expansion Results (All Restraint Rods, 19% Komponent - First Trial)

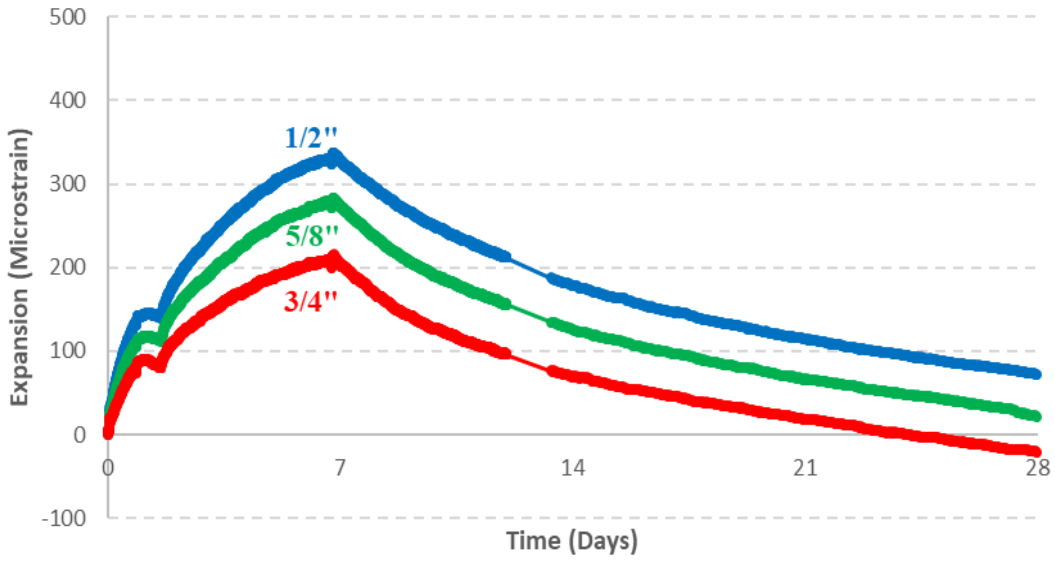

Figure 125: Restrained Column Expansion Results (All Restraint Rods, 21% Komponent - First Trial)

Due to the unexpected curing glitch, this test was terminated sooner than all the others, and load data was not retained. Despite this problem, though, Figures 124 and 125 still exhibit several trends worth noting.

First of all, it is apparent that the expansion of the concrete recommenced immediately when the water was turned back on to the curing system. Secondly, despite the curing glitch, the ordering of the trends correlates precisely with what is theoretically predicted. For both mixes (19% and 21%), the columns with ½" restraint rods showed the most expansion, followed by the columns with the ⅝" restraint rods, and then by the columns with the ¾" restraint rods, which exhibited the least expansion. This concept is expected according to the principles of engineering mechanics and is confirmed by these trends. Finally, not only is the layering of the trends correct, but also the curves are each separated by a margin of between 50 and 75 microstrains. This contrasts with some of the other restrained columns (such as the ¾" and ⅝" restrained

columns for the 19% and 21% mixes from the re-batch of this mix), whose curves were sometimes nearly overlaid or only separated by a few microstrains. The only issue with this data was that the lack of complete curing skewed the maximum expansions, making it difficult to compare them to other restrained columns.

Appendix D – Long-Term Results

For the sake of consistency, all figures presented in the body of this work were shown as far out as 28 days. Many of those specimens, however, were tested for longer than 28 days. Since there were only two sets of column frames available, the experiment could not proceed until the previous columns were removed. Because of this, the restrained column expansion and the 6”x12” cylinders could only be measured for up to around 2-3 months each. For the ASTM C157 and C878 prisms, there was no such restriction on the testing period. Thus, these specimens could be monitored out to 6 months. Figure 126 shows the long-term data for the ASTM C157 specimens.

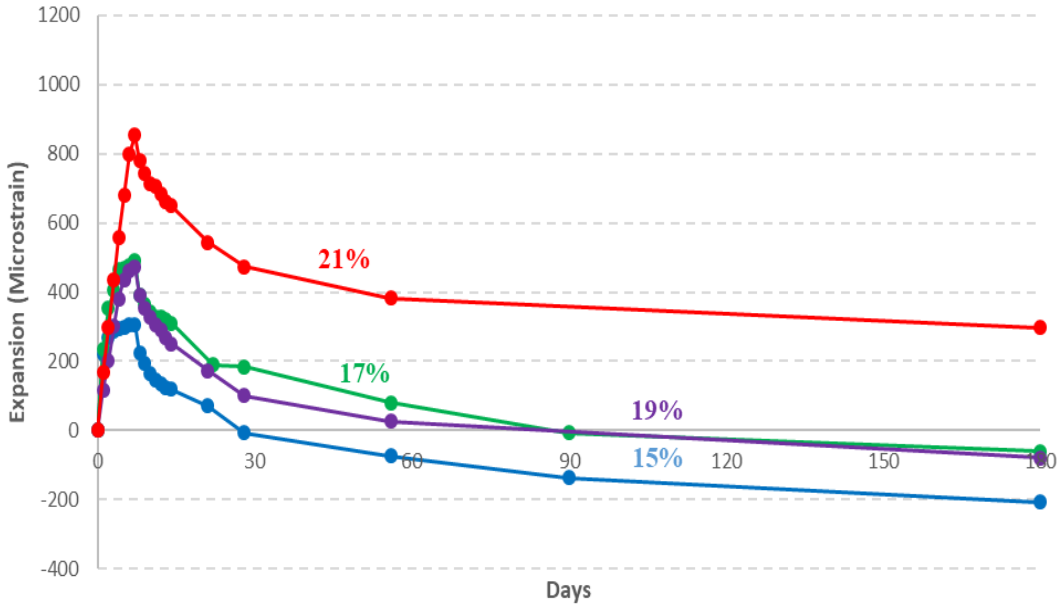

Figure 126: Long-Term ASTM C157 Results

Figure 127 shows the long-term data for the ASTM C878 specimens.

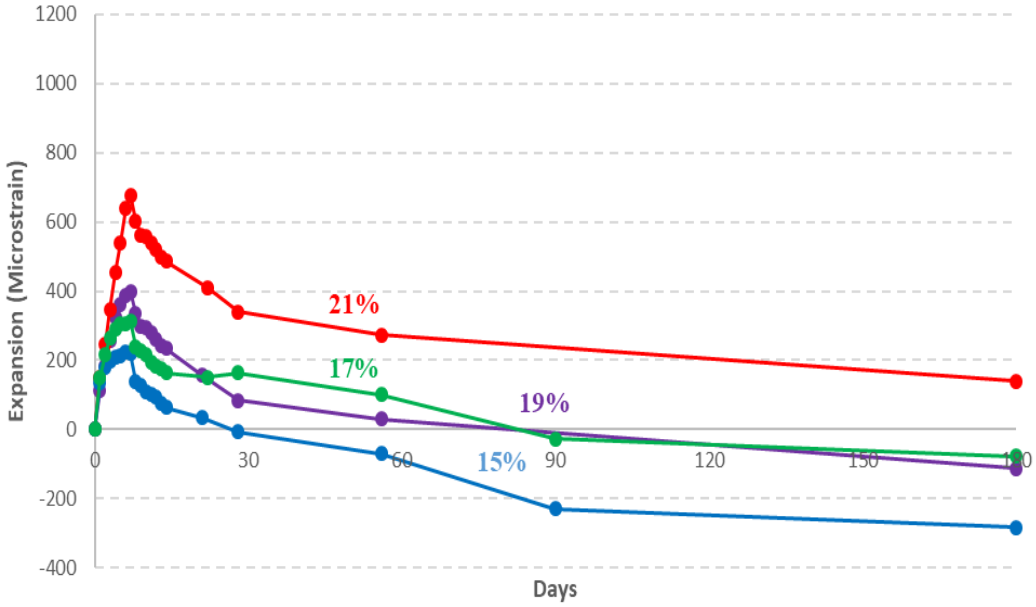

Figure 127: Long-Term ASTM C878 Results

Figure 128 shows the long-term data for the unrestrained 6”x12” specimens.

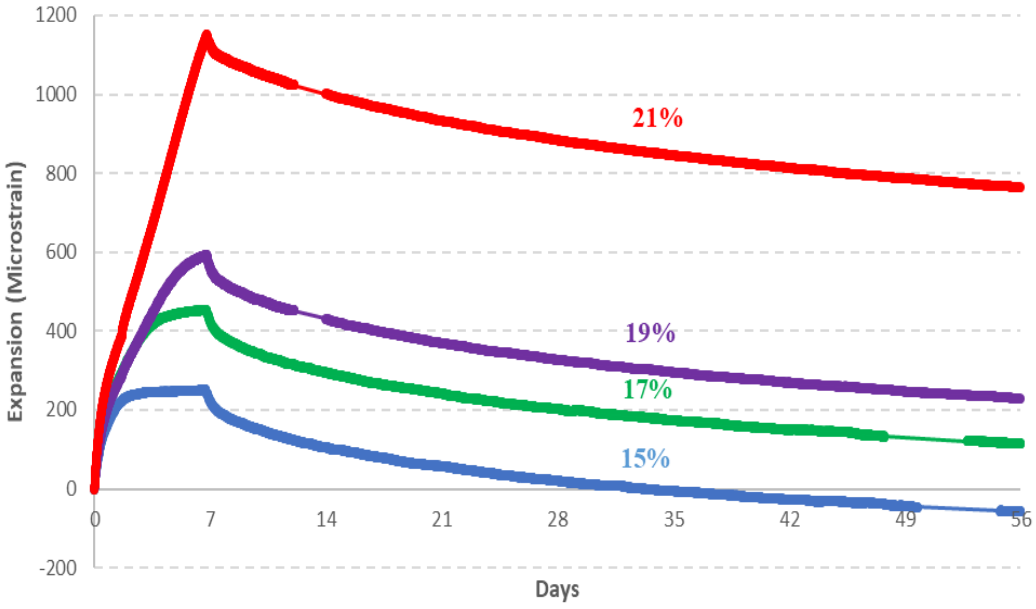

Figure 128: Long-Term VWSG Unrestrained Cylinder Results

Figure 129 shows the long-term data for the restrained 6”x12” specimens.

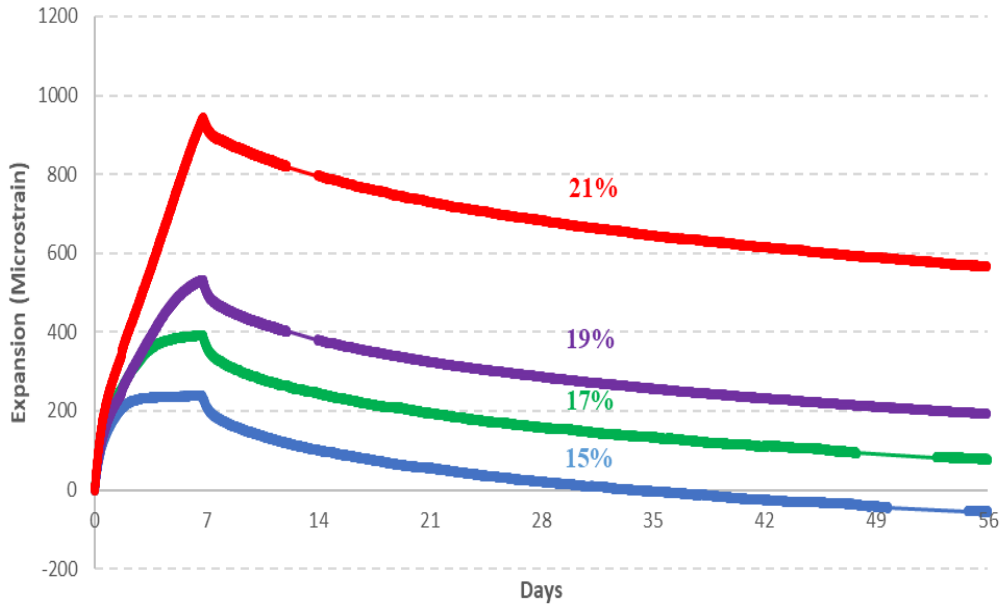

Figure 129: Long-Term VWSG Restrained Cylinder Results

Figure 130 shows the long-term data for the 15% restrained columns, with curing alternative 1.

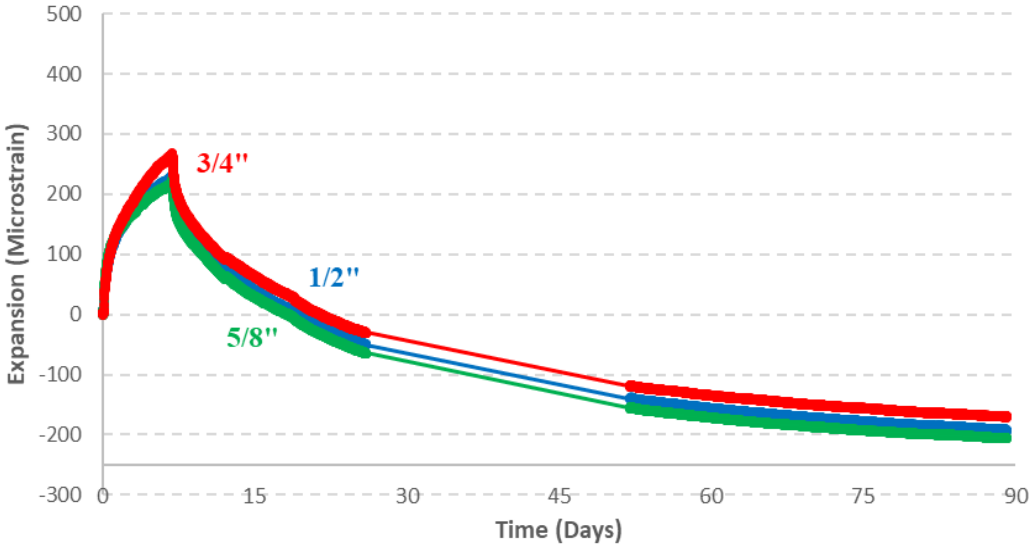

Figure 130: Long-Term Results for 15% Restrained Column Expansion (Curing Alternative 1)

Figure 131 shows the long-term data for the 17% restrained columns, with curing alternative 1.

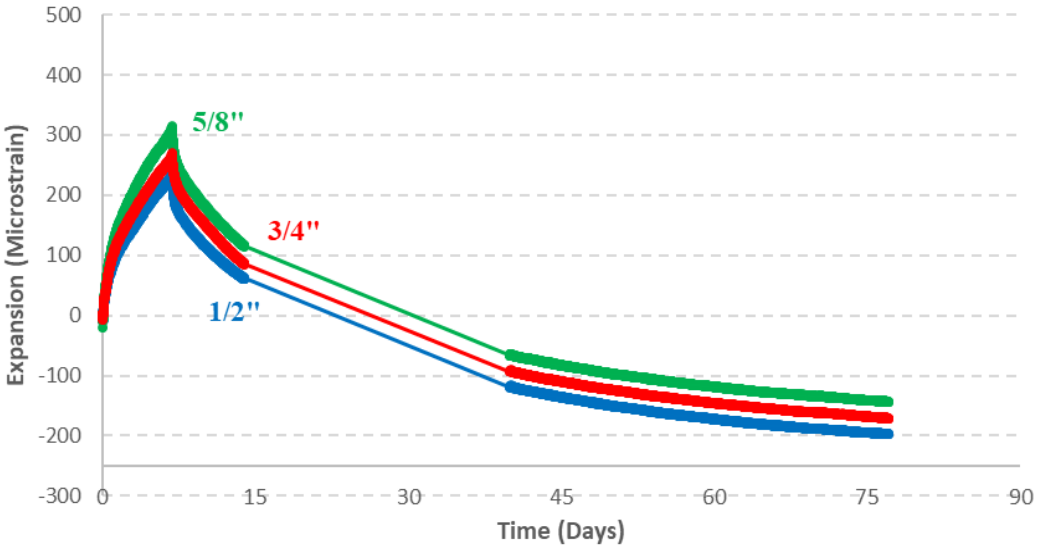

Figure 131: Long-Term Results for 17% Restrained Column Expansion (Curing Alternative 1)

Figure 132 shows the long-term data for the 19% restrained columns, with curing alternative 1.

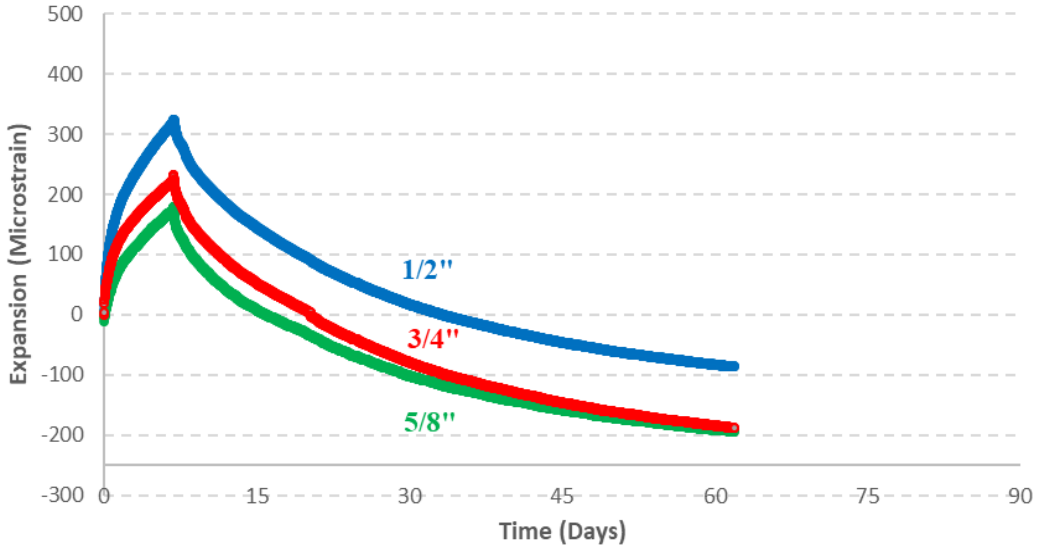

Figure 132: Long-Term Results for 19% Restrained Column Expansion (Curing Alternative 1)

Figure 133 shows the long-term data for the 21% restrained columns, with curing alternative 1.

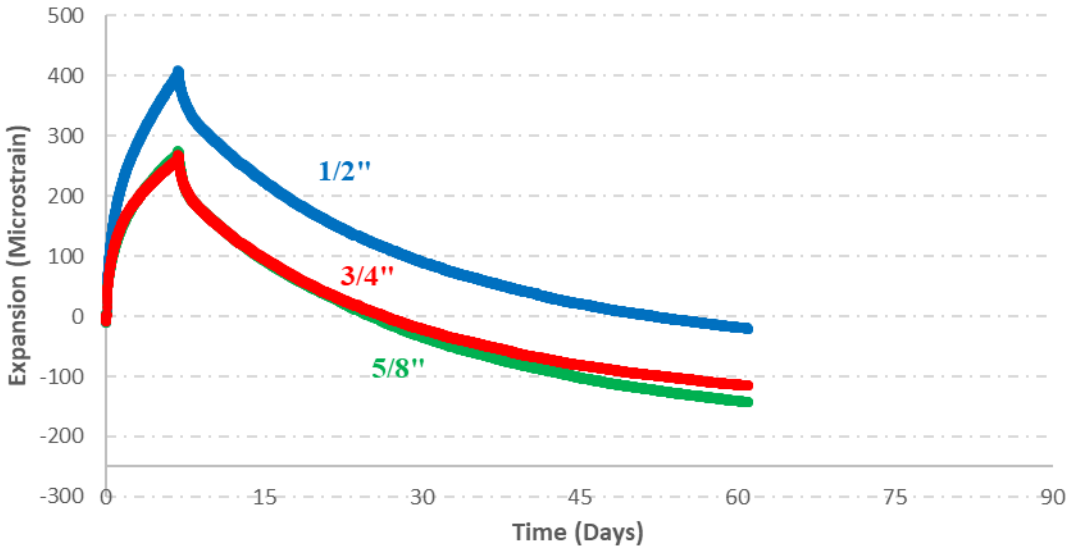

Figure 133: Long-Term Results for 21% Restrained Column Expansion (Curing Alternative 1)